COMPRESSIVE CREEP OF PRESTRESSED CONCRETE MIXTURES WITH AND WITHOUT MINERAL ADMIXTURES

by

Richard Meyerson

Thesis presented to the faculty of the

Virginia Polytechnic and State University

In partial fulfillment of the requirements for the degree of

Master of Science

in

Civil Engineering

Committee:

Richard E. Weyers, Chair

Thomas E. Cousins

Richard Barker

February 2001

Keywords: compressive creep, creep prediction models, time dependent deformation, prestressed concrete mixtures, mineral admixtures

COMPRESSIVE CREEP OF PRESTRESSED CONCRETE MIXTURES WITH AND WITHOUT MINERAL ADMIXTURES

by

Richard Meyerson

(ABSTRACT)

Concrete experiences volume changes throughout its service life. When loaded, concrete experiences an instantaneous recoverable elastic deformation and a slow inelastic deformation called creep. Creep of concrete is composed of two components, basic creep, or deformation under load without moisture loss and drying creep, or deformation under drying conditions only. Deformation of concrete in the absence of applied load is often called shrinkage.

The deformation due to creep is attributed to the movement of water between the different phases of the concrete. When an external load is applied, it changes the attraction forces between the cement gel particles. This change in the forces causes an imbalance in the attractive and disjoining forces. However, the imbalance is gradually eliminated by the transfer of moisture into the pores in cases of compression, and away from the pores in cases of tension.

Designs typically use one of the two code models to estimate creep and shrinkage strain in concrete, ACI 209 model recommended by the American Concrete Institute or the CEB 90 Eurocode 2 model recommended by the Euro-International Committee. The ASSHTO LRFD is based on the ACI 209 model. Three other models are the B3 model, developed by Bazant; the GZ model, developed by Gardner; and the SAK model developed by Sakata.

The development of concrete performance specifications that limit the amount of compressive creep of concrete mixtures used by the Virginia Department of Transportation, specifically concrete mixtures used for prestressed members (A-5 Concrete) were assessed, along with determining the accuracy and precision of the creep models presented in the literature.

The CEB 90 Eurocode 2 model for creep and shrinkage is the most precise and accurate predictor. The total strain for the VDOT portland cement concrete mixtures discussed in this study were found to be between 1200 ± 110 microstrain at 28 days, and 1600 ± 110 microstrain at 97 days, at a five percent significant level.

ACKNOWLEDGEMENTS

First I would like to thank Dr. Richard E. Weyers for his invaluable guidance and assistance. I have a great appreciation for Dr. Thomas Cousins and Dr. Richard Barker for their guidance as members of my research committee.

I express thanks to Steven Lane and the Virginia Transportation Research Council for providing the funding of this project.

My great indebtedness to David Mokarem, without his help and friendship this project could not have been completed.

I would also like to express gratitude to the Faculty of the Structural Engineering and Materials Department along with Dr. Jenson and Wilson Shealy of the Statistics Department for the valuable learning experiences.

Most importantly, I would like to thank my parents Saul and Gail Meyerson, and my brothers Seth, Craig, and Michael for their love and support. I am grateful for the goals and values they have instilled in me.

Finally, I would like to thank my friends, who have supported me both academically and socially. Michael Brown, James Bryant, Terrance W. Carone, Amy Dalrymple, Robert Frasier, Jason W. Jones, Trevor Kirkpatrick, Doug Neely, Michael Neubert, John Ryan, Robert Schottler, Jolyn Senne, and Bob Summers have all contributed to making my experiences at Virginia Tech unforgettable.

TABLE OF CONTENTS

ACKNOWLEDGEMENTS ii

TABLE OF CONTENTS iii

LIST OF FIGURES v

LIST OF TABLES x

CHAPTER 1. INTRODUCTION 1

CHAPTER 2. PURPOSE AND SCOPE 3

CHAPTER 3. METHODS AND MATERIALS 4

Introduction 4

Aggregate Properties 4

Cement Properties 4

Pozzolans 4

Creep Testing 5

REFERENCES 7

CHAPTER 4. RESULTS 8

Introduction 8

Compressive Strength and Modulus 8

Variability of the Total Strain Batch Data 10

Residuals of the Models 10

Chi Squared Analysis 16

REFERENCES 19

CHAPTER 5. DISCUSSION 20

Introduction 20

Compressive Strength and Modulus 20

Variability of the Total Strain Batch Data 21

Creep Prediction Models 23

Performance Specifications 24

References 26

CHAPTER 6. CONCLUSIONS AND RECOMMENDATIONS 27

Conclusions 27

Recommendations 27

FIGURES 28

TABLES 81

APPENDIX A 91

Creep of Concrete Literature Review and Model Equations 91

APPENDIX B 135

Mix Design 135

APPENDIX C 139

Pictures 139

APPENDIX D 142

Creep Frame Calibration 142

APPENDIX E 160

Virginia DOT A-5 Portland Cement Concrete Mixtures 160

APPENDIX F 163

Measurements of Batch Data 163

VITA 170

LIST OF FIGURES

FIGURES.......... 28

FIGURE 1. COMPRESSION STRENGTH OF PORTLAND CEMENT CONCRETE MIXTURES.......... 29

FIGURE 2. COMPRESSION STRENGTH OF PORTLAND CEMENT PLUS MINERAL ADMIXTURE CONCRETE MIXTURES 30

FIGURE 3. ELASTIC MODULUS OF PORTLAND CEMENT CONCRETE MIXTURES 31

FIGURE 4. ELASTIC MODULUS OF PORTLAND CEMENT PLUS MINERAL ADMIXTURE CONCRETE MIXTURES.......... 32

FIGURE 5. PERCENTAGE OF VARIABILITY OF TOTAL STRAIN BETWEEN THE BATCHES OF PORTLAND CEMENT CONCRETE MIXTURES 33

FIGURE 6. PERCENTAGE OF VARIABILITY OF TOTAL STRAIN WINTHIN THE BATCHES OF PORTLAND CEMENT CONCRET MIXTURES 34

FIGURE 7. PERCENTAGE OF VARIABILITY OF TOTAL STRAIN BETWEEN THE BATCHES OF PORTLAND CEMENT PLUS MINERAL ADMIXTURE CONCRETE MIXTURES 35

FIGURE 8. PERCENTAGE OF VARIABILITY OF TOTAL STRAIN WINTHIN THE BATCHES OF PORTLAND CEMENT PLUS MINERAL ADMIXTURE CONCRETE MIXTURES 36

FIGURE 9. RESIDUALS OF TOTAL STRAIN OF PORTLAND CEMENT CONCRETE AND ACI 209 MODEL 37

FIGURE 10. RESIDUALS OF DRYING SHRINKAGE OF PORTLAND CEMENT CONCRETE AND ACI 209 MODEL.......... 38

FIGURE 11. RESIDUALS OF BASIC CREEP OF PORTLAND CEMENT CONCRETE AND ACI 209 MODEL 39

FIGURE 12. RESIDUALS OF TOTAL STRAIN OF PORTLAND CEMENT PLUS MINERAL ADMIXTURE CONCRETE AND ACI 209 MODEL 40

FIGURE 13. RESIDUALS OF DRYING SHRINKAGE OF PORTLAND CEMENT PLUS MINERAL ADMIXTURE CONCRETE AND ACI 209 MODEL.......... 41

FIGURE 14. RESIDUALS OF BASIC CREEP OF PORTLAND CEMENT PLUS MINERAL ADMIXTURE CONCRETE AND ACI 209 MODEL 42

FIGURE 15. RESIDUALS OF TOTAL STRAIN OF PORTLAND CEMENT CONCRETE AND CEB 90 MODEL 43

FIGURE 16. RESIDUALS OF DRYING SHRINKAGE OF PORTLAND CEMENT CONCRETE AND CEB 90 MODEL 44
FIGURE 17. RESIDUALS OF BASIC CREEP OF PORTLAND CEMENT CONCRETE AND CEB 90 MODEL 45
FIGURE 18. RESIDUALS OF TOTAL STRAIN OF PORTLAND CEMENT PLUS MINERAL ADMIXTURE CONCRETE AND CEB 90 MODEL 46
FIGURE 19. RESIDUALS OF DRYING SHRINKAGE OF PORTLAND CEMENT PLUS MINERAL ADMIXTURE CONCRETE AND CEB 90 MODEL 47
FIGURE 20. RESIDUALS OF BASIC CREEP OF PORTLAND CEMENT PLUS MINERAL ADMIXTURE CONCRETE AND CEB 90 MODEL 48
FIGURE 21. RESIDUALS OF TOTAL STRAIN OF PORTLAND CEMENT CONCRETE AND BAZANT MODEL 49
FIGURE 22. RESIDUALS OF DRYING SHRINKAGE OF PORTLAND CEMENT CONCRETE AND BAZANT MODEL 50
FIGURE 23. RESIDUALS OF BASIC CREEP OF PORTLAND CEMENT CONCRETE AND BAZANT MODEL 51
FIGURE 24. RESIDUALS OF TOTAL STRAIN OF PORTLAND CEMENT PLUS MINERAL ADMIXTURE CONCRETE AND BAZANT MODEL 52
FIGURE 25. RESIDUALS OF DRYING SHRINKAGE OF PORTLAND CEMENT PLUS MINERAL ADMIXTURE CONCRETE AND BAZANT MODEL 53
FIGURE 26. RESIDUALS OF BASIC CREEP OF PORTLAND CEMENT PLUS MINERAL ADMIXTURE CONCRETE AND BAZANT MODEL 54
FIGURE 27. RESIDUALS OF TOTAL STRAIN OF PORTLAND CEMENT CONCRETE AND GARDNER MODEL 55
FIGURE 28. RESIDUALS OF DRYING SHRINKAGE OF PORTLAND CEMENT CONCRETE AND GARDNER MODEL 56
FIGURE 29. RESIDUALS OF BASIC CREEP OF PORTLAND CEMENT CONCRETE AND GARDNER MODEL 57
FIGURE 30. RESIDUALS OF TOTAL STRAIN OF PORTLAND CEMENT PLUS MINERAL ADMIXTURE CONCRETE AND GARDNER MODEL 58

FIGURE 31. RESIDUALS OF DRYING SHRINKAGE OF PORTLAND CEMENT PLUS MINERAL ADMIXTURE CONCRETE AND GARDNER MODEL 59
FIGURE 32. RESIDUALS OF BASIC CREEP OF PORTLAND CEMENT PLUS MINERAL ADMIXTURE CONCRETE AND GARDNER MODEL 60
FIGURE 33. RESIDUALS OF TOTAL STRAIN OF PORTLAND CEMENT CONCRETE AND SAKATA MODEL 61
FIGURE 34. RESIDUALS OF DRYING SHRINKAGE OF PORTLAND CEMENT CONCRETE AND SAKATA MODEL 62
FIGURE 35. RESIDUALS OF BASIC CREEP OF PORTLAND CEMENT CONCRETE AND SAKATA MODEL 63
FIGURE 36. RESIDUALS OF TOTAL STRAIN OF PORTLAND CEMENT PLUS MINERAL ADMIXTURE CONCRETE AND SAKATA MODEL 64
FIGURE 37. RESIDUALS OF DRYING SHRINKAGE OF PORTLAND CEMENT PLUS MINERAL ADMIXTURE CONCRETE AND SAKATA MODEL 65
FIGURE 38. RESIDUALS OF BASIC CREEP OF PORTLAND CEMENT PLUS MINERAL ADMIXTURE CONCRETE AND SAKATA MODEL 66
FIGURE 39. CHI SQUARED ANALYSIS FOR TOTAL STRAIN OF PORTLAND CEMENT CONCRETE AT 28 DAYS AFTER CASTING 67
FIGURE 40. CHI SQUARED ANALYSIS FOR DRYING SHRINKAGE OF PORTLAND CEMENT CONCRETE AT 28 DAYS AFTER CASTING 68
FIGURE 41. CHI SQUARED ANALYSIS FOR BASIC CREEP OF PORTLAND CEMENT CONCRETE AT 28 DAYS AFTER CASTING 69
FIGURE 42. CHI SQUARED ANALYSIS FOR TOTAL STRAIN OF PORTLAND CEMENT PLUS MINERAL ADMIXTURE CONCRETE AT 28 DAYS AFTER CASTING 70
FIGURE 43. CHI SQUARED ANALYSIS FOR DRYING SHRINKAGE OF PORTLAND CEMENT PLUS MINERAL ADMIXTURE CONCRETE AT 28 DAYS AFTER CASTING 71
FIGURE 44. CHI SQUARED ANALYSIS FOR BASIC CREEP OF PORTLAND CEMENT PLUS MINERAL ADMIXTURE CONCRETE AT 28 DAYS AFTER CASTING 72
FIGURE 45. CHI SQUARED ANALYSIS FOR TOTAL STRAIN OF PORTLAND CEMENT CONCRETE AT 97 DAYS AFTER CASTING 73

FIGURE 46. CHI SQUARED ANALYSIS FOR DRYING SHRINKAGE OF PORTLAND CEMENT CONCRETE AT 97 DAYS AFTER CASTING ... 74
FIGURE 47. CHI SQUARED ANALYSIS FOR BASIC CREEP OF PORTLAND CEMENT CONCRETE AT 97 DAYS AFTER CASTING ... 75
FIGURE 48. CHI SQUARED ANALYSIS FOR TOTAL STRAIN OF PORTLAND CEMENT PLUS MINERAL ADMIXTURE CONCRETE AT 97 DAYS AFTER CASTING ... 76
FIGURE 49. CHI SQUARED ANALYSIS FOR DRYING SHRINKAGE OF PORTLAND CEMENT PLUS MINERAL ADMIXTURE CONCRETE AT 97 DAYS AFTER CASTING ... 77
FIGURE 50. CHI SQUARED ANALYSIS FOR BASIC CREEP OF PORTLAND CEMENT PLUS MINERAL ADMIXTURE CONCRETE AT 97 DAYS AFTER CASTING ... 78
FIGURE 51. DIFFERENCE BETWEEN MODELS PREDICTION AND AASHTO LRFD DESIGN VALUES FOR CREEP STRAIN (PERCENT) ... 79
FIGURE 52. DIFFERENCE BETWEEN MODELS PREDICTION AND AASHTO LRFD DESIGN VALUES FOR CREEP STRAIN (PERCENT) ... 80
FIGURE 1C. GAGE POINT, SIDE B ... 140
FIGURE 2C. CREEP ROOM: FOUR COMPRESSION FRAMES WITH THREE SPECIMENS PER FRAME. 140
FIGURE 3C. PRESSURE GAGES ... 141
FIGURE 4C. STRAIN GAGE (ONE PER STEEL ROD) ... 141
FIGURE 1D. FRAME 1 GAGE PRESSURE VS. LOAD ... 144
FIGURE 2D. FRAME 1 STRAIN VS. LOAD CELL ... 145
FIGURE 3D. FRAME 1 GAGE PRESSURE VS. DESIRED CONCRETE PRESSURE ... 146
FIGURE 4D. FRAME 1 GAGE PRESSURE VS. STRAIN GAGE ... 147
FIGURE 5D. FRAME 2 GAGE PRESSURE VS. LOAD CELL ... 148
FIGURE 6D. FRAME 2 STRAIN VS. LOAD CELL ... 149
FIGURE 7D. FRAME 2 GAGE PRESSURE VS. DESIRED CONCRETE PRESSURE ... 150
FIGURE 8D. FRAME 2 GAGE PRESSURE VS. STRAIN GAGE ... 151
FIGURE 9D. FRAME 3 GAGE PRESSURE VS. LOAD CELL ... 152
FIGURE 10D. FRAME 3 STRAIN VS. LOAD CELL ... 153
FIGURE 11D. FRAME 3 GAGE PRESSURE VS. DESIRED CONCRETE PRESSURE ... 154
FIGURE 12D. FRAME 3 GAGE PRESSURE VS. STRAIN GAGE ... 155
FIGURE 13D. FRAME 4 GAGE PRESSURE VS. LOAD CELL ... 156

FIGURE 14D. FRAME 4 STRAIN VS. LOAD CELL 157
FIGURE 15D. FRAME 4 GAGE PRESSURE VS. DESIRED CONCRETE PRESSURE 158
FIGURE 16D. FRAME 4 GAGE PRESSURE VS. STRAIN GAGE 159

LIST OF TABLES

TABLES.. 81

TABLE 1. SPECIMENS FOR COMPRESSIVE CREEP TESTING CYCLES 82

TABLE 2. A5 GRAVEL BATCH QUANTITIES AND FRESH CONCRETE PROPERTIES...................... 83

TABLE 3. A5 LIMESTONE BATCH QUANTITIES AND FRESH CONCRETE PROPERTIES 84

TABLE 4. A5 DIABASE BATCH QUANTITIES AND FRESH CONCRETE PROPERTIES..................... 85

TABLE 5. A5 LIMESTONE GGBFS BATCH QUANTITIES AND FRESH CONCRETE PROPERTIES.... 86

TABLE 6. A5 LIMESTONE FLY ASH BATCH QUANTITIES AND FRESH CONCRETE PROPERTIES... 87

TABLE 7. A5 LIMESTONE MICROSILICA BATCH QUANTITIES AND FRESH CONCRETE PROPERTIES 88

TABLE 8. COMPRESSION STRENGTH AND ELASTIC MODULUS OF CONCRETE MIXTURES............. 89

TABLE 9. CHI SQUARE ANALYSIS FOR TOTAL STRAIN 90

TABLE 1B. CONCRETE AGGREGATE PROPERTIES.. 136

TABLE 2B. CEMENT PROPERTIES 137

TABLE 3B. X RAY ANALYSIS OF MICROSILICA, AND GGBFS... 138

TABLE 1E. VDOT APPROVED A5 PORTLAND CEMENT CONCRETE MIXTURES, SSD (QUANTITIES/CUBIC METER).. 161

TABLE 2E. A5 PORTLAND CEMENT CONCRETE MIXTURES CALCULATED FROM VDOT APPROVED MIXTURES, SSD (QUANTITIES/CUBIC METER) 162

TABLE 1F. DATA FOR A5 GRAVEL PORTLAND CEMENT CONCRETE MIXTURES 164

TABLE 2F. DATA FOR A5 LIMESTONE PORTLAND CEMENT CONCRETE MIXTURES 165

TABLE 3F. DATA FOR A5 DIABASE PORTLAND CEMENT CONCRETE MIXTURES 166

TABLE 4F. DATA FOR A5 LIMESTONE FLY ASH PORTLAND CEMENT CONCRETE MIXTURES.. 167

TABLE 5F. DATA FOR A5 LIMESTONE GGBFS PORTLAND CEMENT CONCRETE MIXTURES... 168

TABLE 6F. DATA FOR A5 LIMESTONE MICROSILICA PORTLAND CEMENT CONCRETE MIXTURES 169

CHAPTER 1. INTRODUCTION

Concrete experiences volume changes throughout its service life. The total in-service volume change of concrete is the resultant of applied loads and shrinkage. When loaded, concrete experiences an instantaneous recoverable elastic deformation and a slow inelastic deformation called creep. Creep of concrete is composed of two components, basic creep, or deformation under load without moisture loss and drying creep, or deformation under drying conditions only. Deformation of concrete in the absence of applied load is often called shrinkage.

There are three types of shrinkage; autogeneous, drying, and carbonation shrinkage. Autogeneous shrinkage is the resultant of the hydration process. The hydrated cement paste is smaller in volume than the solid volume of the cement paste and water. Drying shrinkage is caused by the loss of evaporable water. Carbonation shrinkage is caused by the carbonation of hydrated cement products and possibly from the movement of water from the gel pores to the capillary pores.

Creep testing of concrete may be performed on sealed specimens or unsealed specimens. The deformation of sealed-loaded specimens is the result of elastic deformation, water movement from the gel pores to the capillary pores, and autogeneous shrinkage. Whereas, the deformation of unsealed-loaded specimens is the result of internal moisture movement, moisture loss, autogeneous shrinkage, and carbonation shrinkage. The deformation of unsealed-unloaded, or drying shrinkage is the result of moisture loss, autogeneous shrinkage, and carbonation shrinkage. Thus, the difference in deformations between loaded specimens, minus the elastic deformation, and unloaded specimens, is basic creep, which is the resultant of internal moisture movement.

Creep of concrete is normally evaluated using unsealed loaded and unloaded companion specimens exposed at a constant drying environment. Thus, the total deformation may be separated into the elastic compression, basic creep, and drying creep (moisture loss, autogeneous and carbonation shrinkage.)

The deformation due to creep is attributed to the movement of water between the different phases of the concrete. When an external load is applied, it changes the attraction forces between the cement gel particles. This change in the forces causes an imbalance in the attractive and disjoining forces. However, the imbalance is gradually eliminated by the transfer of moisture into the pores in cases of compression, and away from the pores in cases of tension.

Creep coefficient, specific creep, or creep compliance are generally used to describe creep strain by different mathematical prediction models. The creep coefficient is defined as the ratio of creep strain (basic plus drying creep) at a given time to the initial elastic strain. The specific creep is defined as the creep strain per unit stress. The creep compliance is defined as the creep strain plus elastic strain per unit stress, whereas the elastic strain is defined as the instantaneous recoverable deformation per unit length of a concrete specimen during the initial stage of loading.

Designs typically use one of the two code models to estimate creep and shrinkage strain in concrete, ACI 209 model recommended by the American Concrete Institute or the Eurocode 2 model recommended by the Euro-International Committee. The ASSHTO LRFD is based on the ACI 209 model. Three other models are the B3 model, developed by Bazant; the GZ model, developed by Gardner; and the SAK model, developed by Sakata.

Creep estimates are necessary when designing prestressed concrete members. Losses in prestress due to creep are determined by the calculated creep coefficient and creep strain. Thus, the study will be limited to VDOT approved prestressed concrete mixtures.

CHAPTER 2. PURPOSE AND SCOPE

The objective of this research is to develop concrete performance specifications that limit the amount of compressive creep of prestressed concrete mixtures used by the Virginia Department of Transportation, specifically concrete mixtures used for prestressed members (A-5 Concrete). A secondary objective is to assess the accuracy and precision of the creep models presented in the literature. With the development of these concrete performance specifications and the identification of the most accurate and precise creep model, prestress losses will be limited and the most reliable prediction model will be identified.

The aggregate, the cement and water content, and mineral admixtures will be varied, while the cement type and fineness, chemical admixtures, curing conditions, and ambient conditions will be held constant.

CHAPTER 3. METHODS AND MATERIALS

Introduction

The objective of this study is to develop concrete performance specifications, based on a selected test method, which limit the amount of compressive creep of the Virginia Department of Transportation (VDOT) A-5 General Prestress Concrete mixtures. The study variables included two cement types, two pozzolans, and three coarse aggregates with their associated natural fine aggregate. An air entrainment agent and high range water reducer were used to achieve the specified air content and slump. A review of the creep literature including model equations is presented in Appendix A for the interested reader.

Aggregate Properties

The three types of coarse aggregate limestone, gravel, and diabase all meet the requirements of # 57 stone according to VDOT Road and Bridge 1997 Specifications. The fine aggregate used in each mixture corresponded to that of each respective coarse aggregate and also meet VDOT Road and Bridge 1997 Specifications.[1] The aggregate properties are presented in Appendix B.

Cement Properties

The portland cement (PC) was a Type I/II and meet ASTM B 150-98 specifications. A blended cement of Type I/II portland cement and ground granulated blast furnace slag (GGBFS) was used. The GGBFS was grade 120 and met ASTM C 989-89 and ASTM C 595-89, Type IS, when blended with portland cement, specifications.[2,3] Chemical analysis of the PC and GGBFS are presented in Appendix B. Type III cement was not used in this study because it was not representative of the approved VDOT prestressed concrete mixtures.

Pozzolans

The pozzolans were a Class F fly ash (FA), and microsilica (MS) meeting ASTM C 311– 97 specifications. Chemical analysis of the FA and MS are presented in Appendix B.[4]

Creep Testing

The creep test specimens were cast in 150mm x 300mm (6 in x 12 in) steel cylinder molds and moist cured for 7 days in accordance with ASTM C 192-95.[5] In addition, eight 100mm x 200 mm (4 in x 8 in) compressive strength cylinders were cast from each batch.

Compressive strength cylinders were also moist cured for 7 days and then placed in the creep environmental conditioning room, 50 % ± 4 % relative humidity, and 73.4 °F ± 2 °F. All the concrete specimens were sulfur capped after the curing period according to ASTM C 617-94.[6] Compression strength tests according to ASTM C 39-96 were conducted to obtain 7, 14, 28, and 56 day strengths.[7] Modulus of elasticity was measured at 7 and 28 days in accordance with ASTM C 469-94.[8]

The creep test specimens have two sets of gage points 200mm (8 in) apart on diametrically opposite sides of each cylinder. The two sets of gage points are referred to as, "Side A" and "Side B". Figure 1C in Appendix C illustrates the gage points in the specimen.

Each mixture was repeated three times for a total of six specimens per mixture to allow for statistical evaluation. Two specimens per mixture batch were placed in a compression frame and loaded up to 40 % of the ultimate strength of the concrete. Two specimens per mixture batch were not loaded, and used for drying shrinkage and creep measurements. Three specimens were placed in each frame of the four loading frames. The applied load on the three specimens in a loading frame was equal to 40 % of the ultimate strength of the lowest average compressive strength. The compressive creep tests were conducted in accordance with ASTM C 512-94 for a period of 90 days.[9] A Whitimore Gage was used to measure the creep deformation. Four readings were taken on each side of the specimen, A and B, for a total of eight deformation readings for each test time. The creep deformation for a test period is the average of eight measurements.

Prior to the first test cycle, the creep frames were calibrated using a load cell, pressure gages, and strain gages, see Appendix D.

Creep Testing Cycles

Table 1 presents the specimens for each testing cycle. Test cycle I was the limestone and limestone-microsilica mixtures. Test cycle II was the gravel and diabase mixtures. Test cycle III was the limestone-fly ash and limestone-slag mixtures. A total of six compressive creep specimens, two from each batch, were cast for the two mixtures included in each of the three test cycles. The concrete was consolidated by rodding each of the three equal volume layers 25 times. Three batches of each mixture were prepared in respective testing cycles. Appendix E presents the saturated surface dry (SSD) weights of the concrete mixture proportions. Tables 2 through 7 presents the batch dry weights and fresh concrete properties, slump, air content, unit weight, temperature, and water to cement ratio (w/c) or water to cement plus pozzolan ratio (w/c+p).

REFERENCES

1. Virginia Department of Transportation Road and Bridge Specifications, January 1997, pp 129-134, 195.
2. ASTM C 989-89, Standard Specification of Concrete and Aggregates. Section 4, v. 04.02.
3. ASTM C 595-89, Standard Specification of Concrete and Aggregates. Section 4, v. 04.02.
4. ASTM C 311-97, Standard Specification of Concrete and Aggregates. Section 4, v. 04.02.
5. ASTM C 192-95, Standard Specification of Concrete and Aggregates. Section 4, v. 04.02.
6. ASTM C 617-94, Standard Specification of Concrete and Aggregates. Section 4, v. 04.02.
7. ASTM C 39-96, Standard Specification of Concrete and Aggregates. Section 4, v. 04.02.
8. ASTM C 469-94, Standard Specification of Concrete and Aggregates. Section 4, v. 04.02.
9. ASTM C 512-94, Standard Specification of Concrete and Aggregates. Section 4, v. 04.02.

CHAPTER 4. RESULTS

Introduction

This section presents the results of the ASTM C 39-96 and ASTM C 469-94 test methods, the variability of total strain between and within the batches, and the residuals of the experimental data and each prediction model: the ACI 209, CEB 90 Euro-Code, Bazant Model, Gardner Model, and Sakata Model. The total strain data for each batch is presented in Appendix F. The residual is expressed as the difference between the experimental mean and the prediction models. Residuals were calculated for the total strain, drying shrinkage strain, and basic creep. A chi squared analysis was conducted to choose the model that was most accurate. Mixtures with portland cement concrete, and mixtures with portland cement concrete plus a mineral admixtures were analyzed separately.

Compressive Strength and Modulus

ASTM C 39-96

Table 8 presents the average compressive strength and elastic modulus for all of the prestressed concrete mixtures.

Figure 1 presents the compressive strength of the portland cement concrete mixtures. The compressive strength seven days after casting is 44 MPa, 36 MPa, and 33 MPa (6,300 psi, 5,200 psi, 4,700 psi) for limestone, diabase, and gravel concrete mixtures, respectively. The compressive strength 28 days after casting, f_c', is 42 MPa, 42 MPa, and 51 MPa (6,000 psi, 6,000 psi, and 7,400 psi) for limestone, diabase, and gravel concrete mixtures, respectively. The compressive strength 56 days after casting is 52 MPa, 43 MPa, and 41 MPa (7,600 psi, 6,200 psi, 5,900 psi) for limestone, diabase, and gravel concrete mixtures, respectively. The limestone mixture has a larger compressive strength and lower w/c ratio than the gravel and diabase mixtures. The compressive strengths for the gravel and diabase mixtures are not significantly different.

Figure 2 presents the compressive strength of the portland cement plus mineral admixture concrete mixtures. The compressive strength seven days after casting is 50 MPa, 41 MPa, and

34 MPa (7,300 psi, 5,900 psi, 4,900 psi) for limestone MS, limestone GGBFS, and limestone FA concrete mixtures respectively. The compressive strength 28 days after casting, f_c', is 42 MPa, 42 MPa, and 51 MPa (6,000 psi, 6,000 psi, and 7,400 psi) for limestone MS, limestone GGBFS, and limestone FA concrete mixtures respectively. The compressive strength 56 days after casting is 65 MPa, 47 MPa, and 46 MPa (9,400 psi, 6,800 psi, 6,600 psi) for limestone MS, limestone GGBFS, and limestone FA concrete mixtures, respectively. The limestone MS mixture has a larger compressive strength and lower w/c ratio than the limestone GGBFS and limestone FA mixtures. The compressive strengths for the limestone GGBFS and limestone FA mixtures are not significantly different.

The compressive strength for the limestone MS mixture is larger than the compressive strength of the limestone mixture without a mineral admixture. The limestone GGBFS mixture has a slightly lower compressive strength than the limestone mixture without a mineral admixture. The limestone FA mixture at early ages has a considerable lower compressive strength than the limestone mixture with portland cement. As the concrete ages, the limestone FA compressive strength increases nearing the strength of the limestone mixture with portland cement.

ASTM C 469-94

Figure 3 presents the elastic modulus of the portland cement concrete mixtures. The seven-day modulus for the limestone and diabase and gravel concrete mixtures are 41 x 10^3 MPa, 41 x 10^3 MPa, and 32 x 10^3 MPa (5.9 x10^6 psi, 5.9 x10^6 psi, and 4.7 x10^6 psi) respectively. The limestone concrete mixture remains at 41 x 10^3 MPa (5.9 x10^6 psi) at 28 days. The diabase modulus exhibits a decrease in modulus to 36 x 10^3 MPa (5.2 x10^6 psi), and the gravel modulus increases to 34 x 10^3 MPa (5.0 x10^6 psi) at 28 days.

Figure 4 presents the elastic modulus of portland cement plus mineral admixture concrete mixtures. The limestone GGBFS, limestone MS, and limestone FA concrete mixtures have a seven day modulus of 41 x10^3 MPa, 40 x10^3 MPa, and 39 x10^3 MPa (5.9 x10^6 psi, 5.8 x10^6 psi, and 5.6 x10^6 psi) respectively. The limestone GGBFS, limestone MS, and limestone FA have a 28 day modulus of 38 x10^3 MPa, 41 x10^3 MPa, and 38 x10^3 MPa (5.5 x10^6 psi, 6.0 x10^6 psi, and 5.5 x10^6 psi), respectively.

The elastic modulus for the limestone mixture with portland cement is similar to the values produced by the mixtures with mineral admixtures.

Variability of the Total Strain Batch Data

The variability of total strain between the batches is the variation of the process from day to day, or batch-to-batch, batching and mixing combined. The variability within the batch is the inherent variation of experimental error. The experimental error represents the variability of each strain reading for one test cycle.

Portland Cement Concrete Mixtures

The variability of total strain between the batches of portland cement concrete mixtures is presented in Figure 5. The limestone, diabase, and gravel total strain variability between batches is approximately 75%, 65%, and 45% respectively.

The variability of total strain within the batches of portland cement concrete mixtures is presented in Figure 6. The limestone, diabase, and gravel total strain variability within batches is approximately 25%, 35%, and 55% respectively.

Portland Cement plus Mineral Admixture Concrete Mixtures

The variability of total strain between the batches of portland cement concrete mixtures is presented in Figure 7. The limestone MS, limestone FA, and limestone GGBFS total strain variability between batches is approximately 90%, 70%, and 60% respectively.

The variability of total strain within the batches of portland cement concrete mixtures is presented in Figure 8. The limestone MS, limestone FA, and limestone GGBFS total strain variability within batches is approximately 10%, 30%, and 40% respectively.

Residuals of the Models

The model results are presented as residuals, the difference between the experimental mean and the model value. If the model is under predicting the experimental mean, the residual has a positive value. If the model is over predicting the experimental mean, the residual has a negative residual. All five models predict the total strain as the sum of the drying shrinkage strain and basic creep. The models are limited to concrete mixtures without mineral admixtures, therefore the figures were arranged such that the mixtures with portland cement concrete are presented as one group, and mixtures with portland cement plus mineral admixture concrete are presented as another group.

ACI 209

Portland Cement Concrete Mixtures

Figures 9 through 11 present the residuals of the total strain, drying shrinkage strain, and basic creep, respectively, of the portland cement concrete mixtures for the ACI 209 model. For total strain, the ACI 209 model is a better predictor at early ages for the limestone, diabase, and gravel mixtures. At later ages, after 28 days, the model under predicts and becomes less accurate. The limestone mixture exhibits a larger variability at the five percent significant level than the diabase and gravel mixtures. There is no significant difference between the diabase and gravel mixtures.

The model under predicts the drying shrinkage strain, and becomes less accurate after 28 days. There is no significant difference between the gravel, limestone, and diabase mixtures for the drying shrinkage prediction.

The basic creep is over predicted and the model becomes more accurate after 28 days. There is no significant difference between the mixtures for the basic creep prediction.

Portland Cement plus Mineral Admixture Concrete Mixtures

Figures 12 through 14 present the residuals of the total strain, drying shrinkage strain, and basic creep, respectively, of the portland cement plus mineral admixture concrete mixtures for the ACI 209 model. For total strain, the ACI 209 model is a better predictor at early ages for the limestone FA, limestone GGBFS, and limestone MS mixtures. After 28 days the model under predicts and becomes less accurate. There is no significant difference between the limestone FA, limestone GGBFS, and limestone MS mixtures for the total strain.

The model under predicts the drying shrinkage strain, and becomes less accurate after 28 days. There is no significant difference between the mixtures for the drying shrinkage strain prediction. The limestone MS mixture has a larger variability than the other mixtures.

The basic creep is over predicted, but the precision remains the same over time. There is no significant difference between the mixtures for the basic creep prediction.

CEB 90 Euro-Code

Portland Cement Concrete Mixtures

Figures 15 through 17 present the residuals of the total strain, drying shrinkage strain, and basic creep, respectively, of the portland cement concrete mixtures for the CEB 90 Euro-Code. For total strain, the CEB 90 model is a good predictor. The limestone mixture exhibits a larger variability at the five percent significant level than the diabase and gravel mixtures. There is no significant difference between the diabase and gravel mixtures.

The model under predicts the drying shrinkage strain, while there is no significant difference between the gravel, limestone, and diabase mixtures.

The model over predicts the basic creep, and there is no significant difference between the mixtures for the prediction of basic creep.

Portland Cement plus Mineral Admixture Concrete Mixtures

Figures 18 through 20 present the residuals of the total strain, drying shrinkage strain, and basic creep, respectively, of the portland cement plus mineral admixture concrete mixtures for the CEB 90 Euro-Code model. For total strain, the CEB 90 model is a good predictor for the limestone FA, limestone GGBFS, and limestone MS mixtures. There is no significant difference between the limestone FA, limestone GGBFS, and limestone MS mixtures.

The model under predicts the drying shrinkage strain, and there is no significant difference between the mixtures. The limestone MS mixture has a larger variability than the other mixtures.

The basic creep is over predicted and the accuracy slightly decreases over time. There is no significant difference between the mixtures for the prediction of basic creep.

Bazant Model

Portland Cement Concrete Mixtures

Figures 21 through 23 present the residuals of the total strain, drying shrinkage strain, and basic creep, respectively, of the portland cement concrete mixtures for the Bazant Model. For total strain, the Bazant model over predicts the diabase and gravel mixtures. The model under predicts the limestone mixture, and exhibits a larger variability at the five percent significant level than the diabase and gravel mixtures. There is no significant difference between the diabase and gravel mixtures.

The model under predicts the drying shrinkage strain, and there is no significant difference between the gravel, limestone, and diabase mixtures for the prediction of drying shrinkage.

The model over predicts the basic creep, and becomes a better predictor after 28 days. There is no significant difference between the mixtures for the prediction of basic creep.

Portland Cement plus Mineral Admixture Concrete Mixtures

Figures 24 through 26 present the residuals of the total strain, drying shrinkage strain, and basic creep, respectively, of the portland cement plus mineral admixture concrete mixtures for the Bazant model. For total strain, the Bazant model is a good predictor for the limestone FA, limestone GGBFS, and limestone MS mixtures. There is no significant difference between the limestone FA, limestone GGBFS, and limestone MS mixtures. At later ages, after 40 days, the model over predicts the total strain.

The model under predicts the drying shrinkage strain, and there is no significant difference between the mixtures. The limestone MS mixture has a larger variability than the other mixtures.

The model over predicts the basic creep, and the precision remains constant over time. There is no significant difference between the mixtures for the prediction of basic creep.

Gardner Model

Portland Cement Concrete Mixtures

Figures 27 through 29 present the residuals of the total strain, drying shrinkage strain, and basic creep, respectively, of the portland cement concrete mixtures for the Gardner Model. For total strain, the Gardner model over predicts the diabase and gravel mixtures. The model under predicts the experimental mean of the limestone mixture, but exhibits a larger variability at the five percent significant level than the diabase and gravel mixtures. There is no significant difference between the diabase and gravel mixtures.

The model under predicts the drying shrinkage strain, and there is no significant difference between the gravel, limestone, and diabase mixtures for the prediction of drying shrinkage.

The model over predicts the basic creep, and there is no significant difference between the mixtures for the prediction of basic creep.

Portland Cement plus Mineral Admixture Concrete Mixtures

Figures 30 through 32 present the residuals of the total strain, drying shrinkage strain, and basic creep, respectively, of the portland cement plus mineral admixture concrete mixtures for the Gardner model. For total strain, the Gardner model over predicts the experimental mean for the limestone FA, limestone GGBFS, and limestone MS mixtures, and becomes less accurate over time. There is no significant difference between the limestone FA, limestone GGBFS, and limestone MS mixtures.

The model under predicts the drying shrinkage strain, and there is no significant difference between the mixtures. The limestone MS mixture has a larger variability than the other mixtures.

The model over predicts the basic creep, and becomes less accurate over time. There is no significant difference between the mixtures for the prediction of basic creep.

Sakata Model

Portland Cement Concrete Mixtures

Figures 33 through 35 present the residuals of the total strain, drying shrinkage strain, and basic creep, respectively, of the portland cement concrete mixtures for the Sakata Model. For total strain, the Sakata model is a good predictor for the diabase and gravel mixtures. The model under predicts the experimental mean for the limestone mixture, but exhibits a larger variability at the five percent significant level than the diabase and gravel mixtures. There is no significant difference between the diabase and gravel mixtures.

The model is a good predictor for the drying shrinkage strain. There is no significant difference between the gravel, limestone, and diabase mixtures for the prediction of drying shrinkage. The model slightly under predicts the limestone mixture, while the gravel mixture is slightly over predicted, and the model is a good predictor for the diabase mixture.

The model over predicts the basic creep for the gravel and diabase mixtures. The model over predicts the basic creep for the limestone mixture at early ages. After 28 days, the model under predicts the basic creep values. There is no significant difference between the gravel and diabase mixtures for the prediction of basic creep.

Portland Cement plus Mineral Admixture Concrete Mixtures

Figures 36 through 38 present the residuals of the total strain, drying shrinkage strain, and basic creep, respectively, of the portland cement plus mineral admixture concrete mixtures for the Sakata model. For total strain, the Sakata model is a good predictor for the limestone FA, limestone GGBFS, and limestone MS mixtures. There is no significant difference between the limestone FA, limestone GGBFS, and limestone MS mixtures.

The model under predicts the drying shrinkage strain, and becomes less accurate over time. There is no significant difference between the mixtures. The limestone MS mixture has a larger variability than the other mixtures.

The model over predicts the basic creep, and becomes more accurate over time. There is no significant difference between the mixtures for the prediction of basic creep.

Chi Squared Analysis

The chi squared test statistic is the square of the residual of the experimental mean and the model. The model with the smallest test statistic is the best predictor. The models were divided into the total strain, the drying shrinkage strain, and the basic creep. The 28 day and 97 day residual values were examined to better understand the short-term, and the long-term behavior of each model.

Short term – 28 Days

Portland Cement Concrete Mixtures

Figures 39 through 41 present the chi-squared values of the total strain, drying shrinkage strain, and basic creep, respectively, of the portland cement concrete mixtures. The models that predict the total strain best, in order of accuracy, are the Sakata, ACI 209, and CEB 90 models. The Bazant and Gardner models are the least accurate predictors for the total strain. The limestone mixture has the least accurate prediction of the mixtures.

The drying shrinkage predicted by the Sakata, Gardner, Bazant, and CEB 90 models, are the most accurate. The ACI 209 model does not predict the drying shrinkage accurately.

The Sakata, ACI 209, Bazant, and CEB 90 models predict the basic creep more accurately than the Gardner model.

Portland Cement plus Mineral Admixture Concrete Mixtures

Figures 42 through 44 present the chi-squared values of the total strain, drying shrinkage strain, and basic creep, respectively, of the portland cement plus mineral admixture concrete mixtures. In general, the mineral admixture concrete mixtures are more precise than the mixtures with the portland cement.

The model that predicts the total strain with the most precision and accuracy is the CEB 90 model. The Bazant, the Gardner, ACI 209, and Sakata all predict the total strain fairly accurately, but are not as precise as the CEB 90 model.

The Gardner and Sakata model predict the drying shrinkage strain more precisely and accurately than the Bazant, CEB 90, and ACI 209 models.

The Gardner model is the least accurate when predicting the basic creep. The Sakata, ACI 209, Bazant, and CEB 90 models are similar in precision and accuracy for the prediction of basic creep.

Long term – 97 Days

Portland Cement Concrete Mixtures

Figures 45 through 47 present the chi-squared values of the total strain, drying shrinkage strain, and basic creep, respectively, of the portland cement concrete mixtures. The models that predict the total strain in the order of accuracy are the Sakata, CEB 90, and ACI 209 models. The Bazant and Gardner models are the least accurate predictors for the total strain. All the models predict the limestone mixture with the least accuracy.

The drying shrinkage predicted by the Sakata, Gardner, Bazant, and CEB 90 models, are the most accurate. The ACI 209 model does not predict the drying shrinkage accurately.

The ACI 209, Sakata, Bazant, and CEB 90 models predict the basic creep more accurately than the Gardner model.

Portland Cement plus Mineral Admixture Concrete Mixtures

Figures 48 through 50 present the chi-squared values of the total strain, drying shrinkage strain, and basic creep, respectively, of the portland cement plus mineral admixture concrete mixtures. In general, the mineral admixture concrete mixtures are more precise than the mixtures with the portland cement.

The model that predicts the total strain with the most precision and accuracy is the CEB 90 model. The Sakata, Bazant, and ACI 209, all predict the total strain accurately. The Gardner model is inaccurate when predicting the total strain.

The Gardner, CEB 90, and Bazant models predict the drying shrinkage strain more precisely and accurately than the Sakata and ACI 209 models.

The Gardner model is the least accurate when predicting the basic creep. The Sakata, ACI 209, Bazant, and CEB 90 models are similar in precision and accuracy for the prediction of basic creep.

In general, the limestone portland cement concrete mixture has the most variability and least precision than the other mixtures. When comparing the models for short and long term accuracy and precision, the models for the short term time periods are better predictors.

Figures 51 and 52 present the difference between the prediction models and the AASHTO LRFD design for basic creep strain.[3] Values were calculated by the following equation:

(AASHTO – Model) / Model x 100

The model value was calculated by taking the average prediction values of all the mixtures. The CEB 90, Bazant, and Gardner models ranged from –50% to approximately 150% difference over time. The ACI 209 and Sakata models ranged from –50% to approximately 250% difference over time. A positive value represents the model under predicting the AASHTO design. The percent differences increase as time progresses.

REFERENCES

1. ASTM C 39-96, Standard Specification of Concrete and Aggregates. Section 4, v. 04.02.

2. ASTM C 469-94, Standard Specification of Concrete and Aggregates. Section 4, v. 04.02.

3. Barker, Richard M. and Puckett, Jay A., *Design of Highway Bridges: Based on AASHTO LRFD Bridge Design Specifications.* New York: John Wiley & Sons, Inc., pp. 410-413.

CHAPTER 5. DISCUSSION

Introduction

This section discusses the results of the ASTM C 39-96 and ASTM C 469-94 test methods, the variability of total strain between and within the batches, and the residuals of the experimental data and each prediction model: the ACI 209, CEB 90 Eruo-Code, Bazant Model, Gardner Model, and Sakata Model.

Compressive Strength and Modulus

ASTM C 39-96

Figure 1 presents the compressive strength of the portland cement concrete mixtures. The limestone mixture has a larger compressive strength and lower w/c ratio than the gravel and diabase mixtures. As the w/c ratio decreases, the compressive strength increases for a mixture with the same aggregate. The compressive strengths for the gravel and diabase mixtures are not significantly different, although the gravel mixture has a lower w/c ratio. This is a result of the surface mechanics of the aggregate. The gravel aggregate has fewer fracture surfaces than the diabase aggregate which affects the mechanical bonds between the aggregate and the cement paste.

Figure 2 presents the compressive strength of the portland cement plus mineral admixture concrete mixtures. The limestone MS mixture has a larger compressive strength and lower w/c ratio than the limestone GGBFS and limestone FA mixtures. The compressive strength for the limestone MS mixture is larger than the compressive strength of the limestone mixture without a mineral admixture. This is a result of the MS having a finer particle distribution. The finer particles allow the cement paste to hydrate at a faster rate than normal portland cement. The desired compressive strength is reached at earlier ages. The addition of MS in a concrete mixture will increase the compressive strength at all ages of the concrete compared to the compressive strength of a mixture with normal portland cement.

The compressive strengths for the limestone GGBFS and limestone FA mixtures are not significantly different. The limestone GGBFS mixture has a slightly lower compressive strength than the limestone mixture without a mineral admixture. The limestone FA mixture at early ages has a considerable lower compressive strength than the limestone mixture with portland cement. As the concrete ages, the limestone FA compressive strength increases nearing the strength of the limestone mixture with portland cement. The two mineral admixtures, when added to the mixture, slow the hydration of the cement paste, and the desired compressive strength is reached at later ages.

When compared to the compressive strength of normal portland cement concrete, the addition of GGBFS or FA to a concrete mixture decreases the 7 day compressive strength, and become uniform at later ages.

ASTM C 469-94

Figure 3 presents the elastic modulus of the portland cement concrete mixtures. The seven-day and 28 day modulus for the gravel mixture is lower than the modulus for the limestone and diabase mixtures. The surface area on the gravel aggregate is less than the surface area of the limestone and diabase aggregates. The area of contact between the gravel aggregate and the cement paste is less, resulting in a lower modulus. The 28 day modulus for the diabase mixture decreased, due to variability in the testing procedure.

Figure 4 presents the elastic modulus of portland cement plus mineral admixture concrete mixtures. The modulus for the limestone GGBFS, limestone MS, and limestone FA concrete mixtures are not significantly different. The elastic modulus for the limestone mixture with portland cement is similar to the values produced by the mixtures with mineral admixtures.

Variability of the Total Strain Batch Data

The variability of total strain between the batches is the variation of the process from day-to-day, or batch-to-batch, batching and mixing combined. The variability within the batch is the inherent variation of experimental error. The experimental error represents the variability of each strain reading for one test cycle.

Portland Cement Concrete Mixtures

The variability of total strain between the batches of portland cement concrete mixtures is presented in Figure 5. The limestone, diabase, and gravel total strain variability between batches is approximately 75%, 65%, and 45% respectively. The limestone mixture has the largest between batch variability. The limestone mixture was tested in the first testing cycle. The error due to learning the day-to-day methodology of the test is most likely the cause of the higher variability. The diabase and gravel mixtures were prepared in the second testing cycle and exhibit a lower variability between the batches.

The variability of total strain within the batches of portland cement concrete mixtures is presented in Figure 6. The limestone, diabase, and gravel total strain variability within batches is approximately 25%, 35%, and 55% respectively. The variability of the limestone mixture within the batch is the lowest, because the majority of the variability is between the batches due to learning error. The diabase mixture has a lower within batch variability than the between batch variability, which is to be expected. The gravel mixture variability within and between batches is similar, due to the inherent variability of the material, and the testing procedure.

Portland Cement plus Mineral Admixture Concrete Mixtures

The variability of total strain between the batches of portland cement concrete mixtures is presented in Figure 7. The limestone MS, limestone FA, and limestone GGBFS total strain variability between batches is approximately 90%, 70%, and 60% respectively. The variability between the batches for the limestone MS is particularly high. The limestone MS mixture was also tested in the first testing cycle. Error due to learning the day-to-day methodology in the test is the result of the higher variability. The limestone FA and limestone GGBFS mixtures have similar between batch variability. Both mixtures were tested in the third testing cycle.

The variability of total strain within the batches of portland cement concrete mixtures is presented in Figure 8. The limestone MS, limestone FA, and limestone GGBFS total strain variability within batches is approximately 10%, 30%, and 40% respectively. The variability of the limestone MS mixture within the batch is the lowest, because the majority of the variability is between the batches due to learning error. The limestone FA and limestone GGBFS mixtures have a lower within batch variability than the between batch variability, which is to be expected.

Creep Prediction Models

The models have various factors that contribute to an accurate prediction of creep and shrinkage. Each parameter limitation is further explained in the Model Limitations found in Appendix A. The most influential model parameter, in the case of the VDOT mixtures is the w/c ratio. The Bazant model requires a w/c ratio of 0.35 to 0.85, and the Sakata model requires a w/c ratio of 0.4 to 0.6. The concrete mixtures used have w/c ratio's lower than what is required by the model. This must be taken into consideration when looking for the best prediction model.

The model prediction results are presented as residuals, the difference between the experimental mean and the model value. If the model is under predicting the experimental mean, the residual will have a positive value. If the model is over predicting the experimental mean, the residual will have a negative value. All five models predict the total strain as the sum of the drying shrinkage strain and basic creep.

The limestone mixture has a larger variability than the other mixtures due to learning error. Therefore, the limestone mixture values will not have much weight when deciding which model is the best predictor.

Each model under predicts the drying shrinkage and over predicts the basic creep, resulting in a good prediction of the total strain, some models being more accurate than others. In the context of the models, basic creep is the difference between the total strain and the drying shrinkage. All of the models under predict the drying shrinkage. This calls to question the ability of the test method to predict the drying shrinkage. If the measured drying shrinkage is higher than predicted due to the testing procedure, then the basic creep should be less than predicted. This is the case for the ACI 209, CEB 90, Bazant, Gardner, and Sakata models.

There is no difference between the residuals when comparing mixtures with or without mineral admixtures. The variability of the results is less for the mixtures with mineral admixtures. The mineral admixture concrete mixtures were tested in the third testing cycle. The variability in the third testing cycle appears to be much less than that of the first testing cycle.

Table 9 presents the average chi-squared analysis data for the total strain, drying shrinkage strain, and basic creep strain at 28 and 97 days. The average chi-squared analysis excludes the limestone mixture values. The values are presented in rank order from best predictor to poor predictor.

At 28 days, the order of best prediction of total strain is the CEB 90, Sakata, ACI 209, Bazant, and Gardner models respectively. At 97 days, the order of best prediction of total strain is the Sakata, CEB 90, ACI 209, Bazant, and Gardner models respectively.

At 28 days, the order of best prediction of drying shrinkage strain is the Sakata, Gardner, Bazant, CEB 90, and ACI 209 models respectively. At 97 days, the order of best prediction of drying shrinkage strain is the Gardner, Bazant, CEB 90, Sakata, and ACI 209 models respectively.

At 28 days, the order of best prediction of basic creep strain is the Sakata, ACI 209, Bazant, CEB 90, and Gardner models respectively. At 97 days, the order of best prediction of basic creep strain is the Sakata, ACI 209, Bazant, CEB 90, and Gardner models respectively.

It can be concluded that the CEB 90 model is the best predictor for total strain up to 97 days for concrete mixtures with or with out mineral admixtures. The later ages of the prediction are less accurate. The CEB 90 model for example has a 28-day chi-squared value of 17300, and a 97-day chi-squared value of 39100. The same goes for the ACI 209, Bazant, and Gardner models. The Sakata model remains consistent over time.

Performance Specifications

The performance specifications are limited to all of the mixtures examined in this study. Due to the large error in the limestone mixture, the total strain values will be disregarded when determining the performance limits for the mixtures. Since there is no significant difference between the mixtures at a five percent significant level, the average of the total strain at 28 and 97 days for all the mixtures, except the limestone mixture, will be used.

The total strain for the VDOT portland cement concrete mixtures discussed in this study should be between 1180 ± 110 microstrain at 28 days, and 1620 ± 110 microstrain at 97 days, at a five percent significant level.

The CEB 90 model is the best model to apply to prestress losses. Values obtained apply for the losses due to creep and shrinkage.

The ultimate creep coefficient C_u is defined as the product of the basic creep per unit stress and the elastic modulus of the concrete. The stress losses due to creep is defined as the product of the ultimate creep coefficient, C_u, the ratio of the elastic modulus of the prestressing steel and the elastic modulus of concrete, and the stress of the prestressing steel at the level of the steel centroid. The CEB 90 model accounts for the prediction of the basic creep.

The losses due to shrinkage are expressed as the product of the elastic modulus of the prestressing steel and the shrinkage strain. The CEB 90 model predicts the shrinkage strain and there is a direct correlation between the model and prestress losses.

The prediction of creep and shrinkage combined, apply to the total affects of the losses of prestressing force in prestressed beams.

Figures 51 and 52 present the difference between the prediction models and the AASHTO LRFD design for basic creep strain.[3] Values were calculated by the following equation:

(AASHTO – Model) / Model x 100

The model value was calculated by taking the average prediction values of all the mixtures. The CEB 90, Bazant, and Gardner models ranged from –50% to approximately 150% difference over time. The ACI 209 and Sakata models ranged from –50% to approximately 250% difference over time. A positive value represents the model under predicting the AASHTO design. The percent differences increase as time progresses.

REFERENCES

1. ASTM C 39-96, Standard Specification of Concrete and Aggregates. Section 4, v. 04.02.

2. ASTM C 469-94, Standard Specification of Concrete and Aggregates. Section 4, v. 04.02.

3. Barker, Richard M. and Puckett, Jay A., *Design of Highway Bridges: Based on AASHTO LRFD Bridge Design Specifications.* New York: John Wiley & Sons, Inc., pp. 410-413.

CHAPTER 6. CONCLUSIONS AND RECOMMENDATIONS

Conclusions

The CEB 90 Model predicts the creep and shrinkage strain of prestressed concrete mixtures with the best precision and accuracy for the VDOT approved mixtures examined in this study.

The prediction of basic creep should be applied to the calculation of prestress losses due to creep, and the prediction of shrinkage strain should be applied to the calculation of prestress losses due to shrinkage.

There is no significant difference between mixtures with or without mineral admixtures.

The total strain for the VDOT portland cement concrete mixtures discussed in this study were found to be less than 1200 ± 110 microstrain at 28 days, and 1600 ± 110 microstrain at 97 days, at a five percent significant level.

Recommendations

- When running at test cycle, no more than two batches of the same mixture should be used.
- Further research should be conducted on the Bazant and Sakata prediction models to allow for limitations of w/c ratio to be lower than the ranges specified by the models.
- Future research may be conducted on the effect of shrinkage reducing admixtures on the compressive creep of concrete mixtures.

FIGURES

FIGURE 1. COMPRESSION STRENGTH OF PORTLAND CEMENT CONCRETE MIXTURES

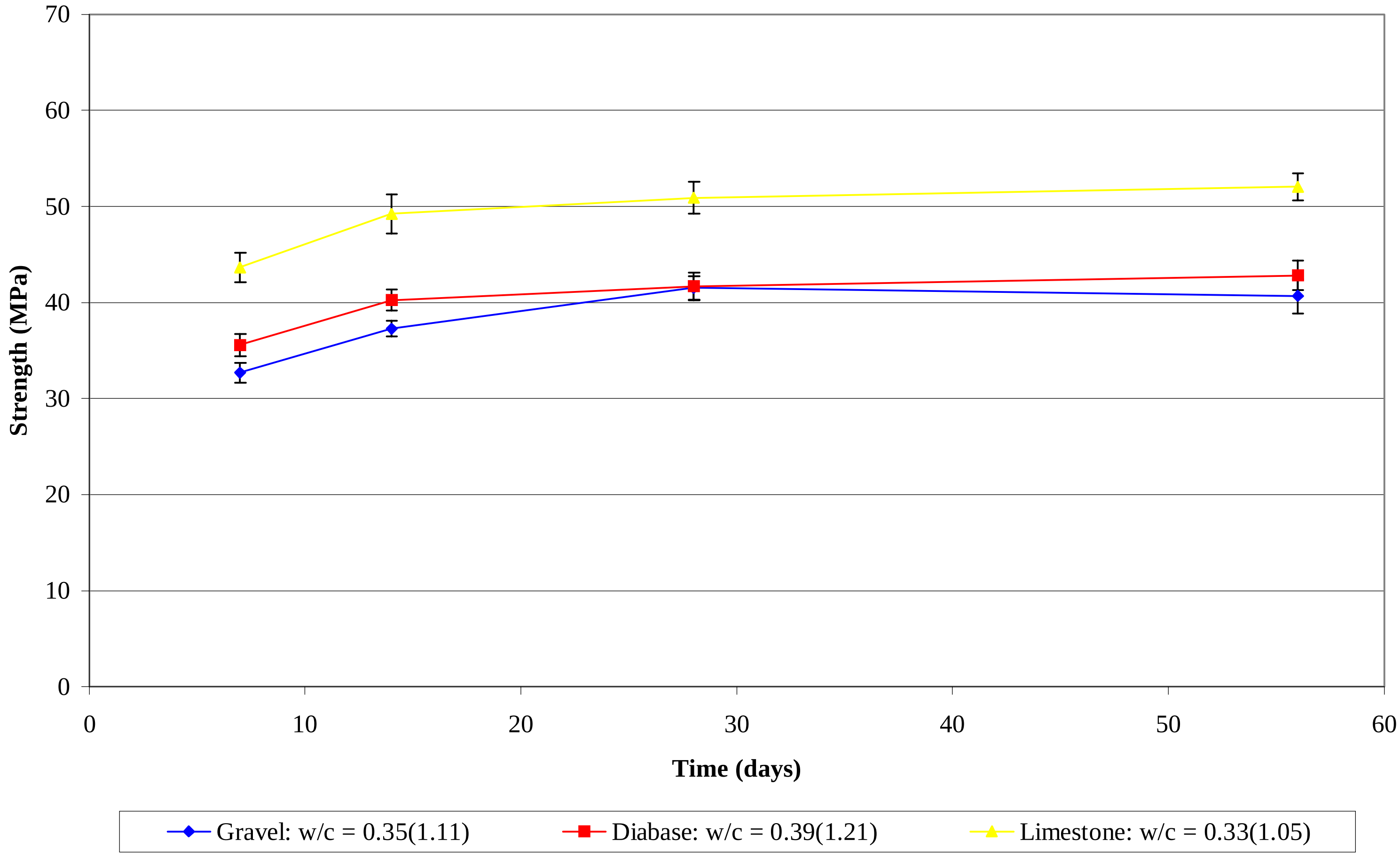

Each point is an average of six measurements.

w/c ratio is expressed by: w/c by weight (w/c ratio by volume)

FIGURE 2. COMPRESSION STRENGTH OF PORTLAND CEMENT PLUS MINERAL ADMIXTURE CONCRETE MIXTURES

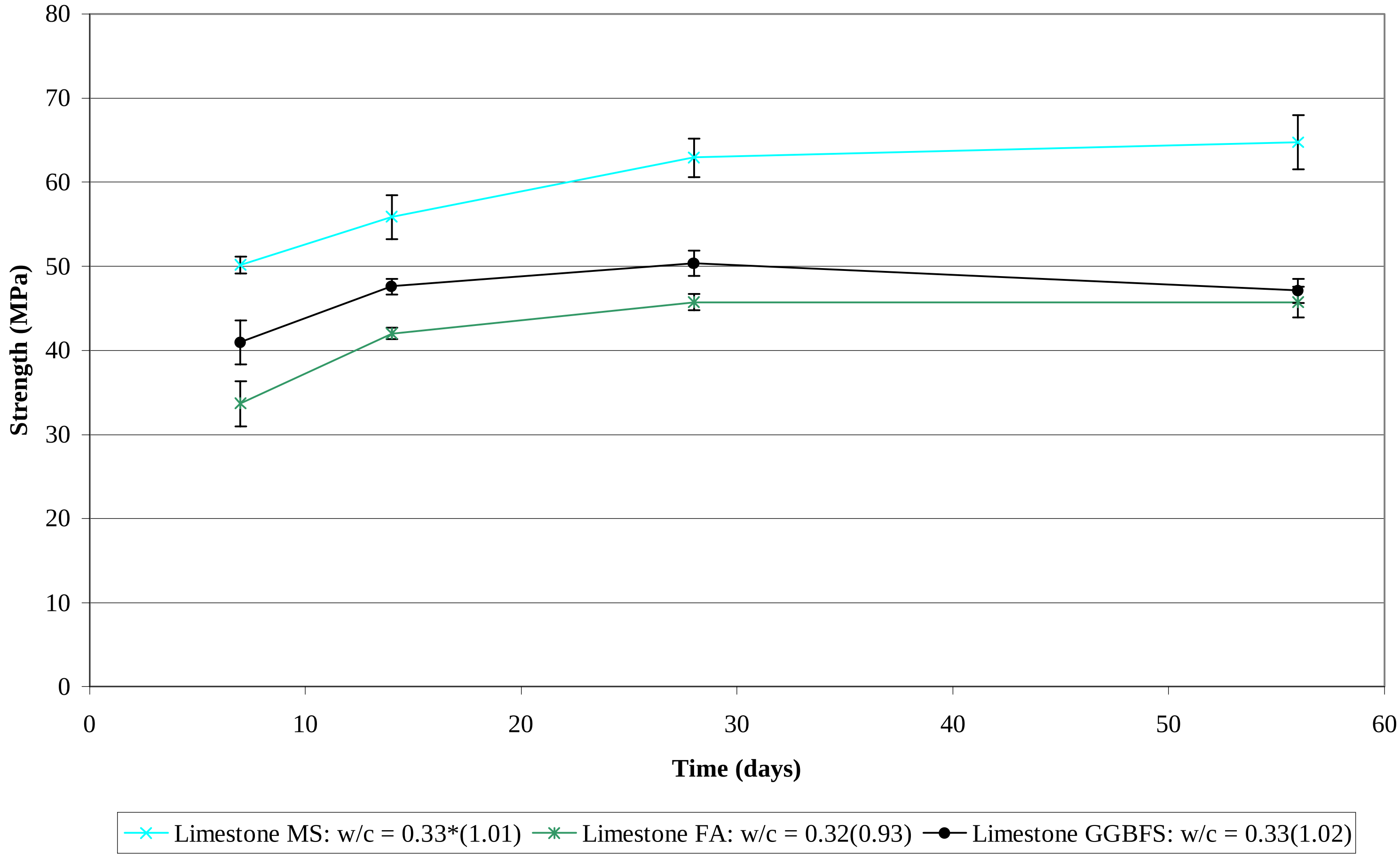

Each point is an average of six measurements.

w/c ratio is expressed by: w/c by weight (w/c ratio by volume)

FIGURE 3. ELASTIC MODULUS OF PORTLAND CEMENT CONCRETE MIXTURES

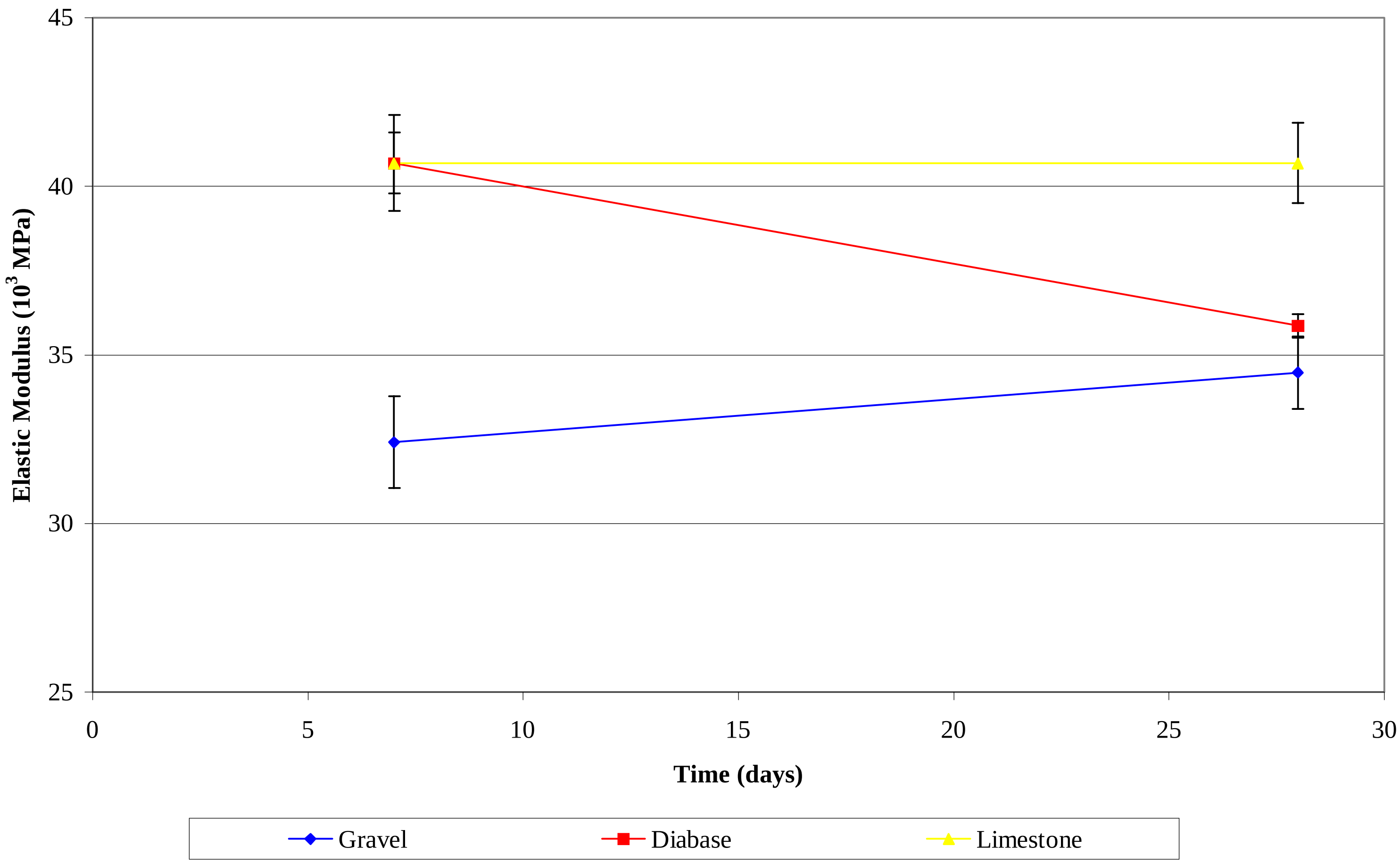

Drying shrinkage specimens were used for the modulus test.

FIGURE 4. ELASTIC MODULUS OF PORTLAND CEMENT PLUS MINERAL ADMIXTURE CONCRETE MIXTURES

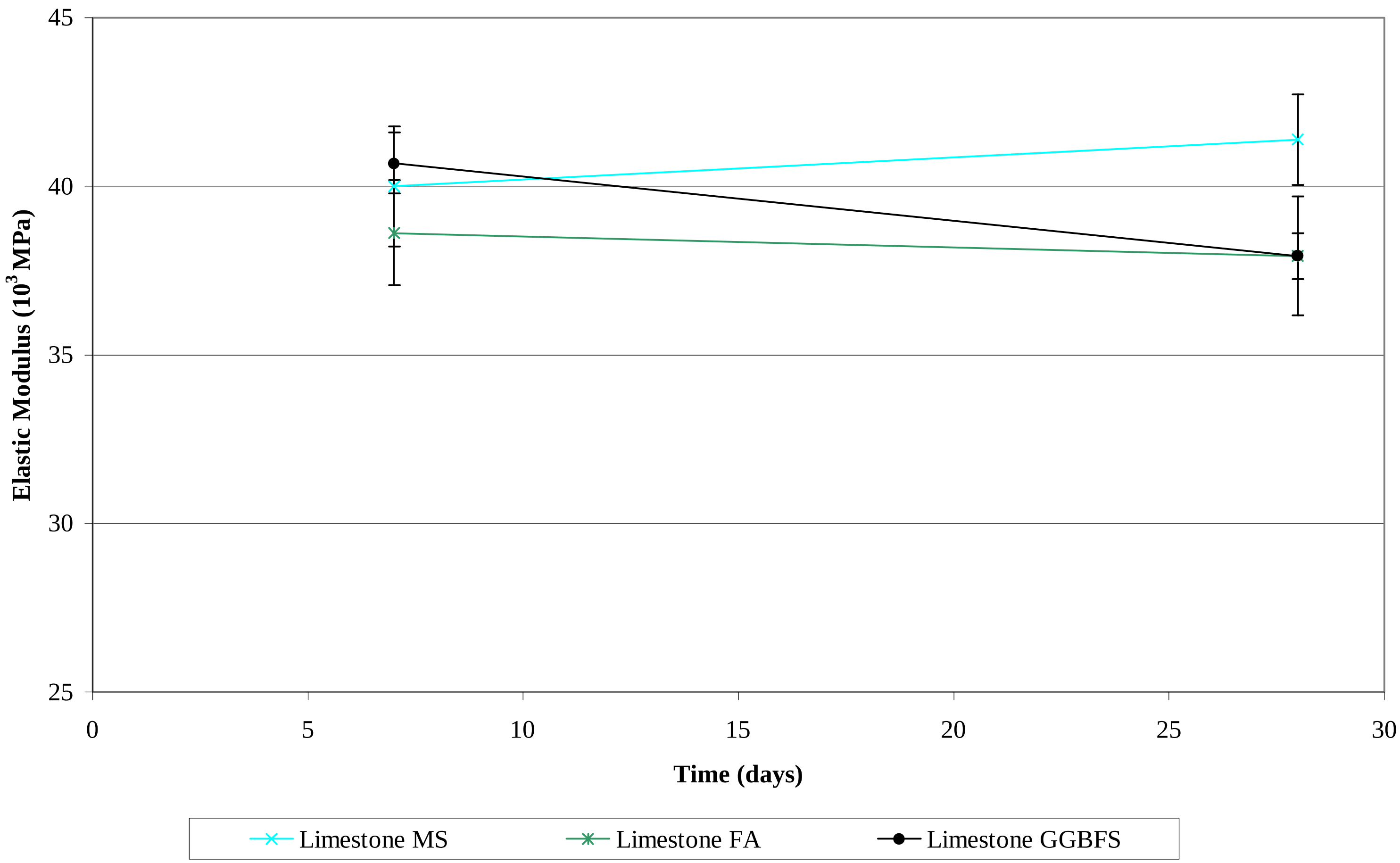

Drying shrinkage specimens were used for the modulus test.

FIGURE 5. PERCENTAGE OF VARIABILITY OF TOTAL STRAIN BETWEEN THE BATCHES OF PORTLAND CEMENT CONCRETE MIXTURES

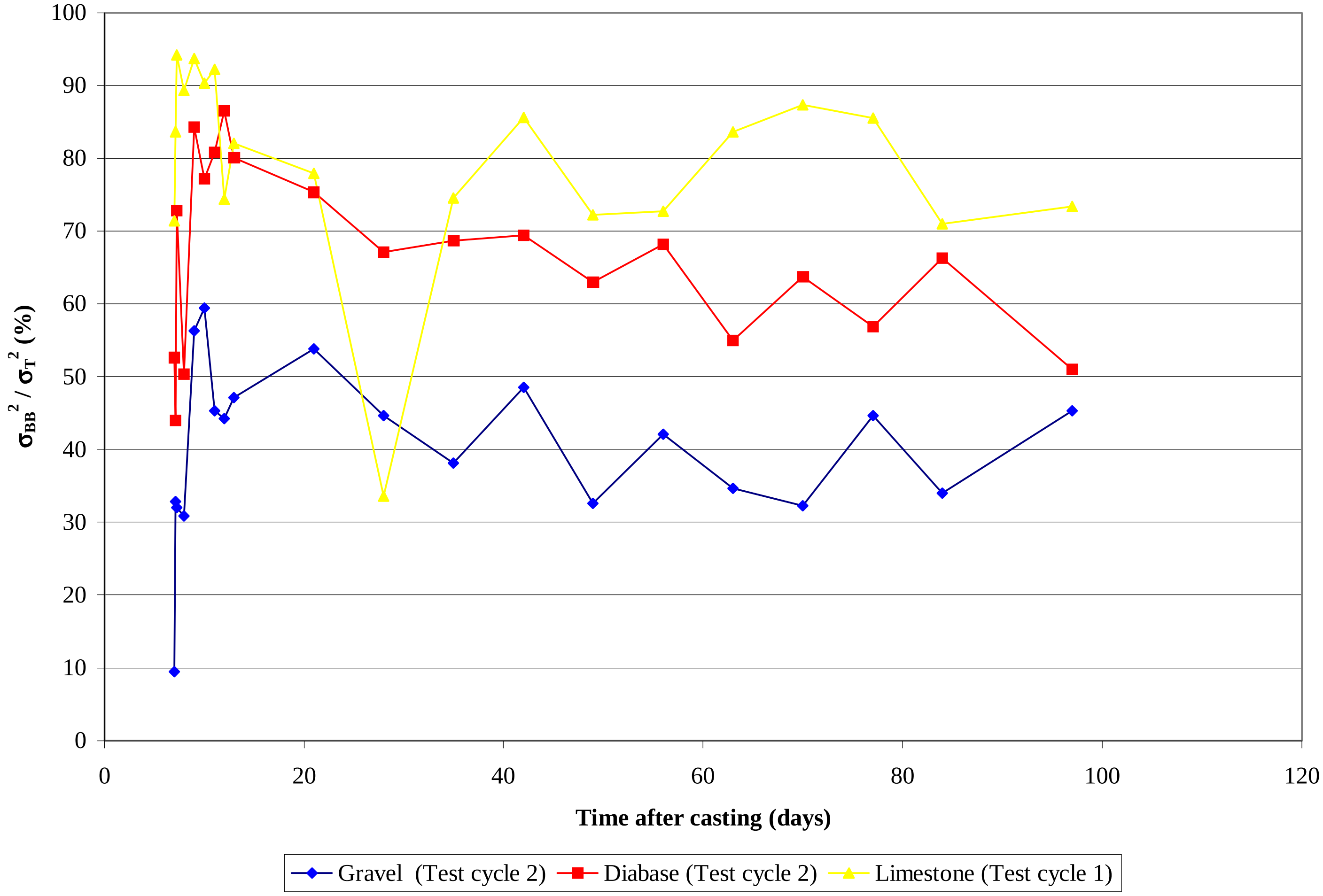

Variability between batches is the variation of the process from day to day, or batch-to-batch, batching and mixing combined.

FIGURE 6. PERCENTAGE OF VARIABILITY OF TOTAL STRAIN WINTHIN THE BATCHES OF PORTLAND CEMENT CONCRETE MIXTURES

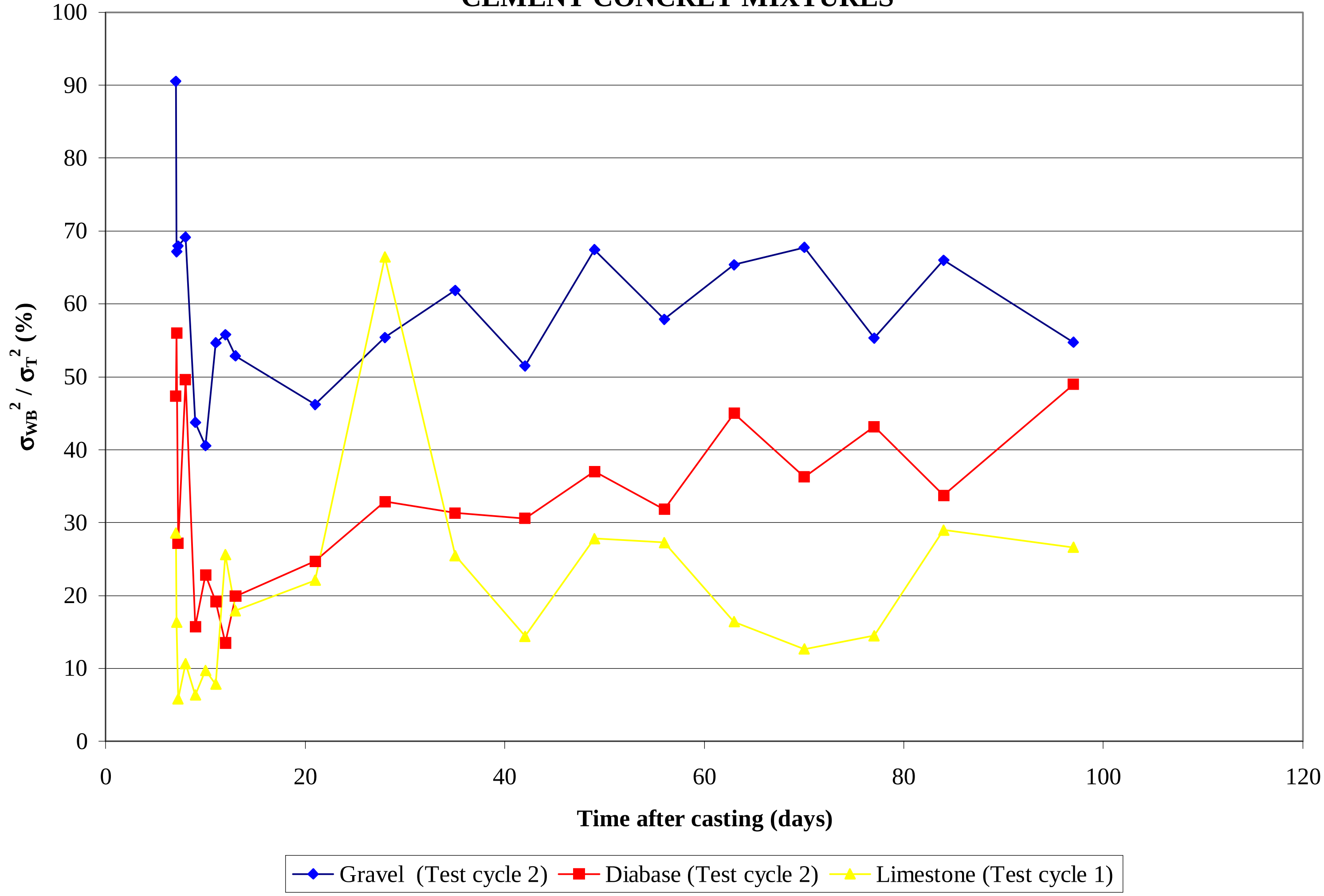

Variability within batches is the inherent variation of experimental / testing error.

FIGURE 7. PERCENTAGE OF VARIABILITY OF TOTAL STRAIN BETWEEN THE BATCHES OF PORTLAND CEMENT PLUS MINERAL ADMIXTURE CONCRETE MIXTURES

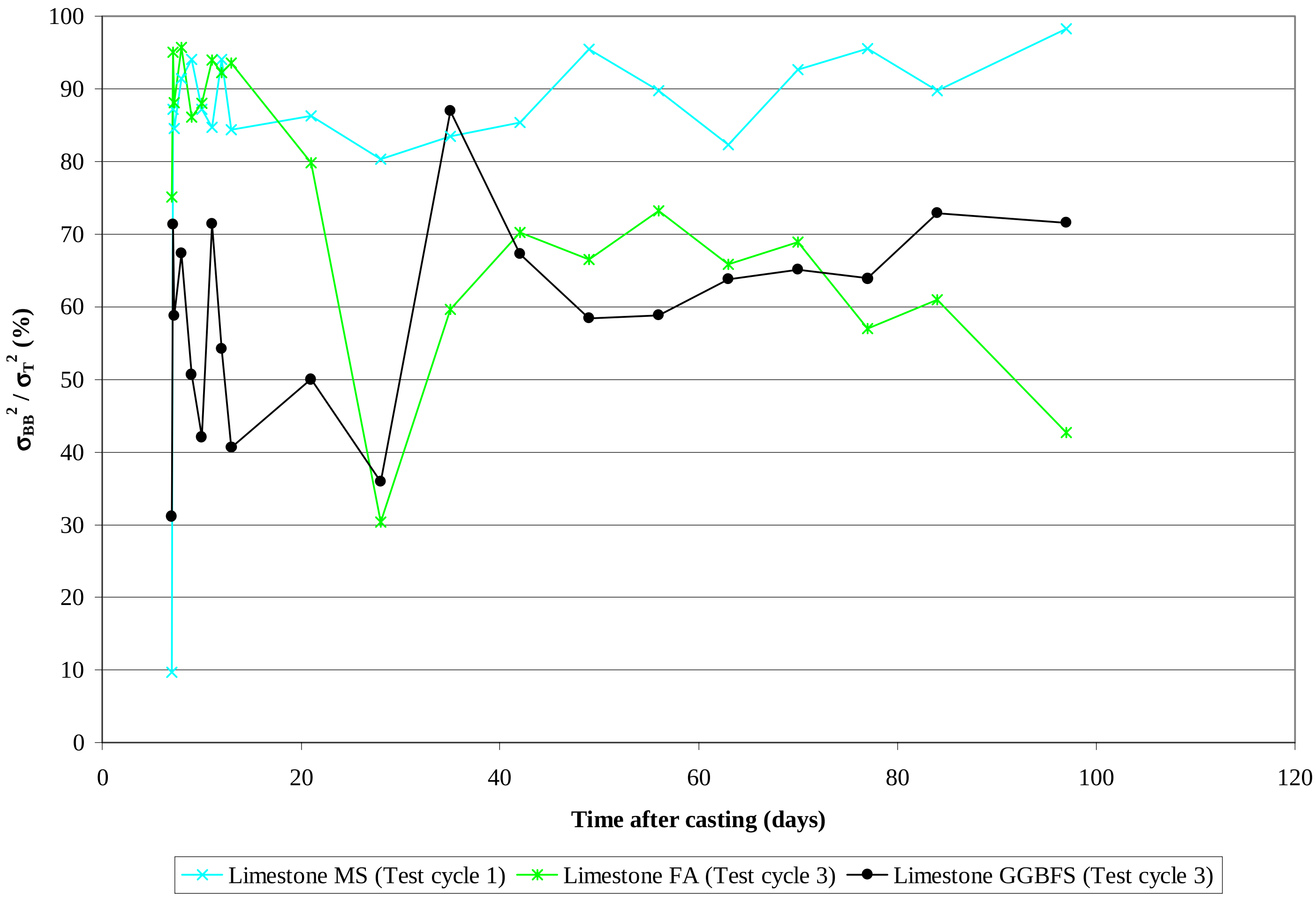

Variability between batches is the variation of the process from day to day, or batch-to-batch, batching and mixing combined.

FIGURE 8. PERCENTAGE OF VARIABILITY OF TOTAL STRAIN WINTHIN THE BATCHES OF PORTLAND CEMENT PLUS MINERAL ADMIXTURE CONCRETE MIXTURES

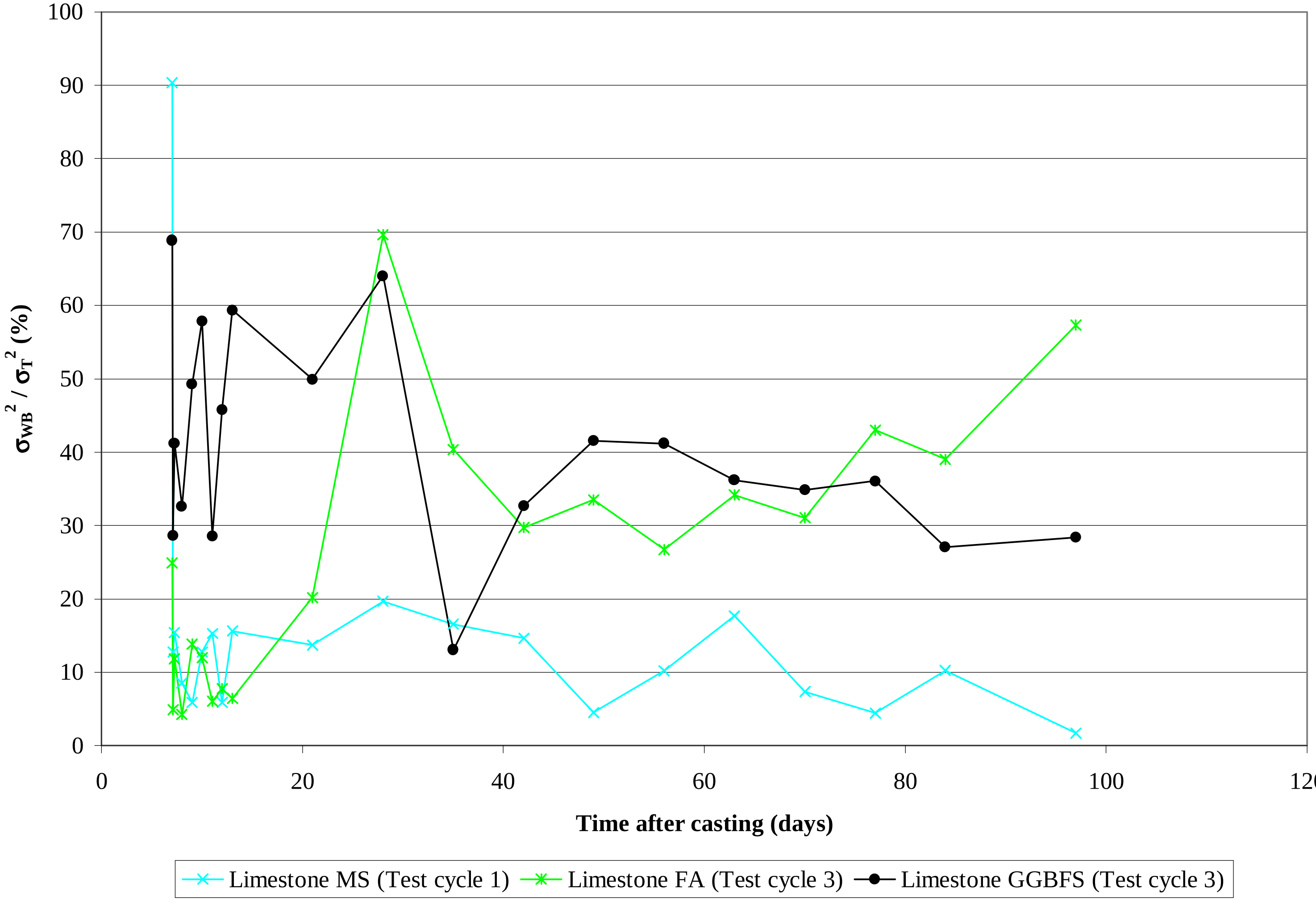

Variability within batches is the inherent variation of experimental / testing error.

FIGURE 9. RESIDUALS OF TOTAL STRAIN OF PORTLAND CEMENT CONCRETE AND ACI 209 MODEL

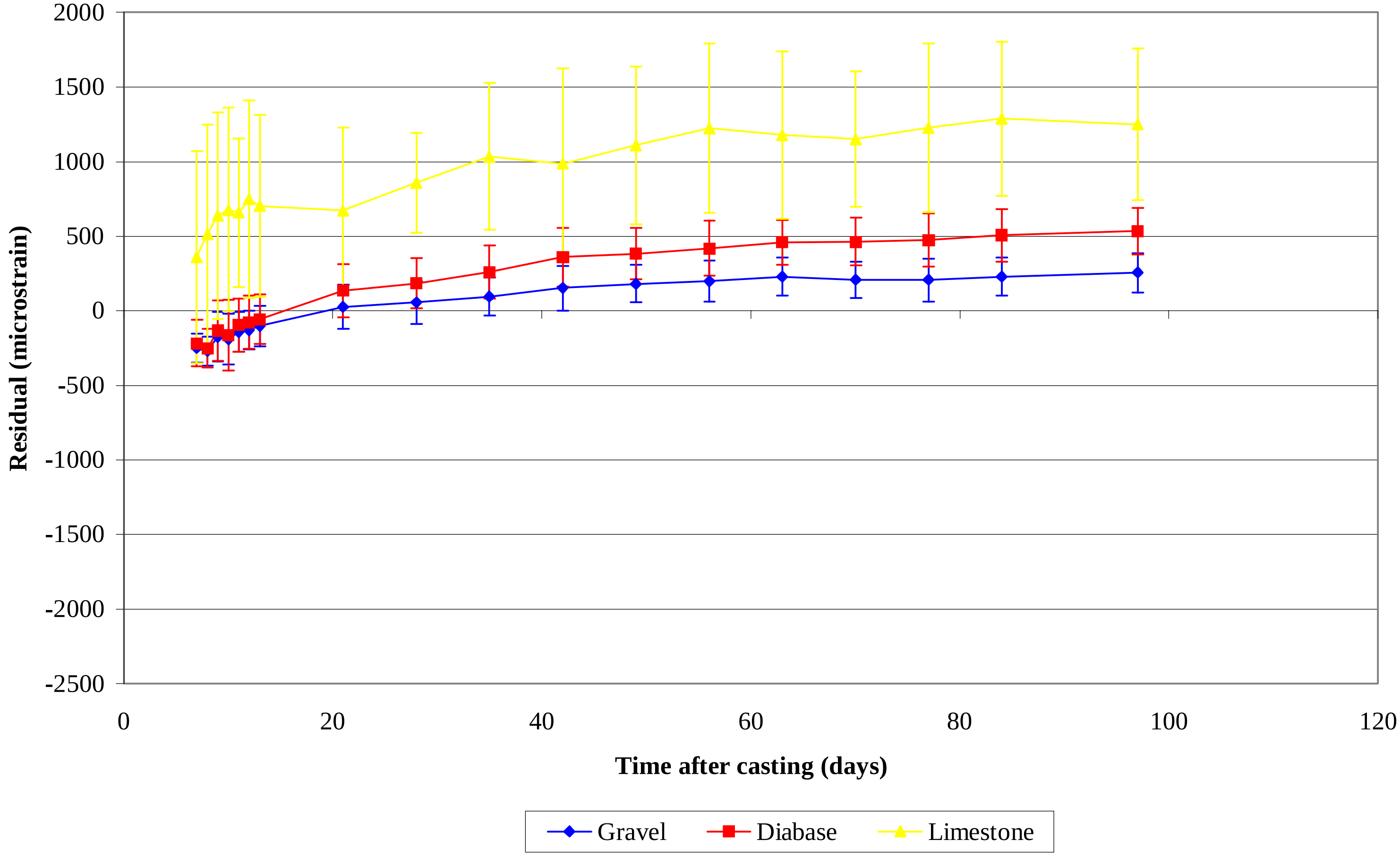

Each data point for a specified time is an average of three measurements. The error bars represent the 95 % confidence interval.

FIGURE 10. RESIDUALS OF DRYING SHRINKAGE OF PORTLAND CEMENT CONCRETE AND ACI 209 MODEL

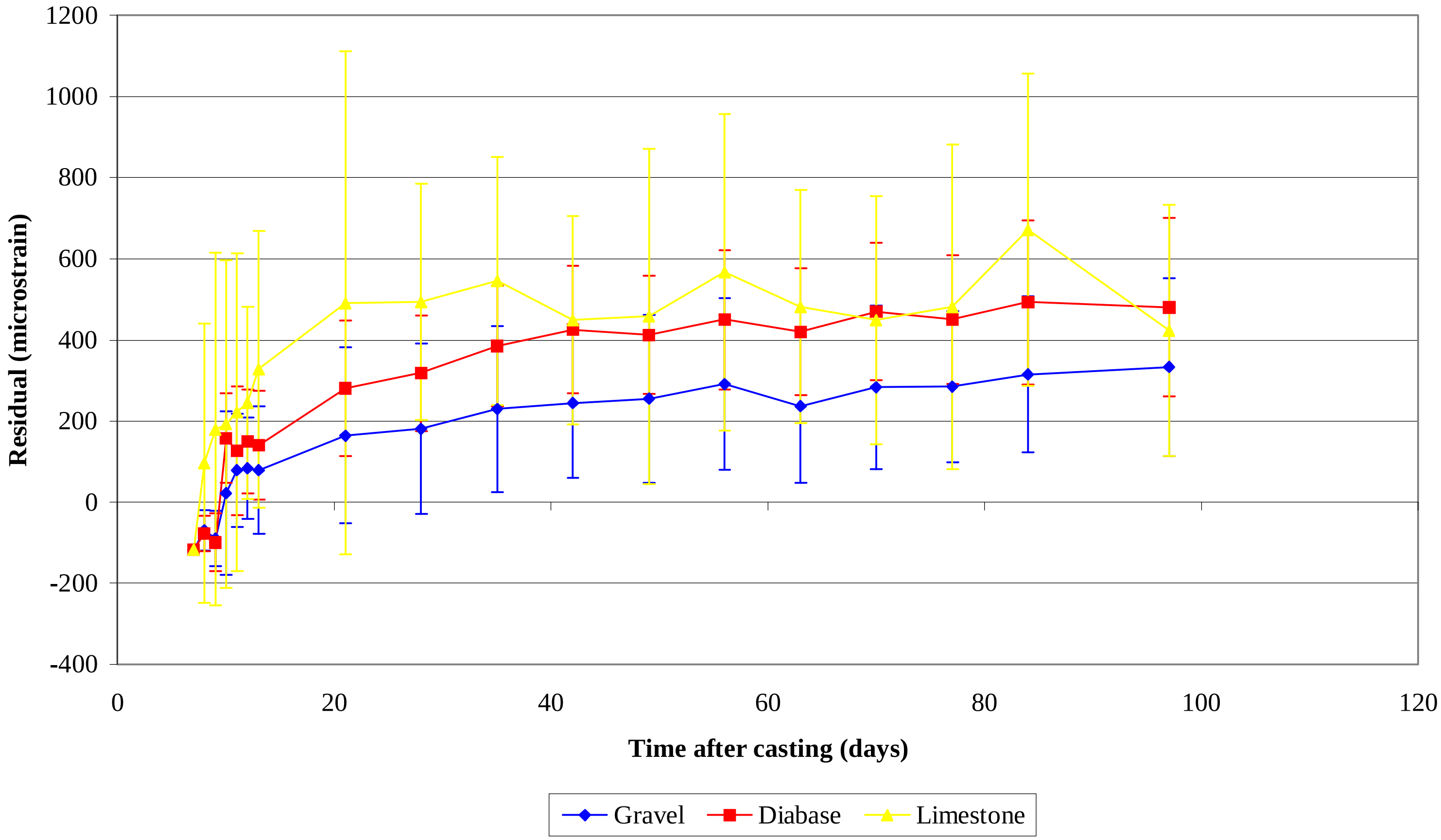

Each data point for a specified time is an average of three measurements. The error bars represent the 95 % confidence interval.

FIGURE 11. RESIDUALS OF BASIC CREEP OF PORTLAND CEMENT CONCRETE AND ACI 209 MODEL

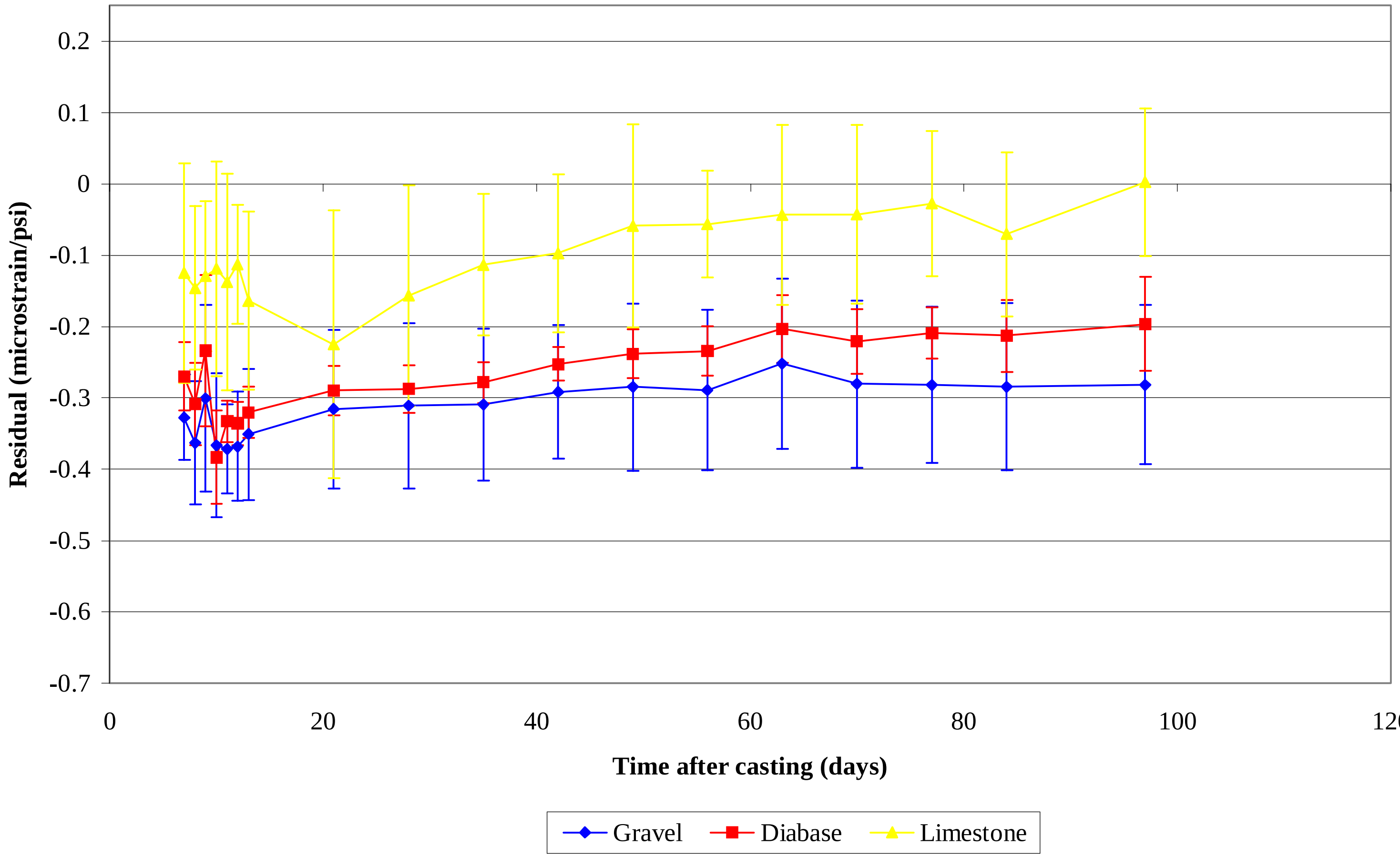

Each data point for a specified time is an average of three measurements. The error bars represent the 95 % confidence interval. 1 psi = 1/145 MPa

FIGURE 12. RESIDUALS OF TOTAL STRAIN OF PORTLAND CEMENT PLUS MINERAL ADMIXTURE CONCRETE AND ACI 209 MODEL

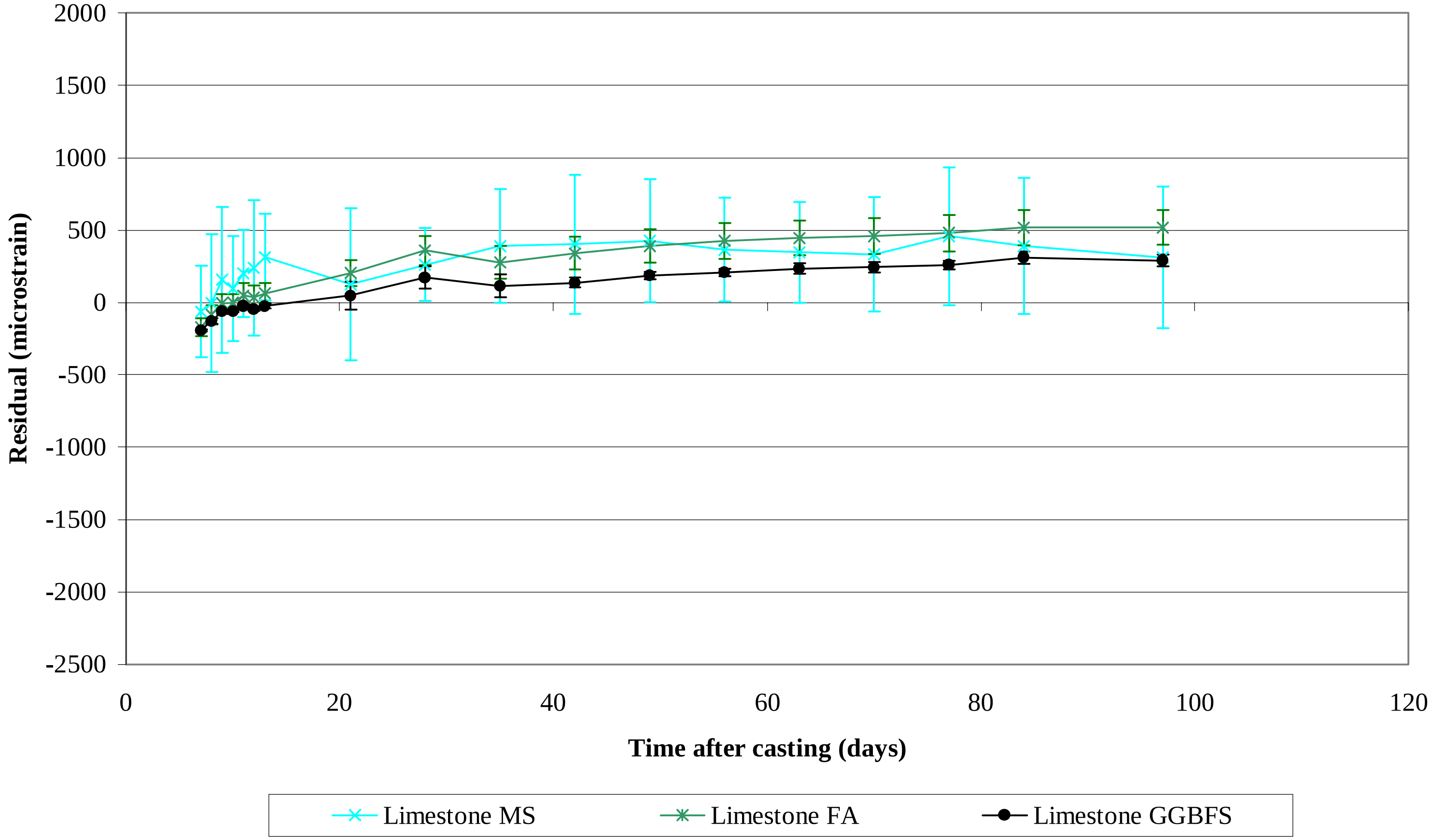

Each data point for a specified time is an average of three measurements. The error bars represent the 95 % confidence interval.

FIGURE 13. RESIDUALS OF DRYING SHRINKAGE OF PORTLAND CEMENT PLUS MINERAL ADMIXTURE CONCRETE AND ACI 209 MODEL

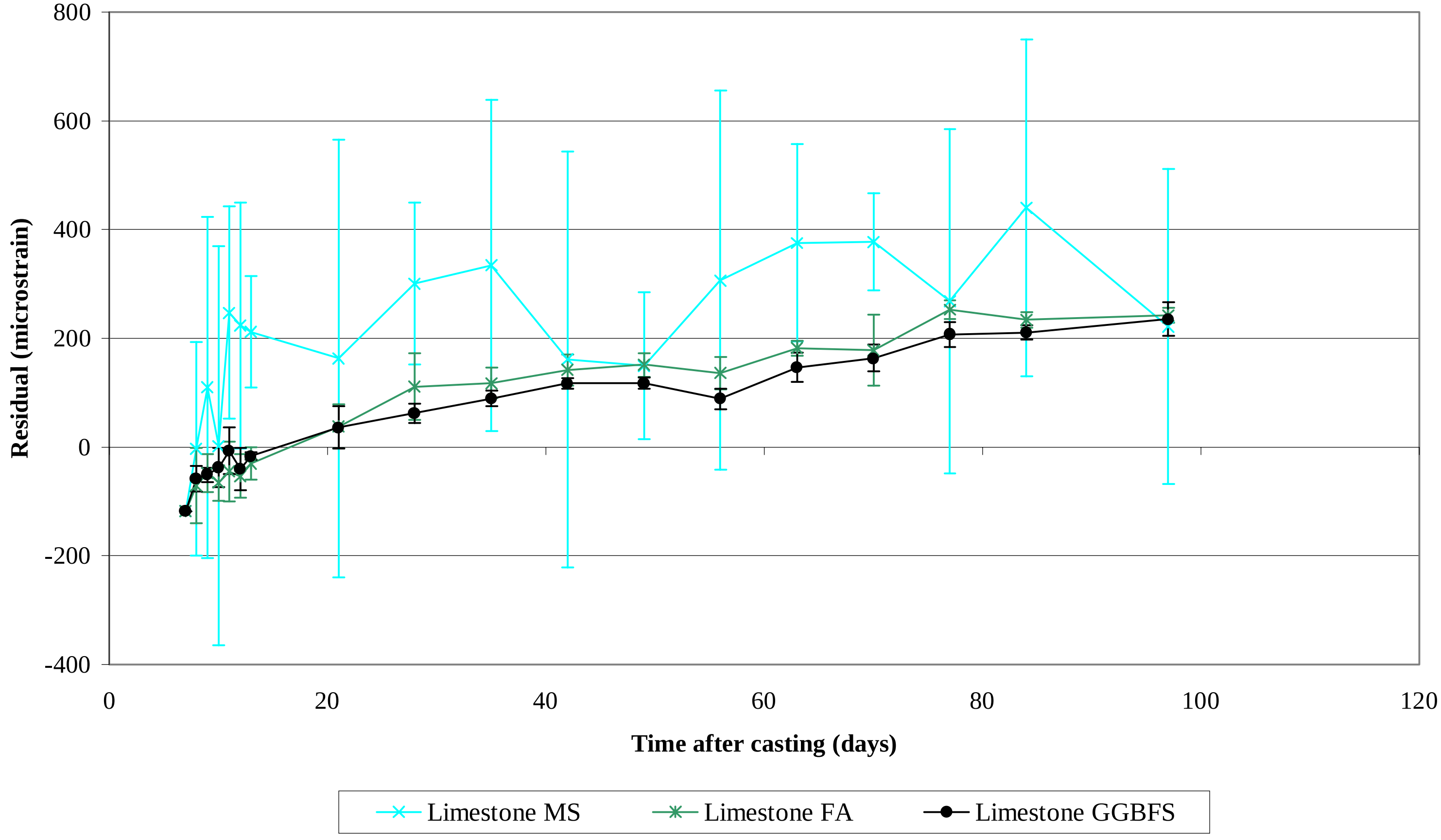

Each data point for a specified time is an average of three measurements. The error bars represent the 95 % confidence interval.

FIGURE 14. RESIDUALS OF BASIC CREEP OF PORTLAND CEMENT PLUS MINERAL ADMIXTURE CONCRETE AND ACI 209 MODEL

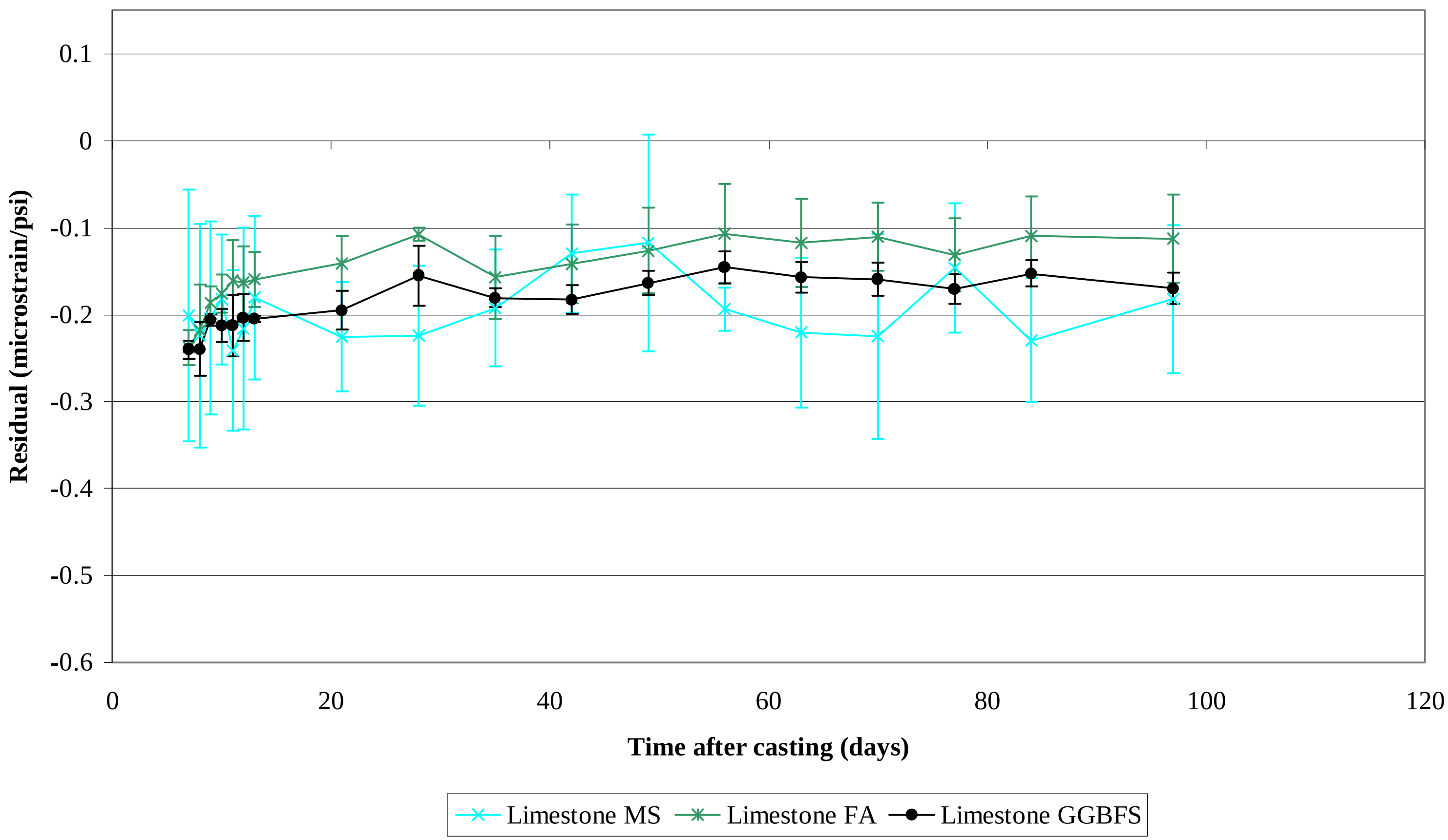

Each data point for a specified time is an average of three measurements. The error bars represent the 95 % confidence interval. 1 psi = 1/145 MPa

FIGURE 15. RESIDUALS OF TOTAL STRAIN OF PORTLAND CEMENT CONCRETE AND CEB 90 MODEL

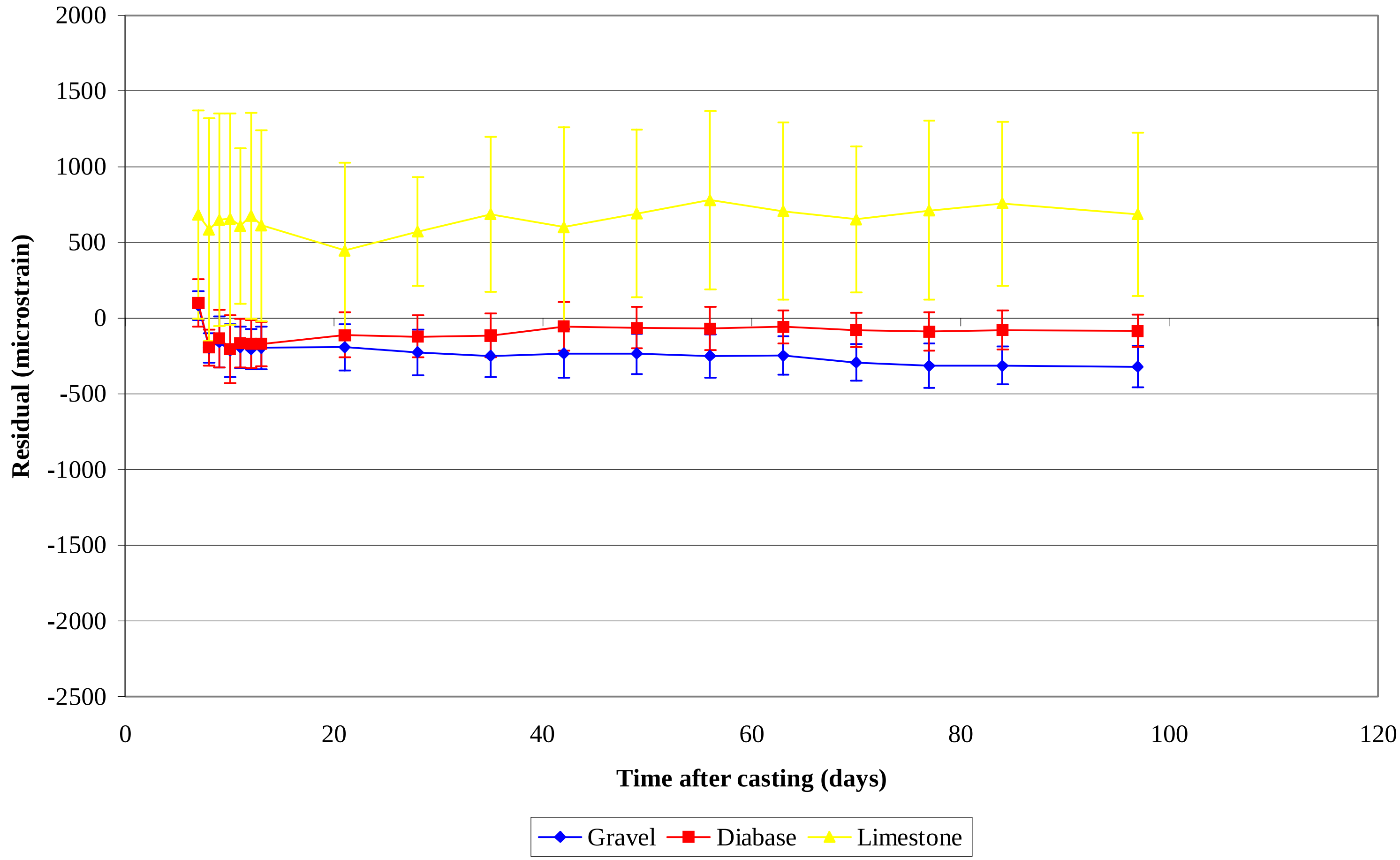

Each data point for a specified time is an average of three measurements. The error bars represent the 95 % confidence interval.

FIGURE 16. RESIDUALS OF DRYING SHRINKAGE OF PORTLAND CEMENT CONCRETE AND CEB 90 MODEL

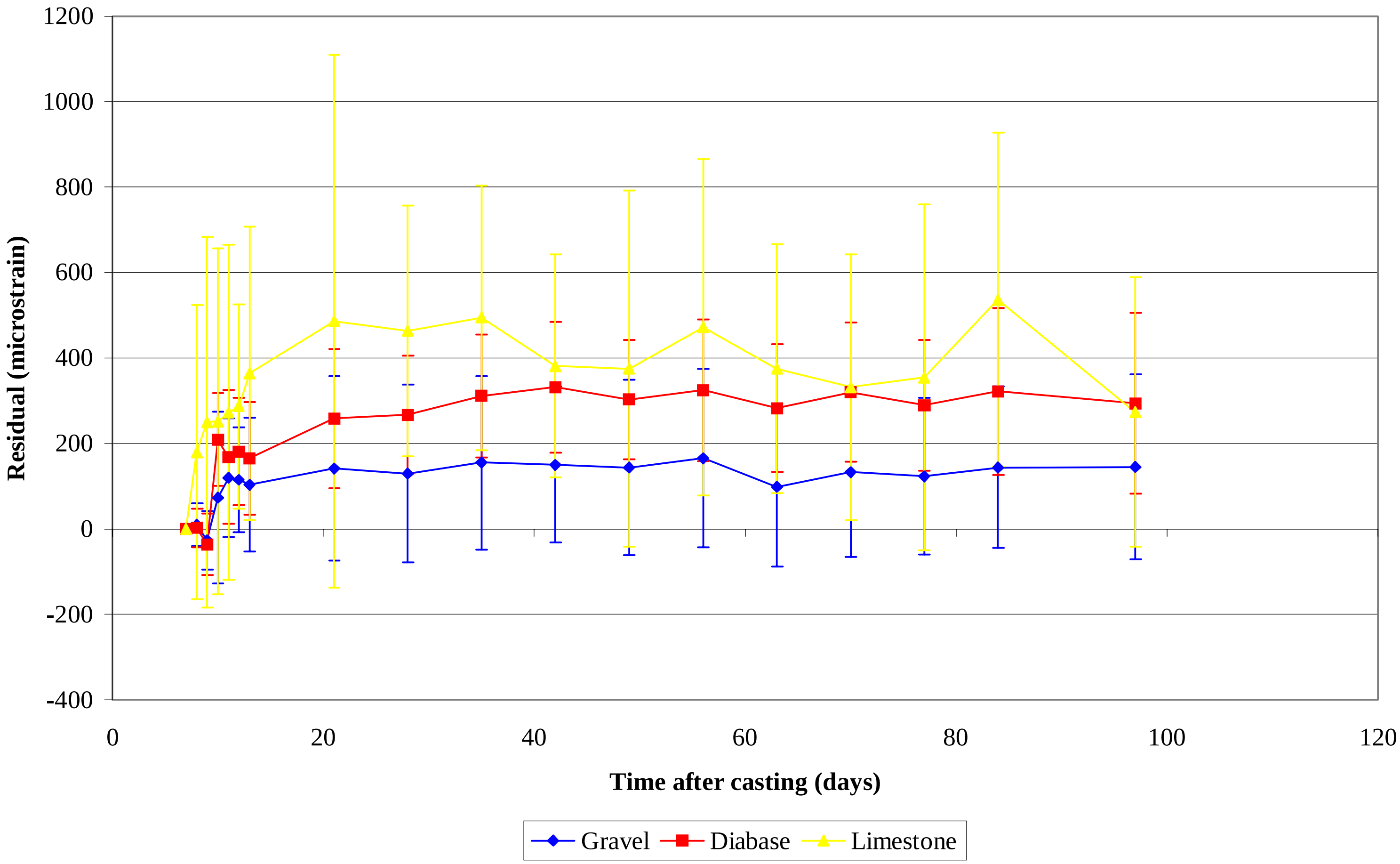

Each data point for a specified time is an average of three measurements. The error bars represent the 95 % confidence interval.

FIGURE 17. RESIDUALS OF BASIC CREEP OF PORTLAND CEMENT CONCRETE AND CEB 90 MODEL

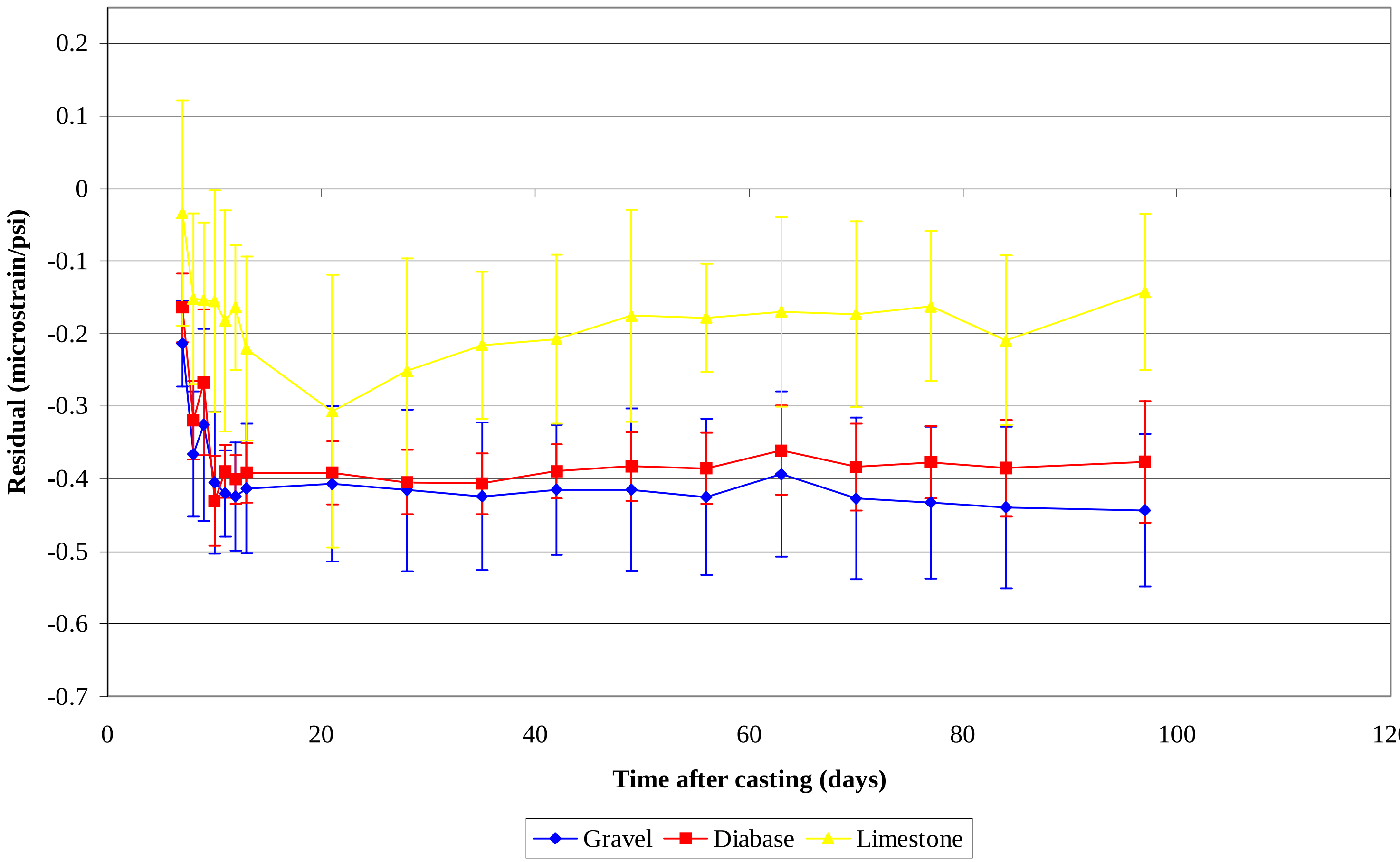

Each data point for a specified time is an average of three measurements. The error bars represent the 95 % confidence interval. 1 psi = 1/145 MPa

FIGURE 18. RESIDUALS OF TOTAL STRAIN OF PORTLAND CEMENT PLUS MINERAL ADMIXTURE CONCRETE AND CEB 90 MODEL

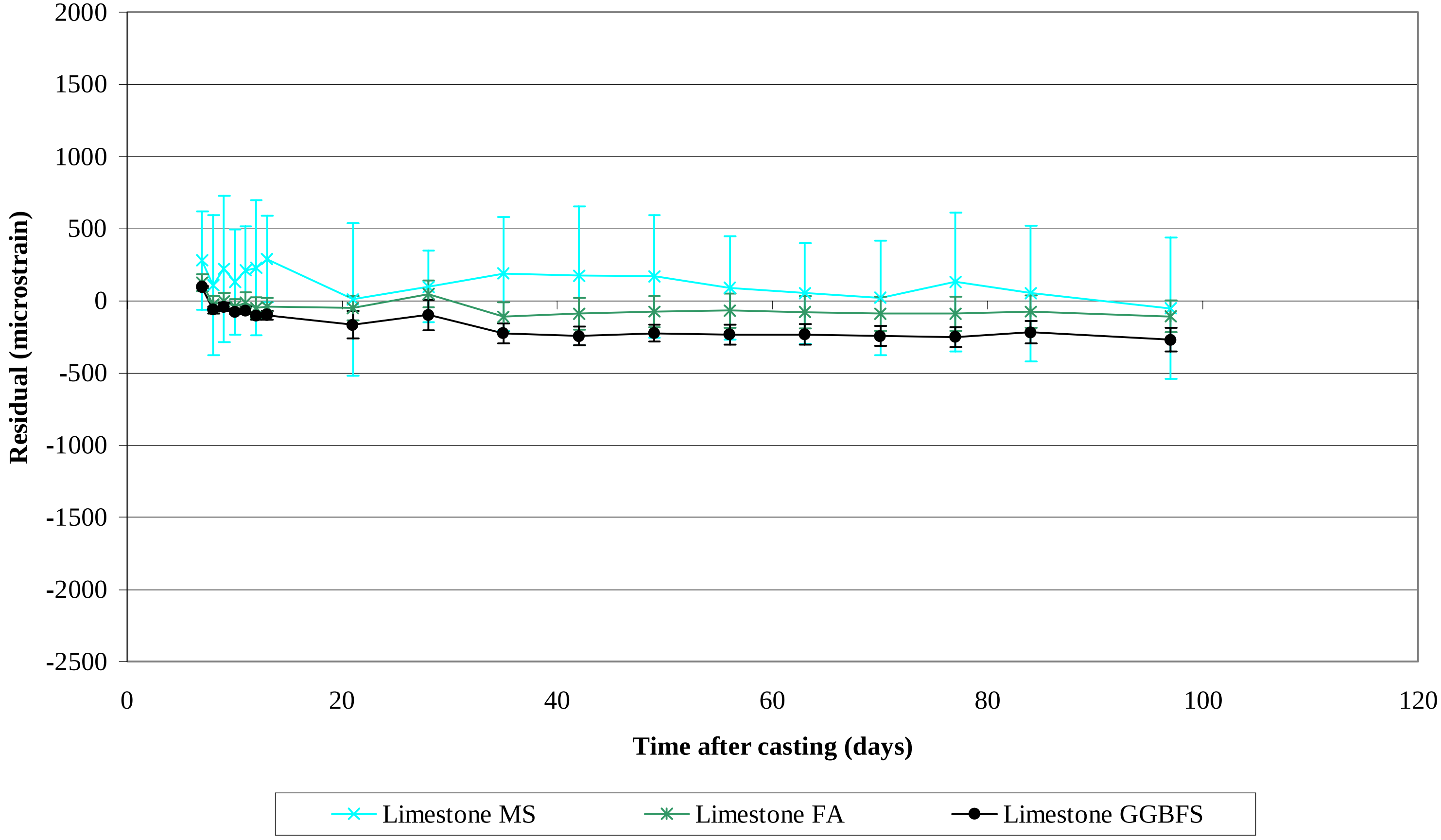

Each data point for a specified time is an average of three measurements. The error bars represent the 95 % confidence interval.

FIGURE 19. RESIDUALS OF DRYING SHRINKAGE OF PORTLAND CEMENT PLUS MINERAL ADMIXTURE CONCRETE AND CEB 90 MODEL

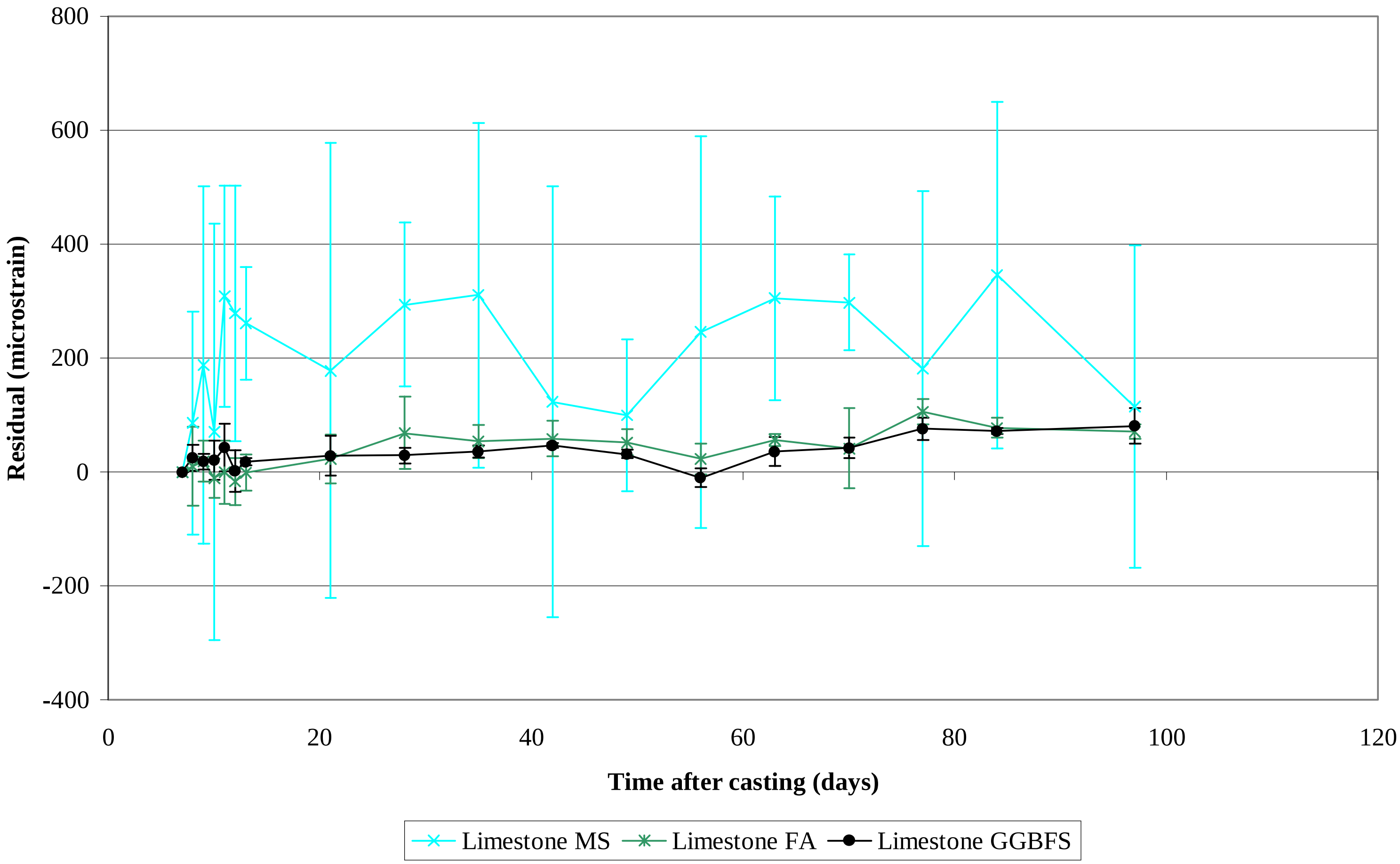

Each data point for a specified time is an average of three measurements. The error bars represent the 95 % confidence interval.

FIGURE 20. RESIDUALS OF BASIC CREEP OF PORTLAND CEMENT PLUS MINERAL ADMIXTURE CONCRETE AND CEB 90 MODEL

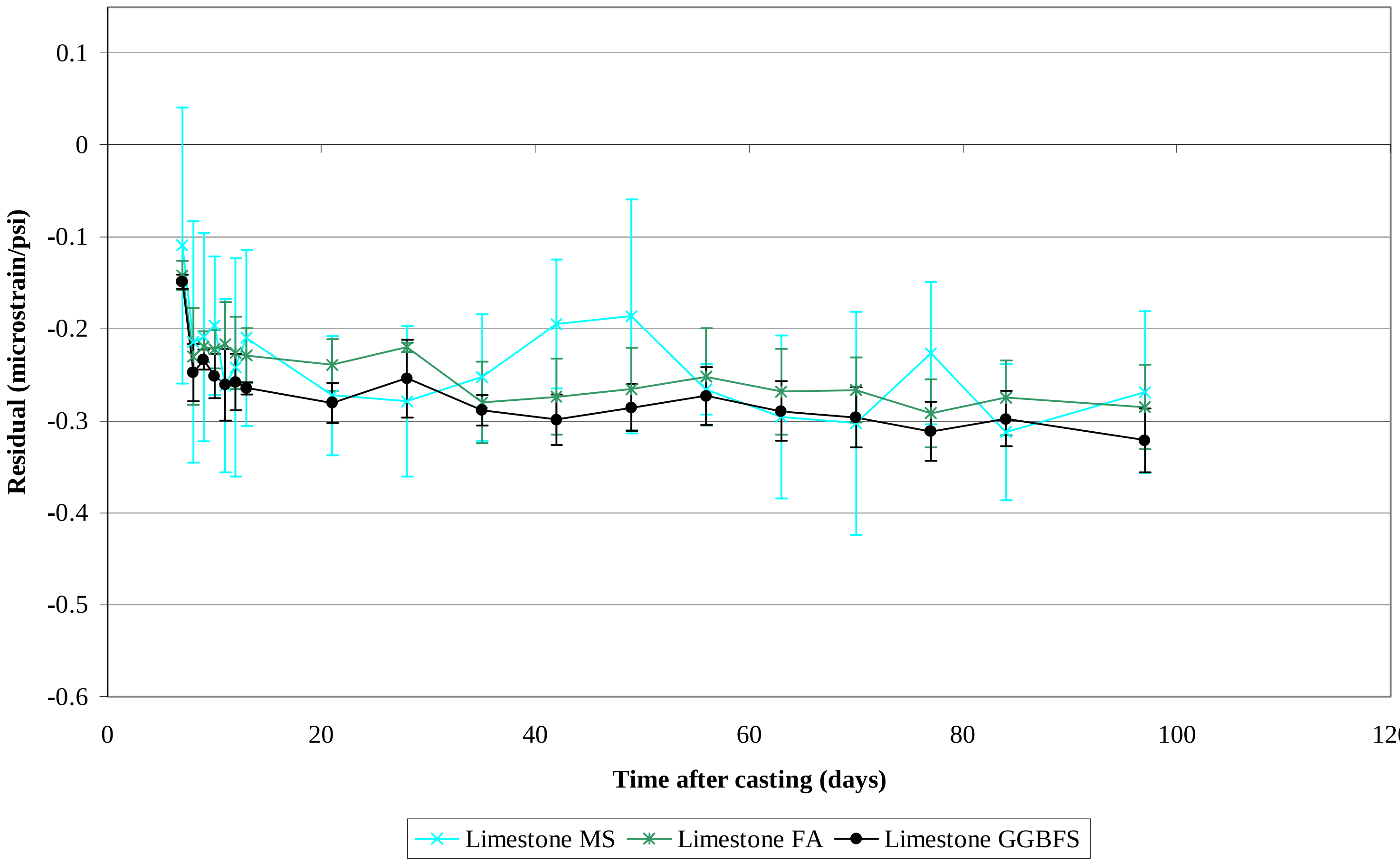

Each data point for a specified time is an average of three measurements. The error bars represent the 95 % confidence interval. 1 psi = 1/145 MPa

FIGURE 21. RESIDUALS OF TOTAL STRAIN OF PORTLAND CEMENT CONCRETE AND BAZANT MODEL

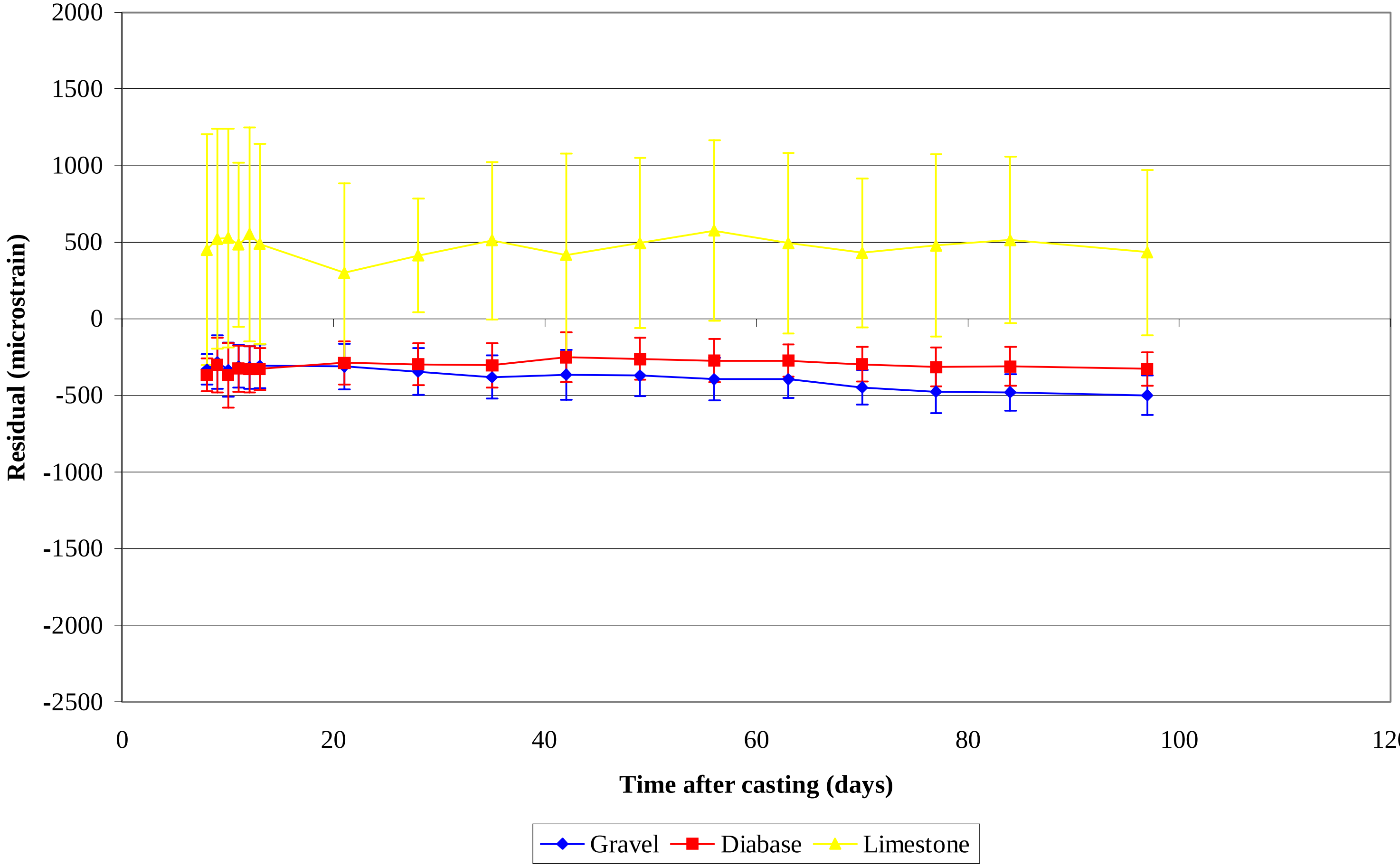

Each data point for a specified time is an average of three measurements. The error bars represent the 95 % confidence interval.

FIGURE 22. RESIDUALS OF DRYING SHRINKAGE OF PORTLAND CEMENT CONCRETE AND BAZANT MODEL

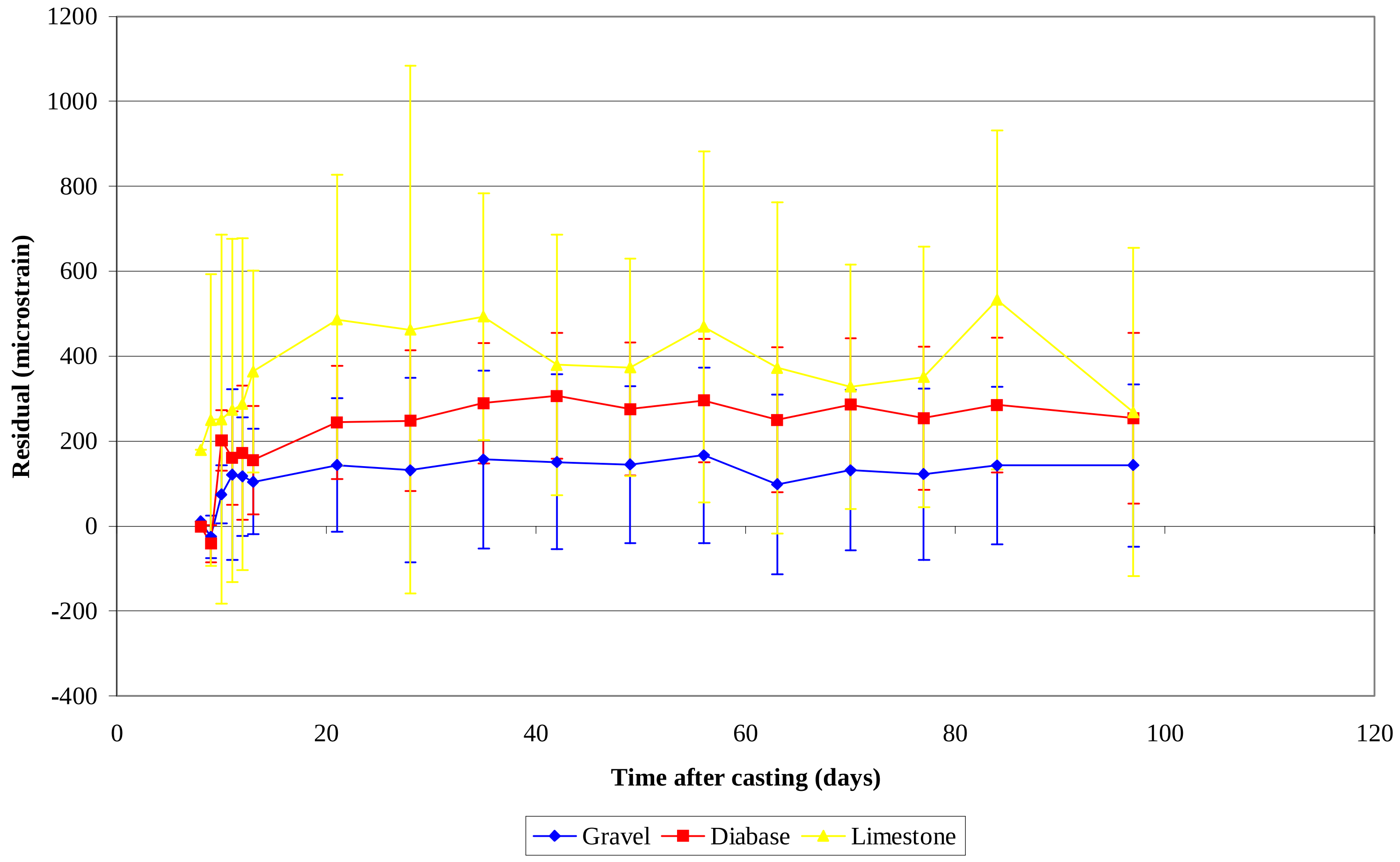

Each data point for a specified time is an average of three measurements. The error bars represent the 95 % confidence interval.

FIGURE 23. RESIDUALS OF BASIC CREEP OF PORTLAND CEMENT CONCRETE AND BAZANT MODEL

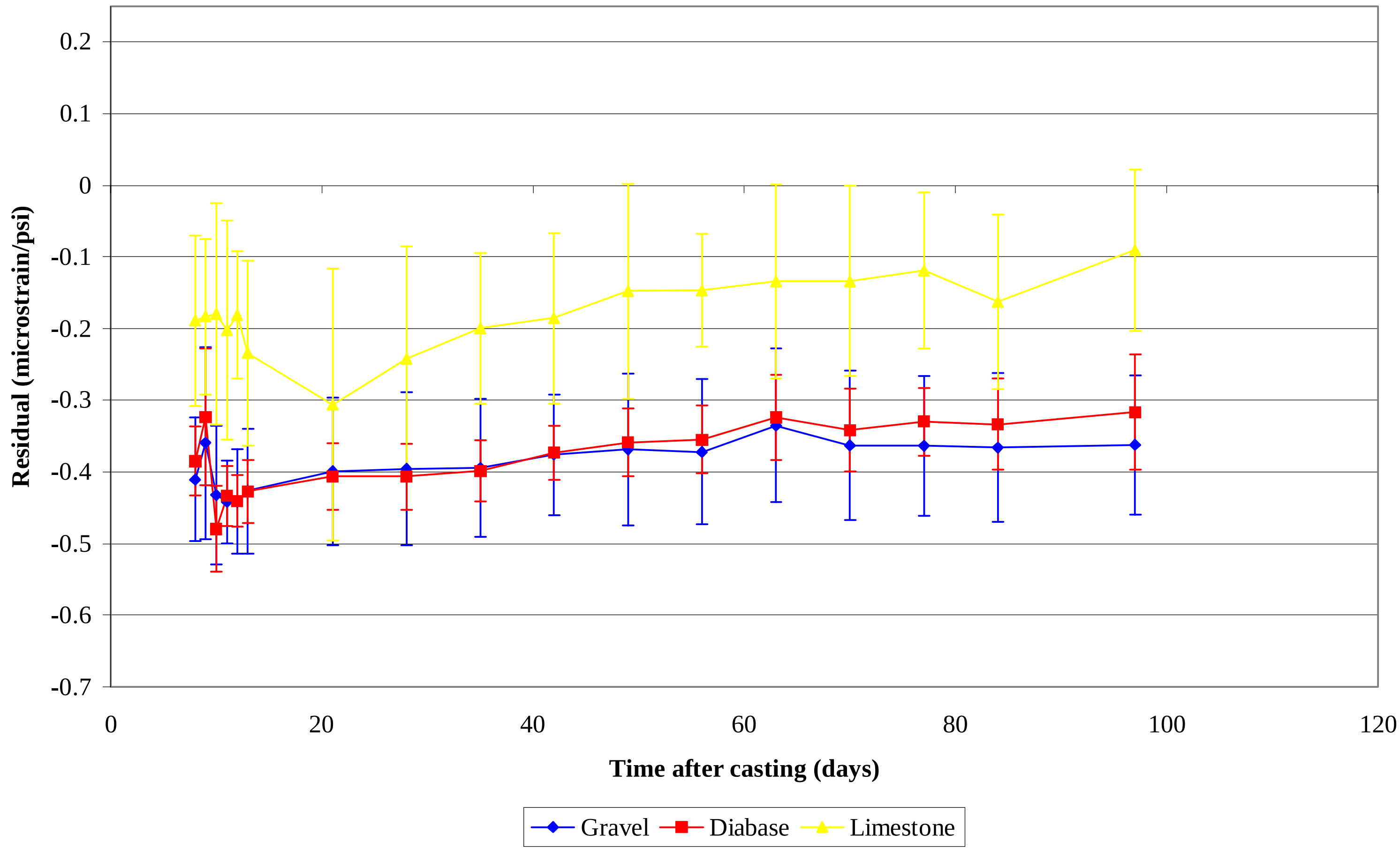

Each data point for a specified time is an average of three measurements. The error bars represent the 95 % confidence interval. 1 psi = 1/145 MPa

FIGURE 24. RESIDUALS OF TOTAL STRAIN OF PORTLAND CEMENT PLUS MINERAL ADMIXTURE CONCRETE AND BAZANT MODEL

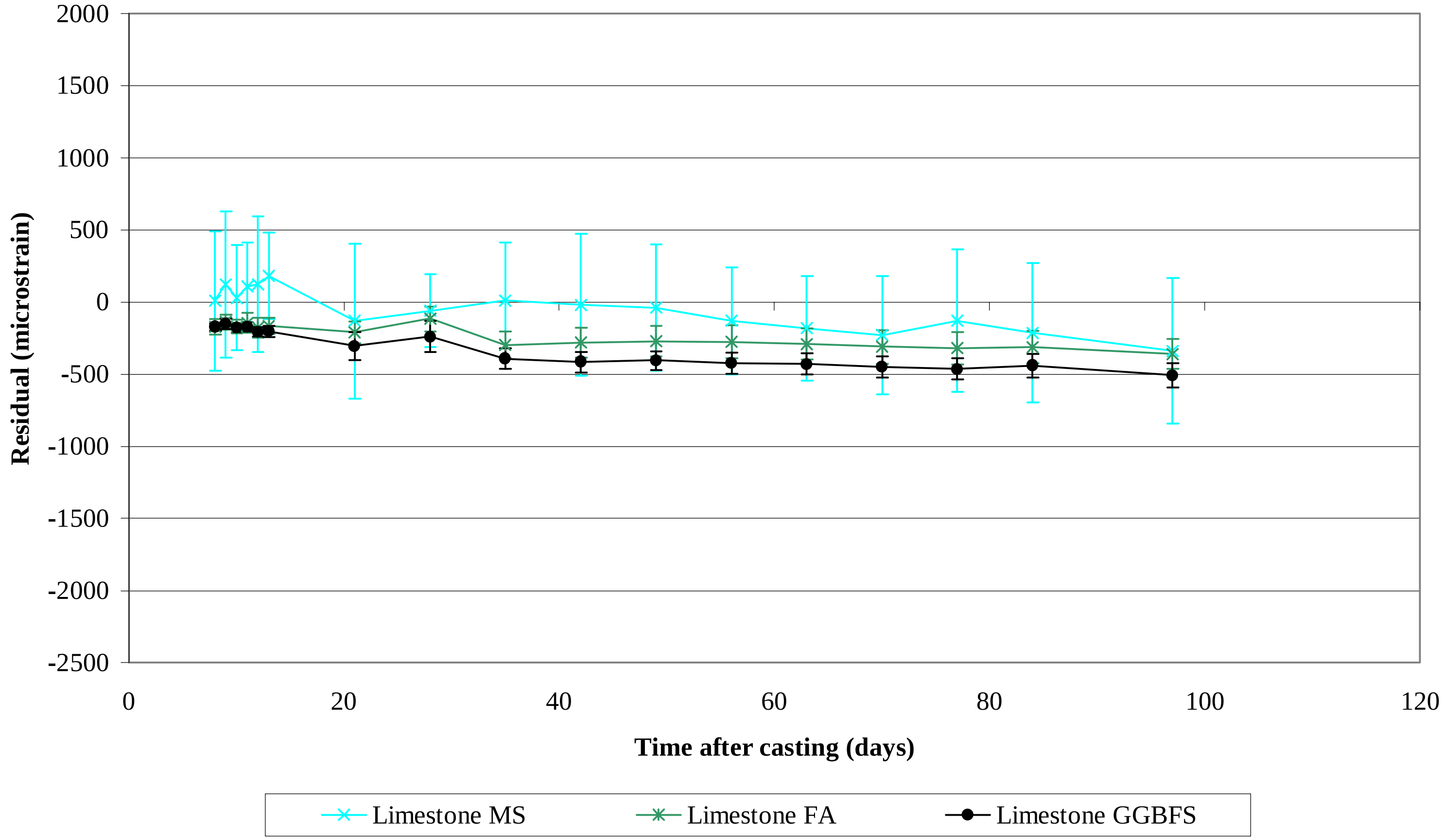

Each data point for a specified time is an average of three measurements. The error bars represent the 95 % confidence interval.

FIGURE 25. RESIDUALS OF DRYING SHRINKAGE OF PORTLAND CEMENT PLUS MINERAL ADMIXTURE CONCRETE AND BAZANT MODEL

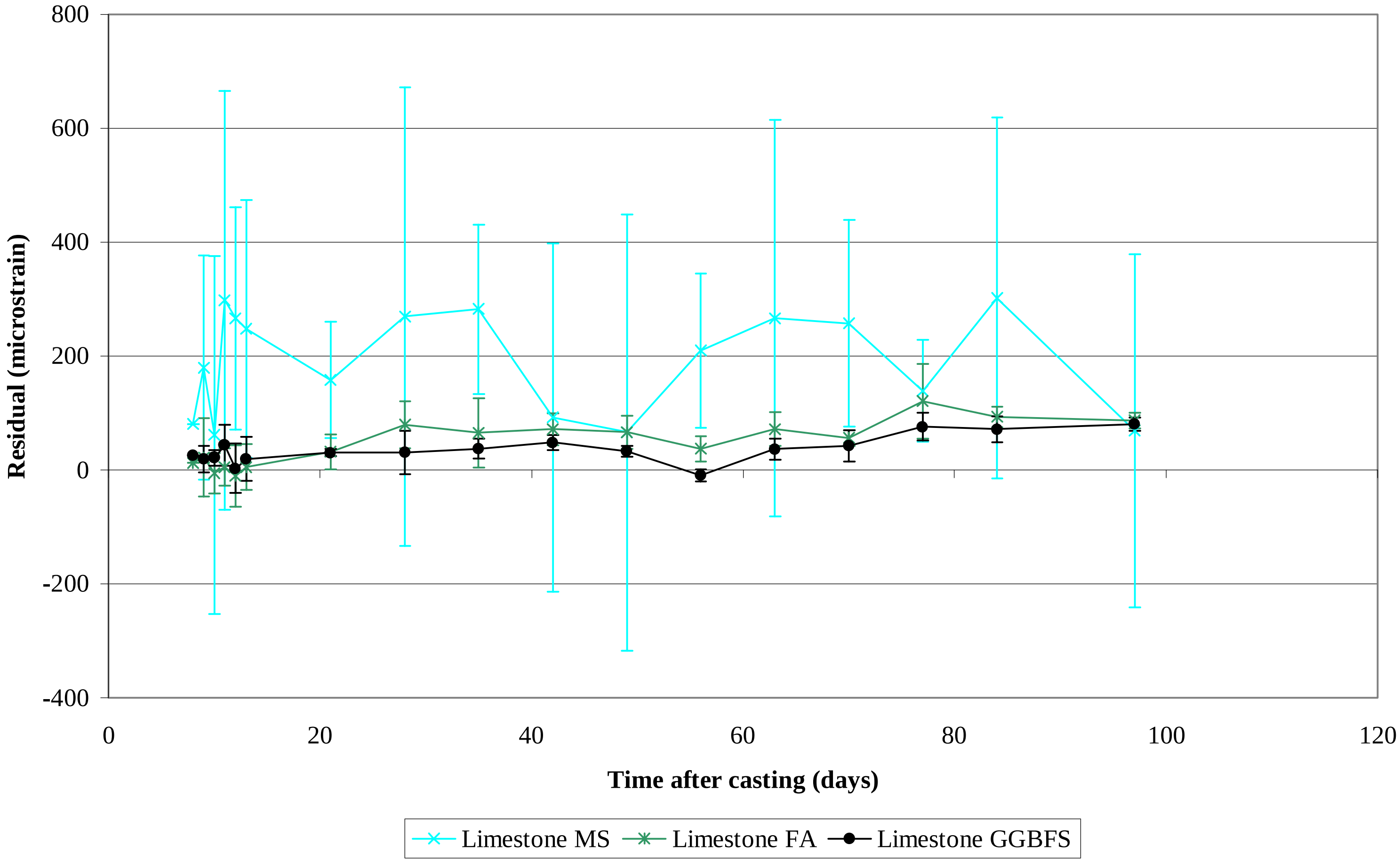

Each data point for a specified time is an average of three measurements. The error bars represent the 95 % confidence interval.

FIGURE 26. RESIDUALS OF BASIC CREEP OF PORTLAND CEMENT PLUS MINERAL ADMIXTURE CONCRETE AND BAZANT MODEL

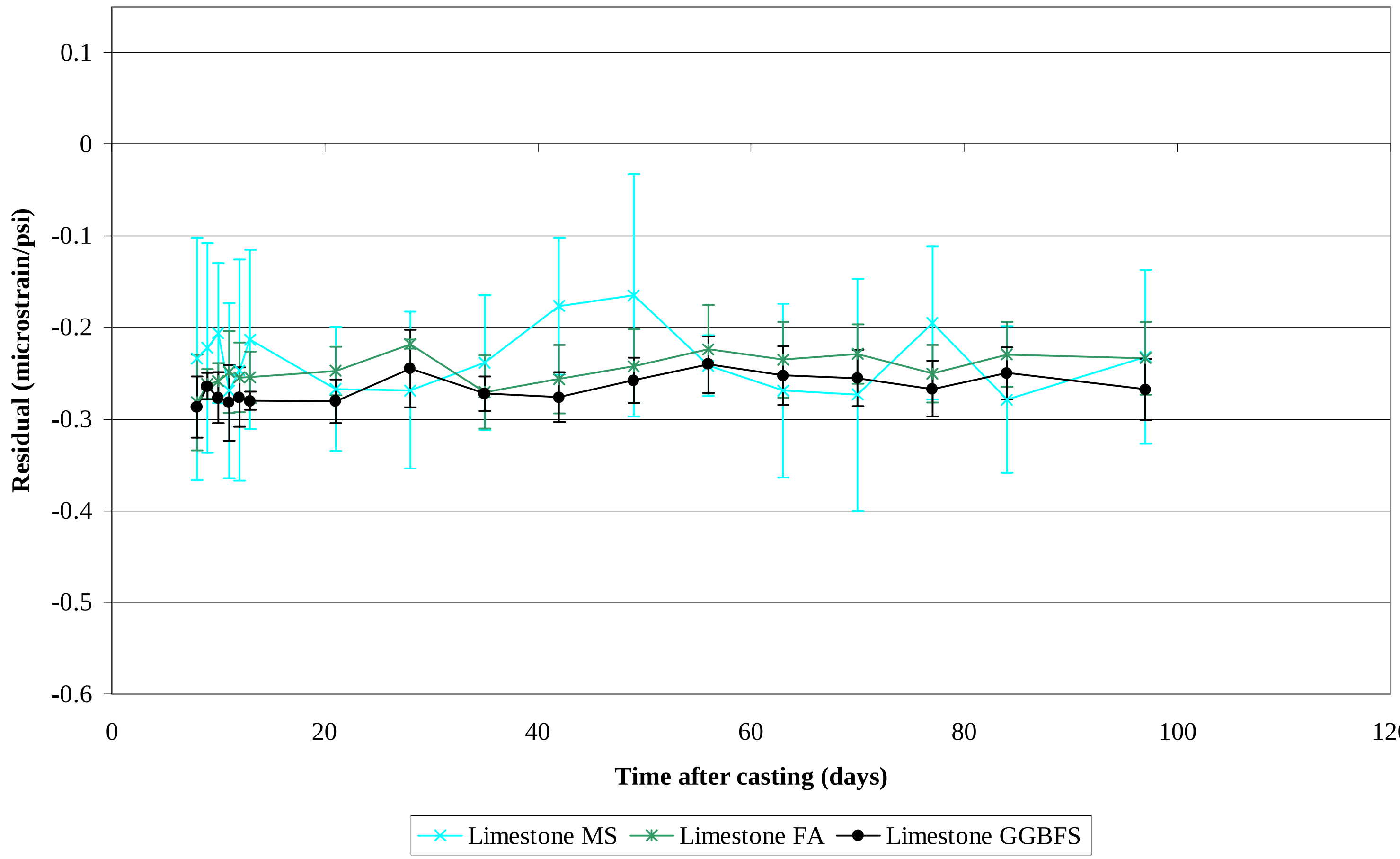

Each data point for a specified time is an average of three measurements. The error bars represent the 95 % confidence interval. 1 psi = 1/145 MPa

FIGURE 27. RESIDUALS OF TOTAL STRAIN OF PORTLAND CEMENT CONCRETE AND GARDNER MODEL

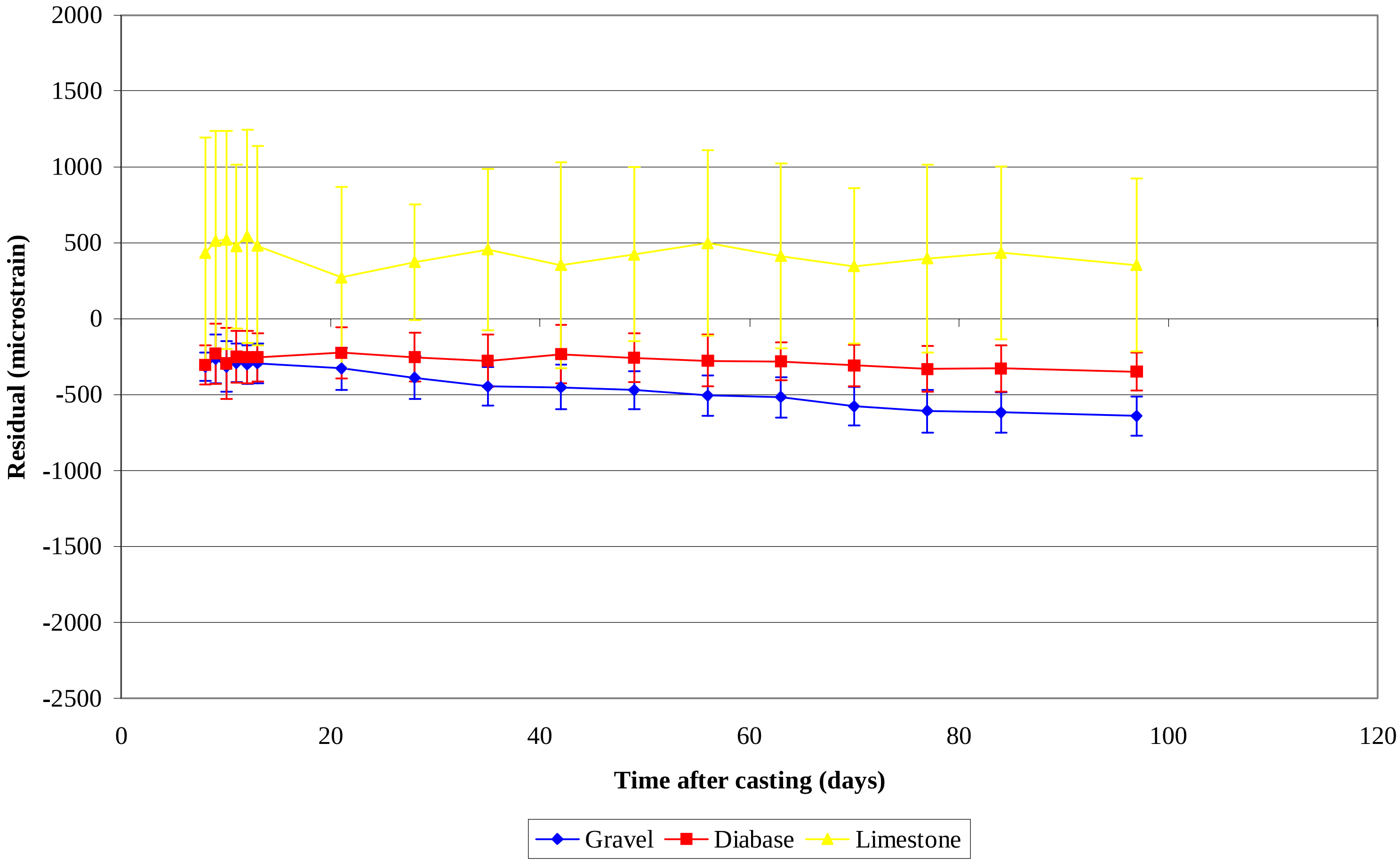

Each data point for a specified time is an average of three measurements. The error bars represent the 95 % confidence interval.

FIGURE 28. RESIDUALS OF DRYING SHRINKAGE OF PORTLAND CEMENT CONCRETE AND GARDNER MODEL

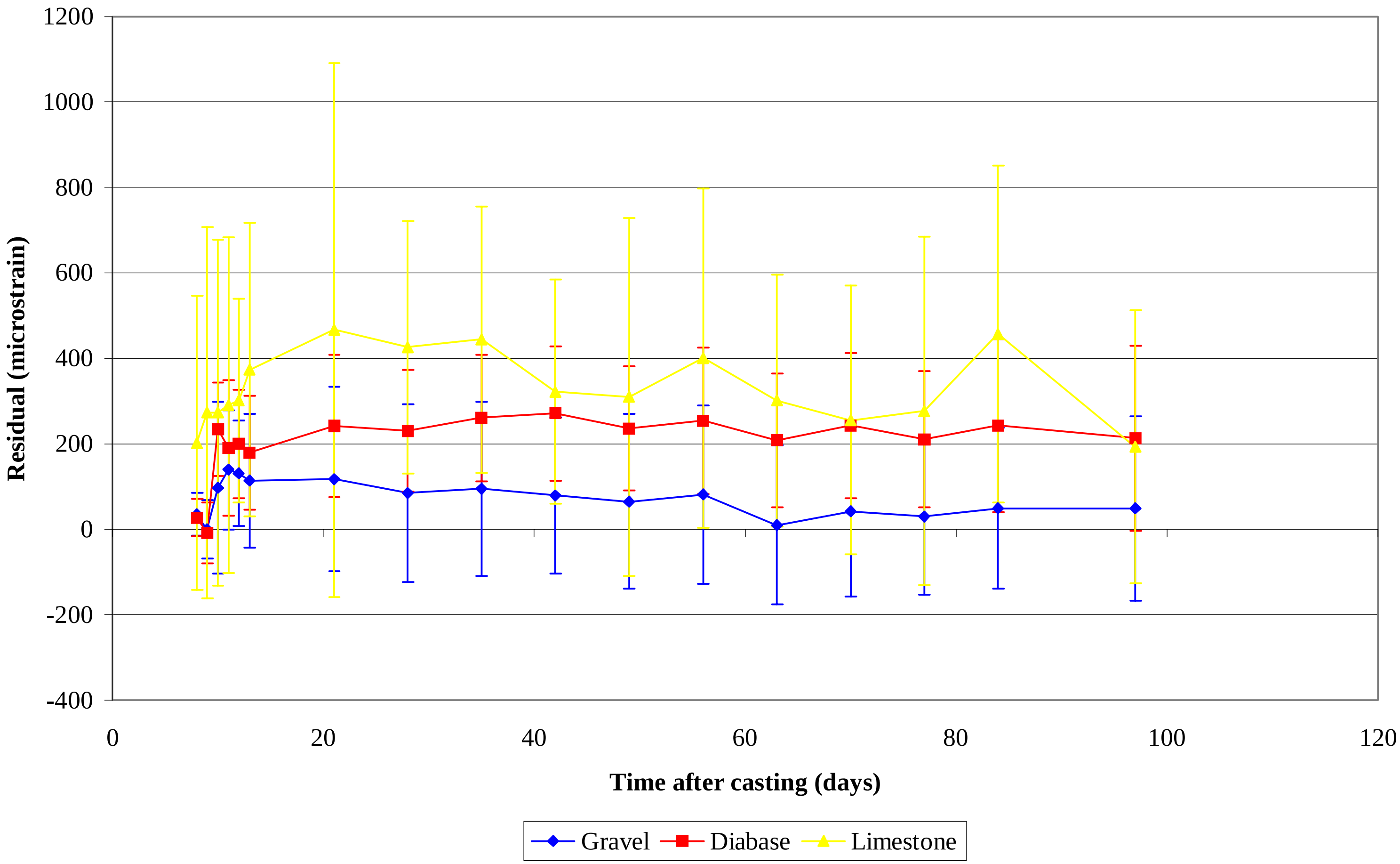

Each data point for a specified time is an average of three measurements. The error bars represent the 95 % confidence interval.

FIGURE 29. RESIDUALS OF BASIC CREEP OF PORTLAND CEMENT CONCRETE AND GARDNER MODEL

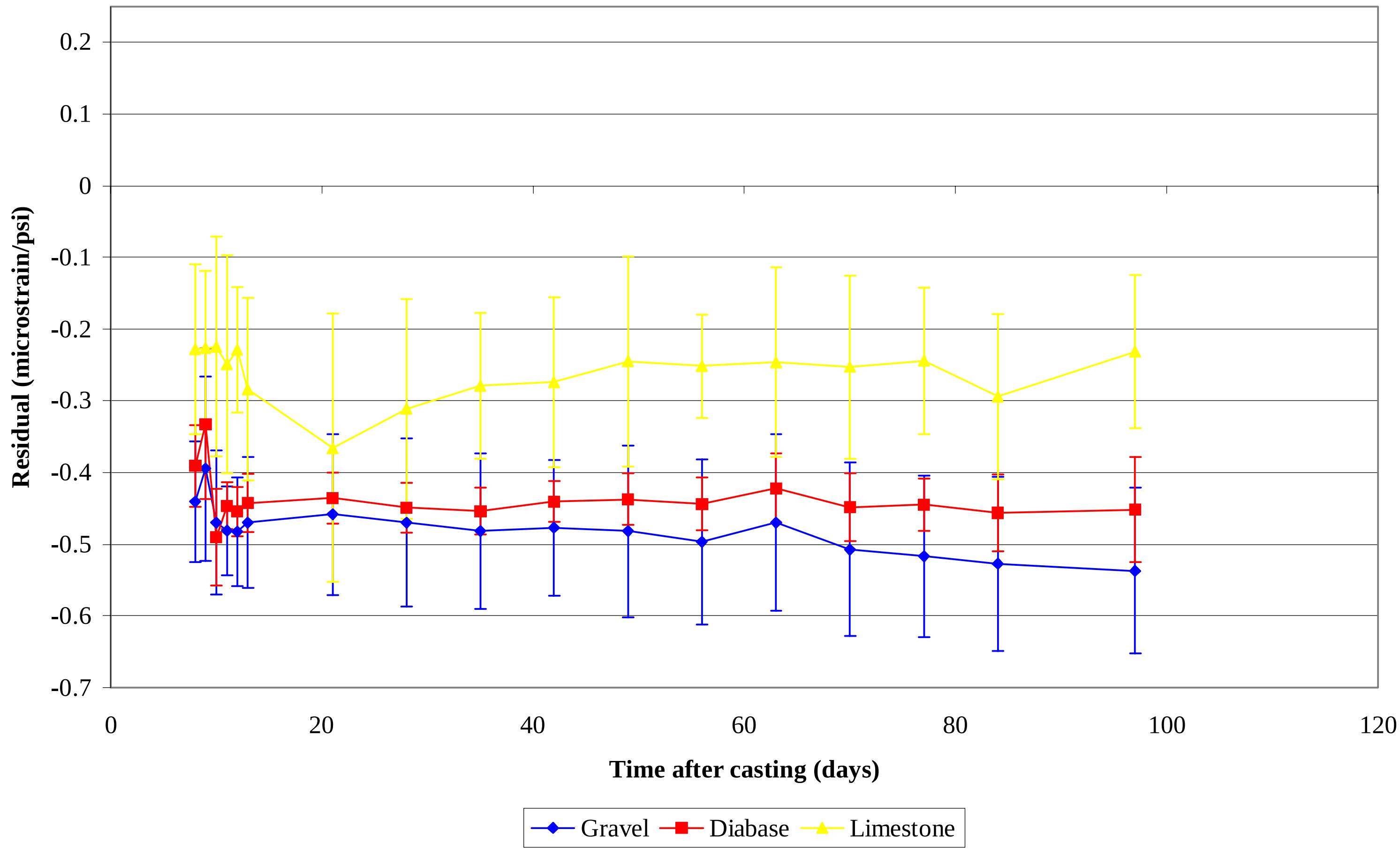

Each data point for a specified time is an average of three measurements. The error bars represent the 95 % confidence interval. 1 psi = 1/145 MPa

FIGURE 30. RESIDUALS OF TOTAL STRAIN OF PORTLAND CEMENT PLUS MINERAL ADMIXTURE CONCRETE AND GARDNER MODEL

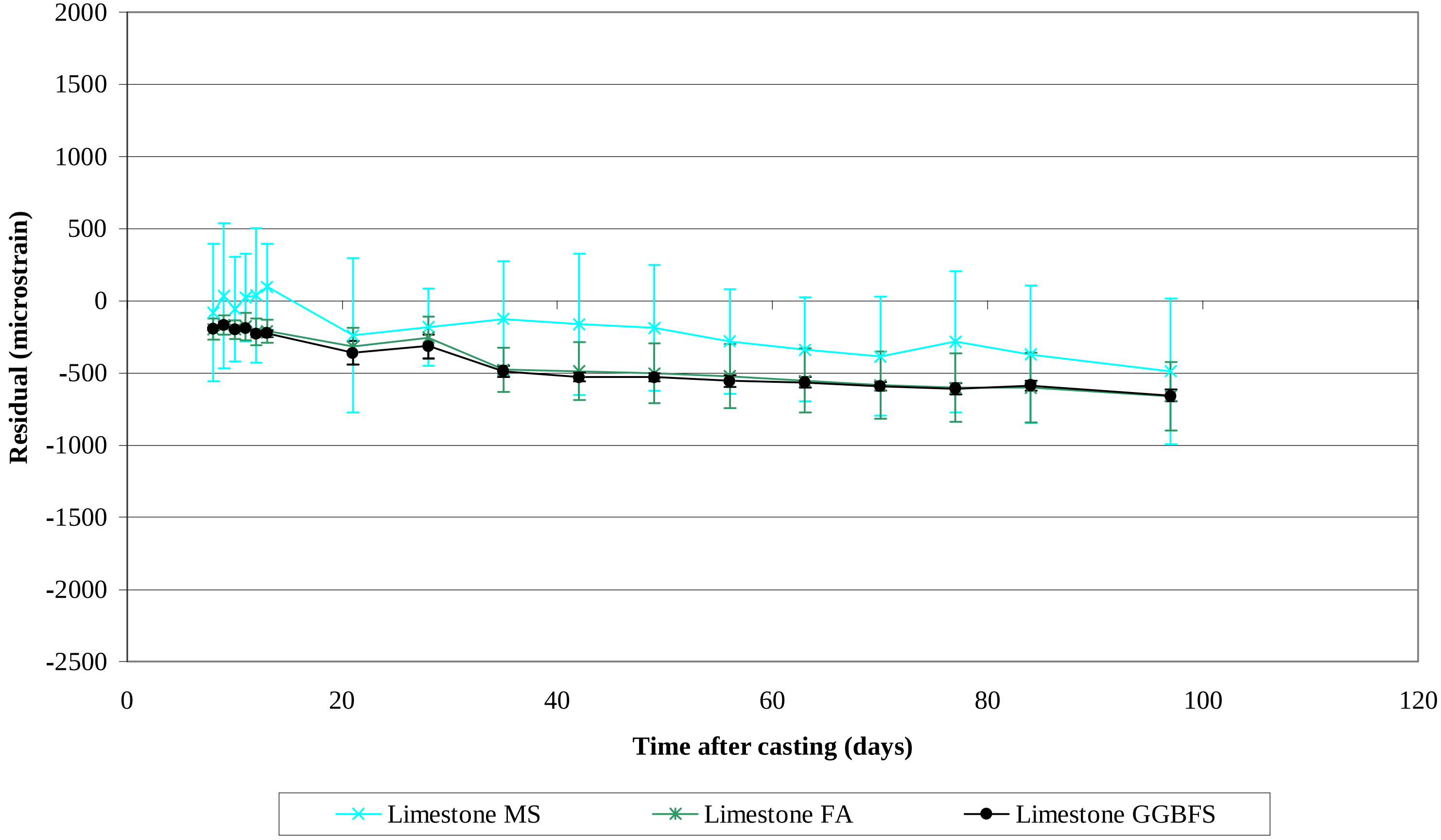

Each data point for a specified time is an average of three measurements. The error bars represent the 95 % confidence interval.

FIGURE 31. RESIDUALS OF DRYING SHRINKAGE OF PORTLAND CEMENT PLUS MINERAL ADMIXTURE CONCRETE AND GARDNER MODEL

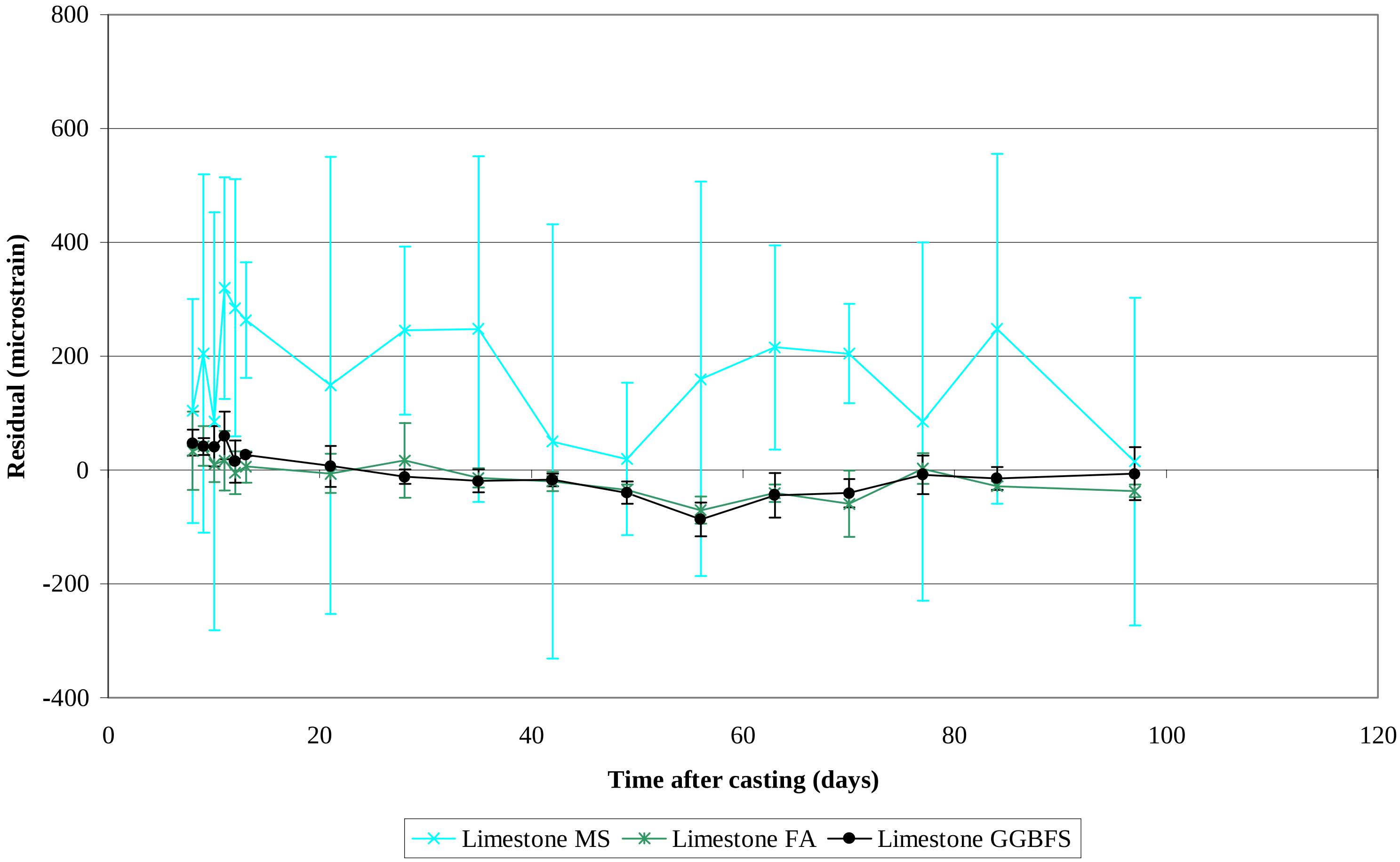

Each data point for a specified time is an average of three measurements. The error bars represent the 95 % confidence interval.

FIGURE 32. RESIDUALS OF BASIC CREEP OF PORTLAND CEMENT PLUS MINERAL ADMIXTURE CONCRETE AND GARDNER MODEL

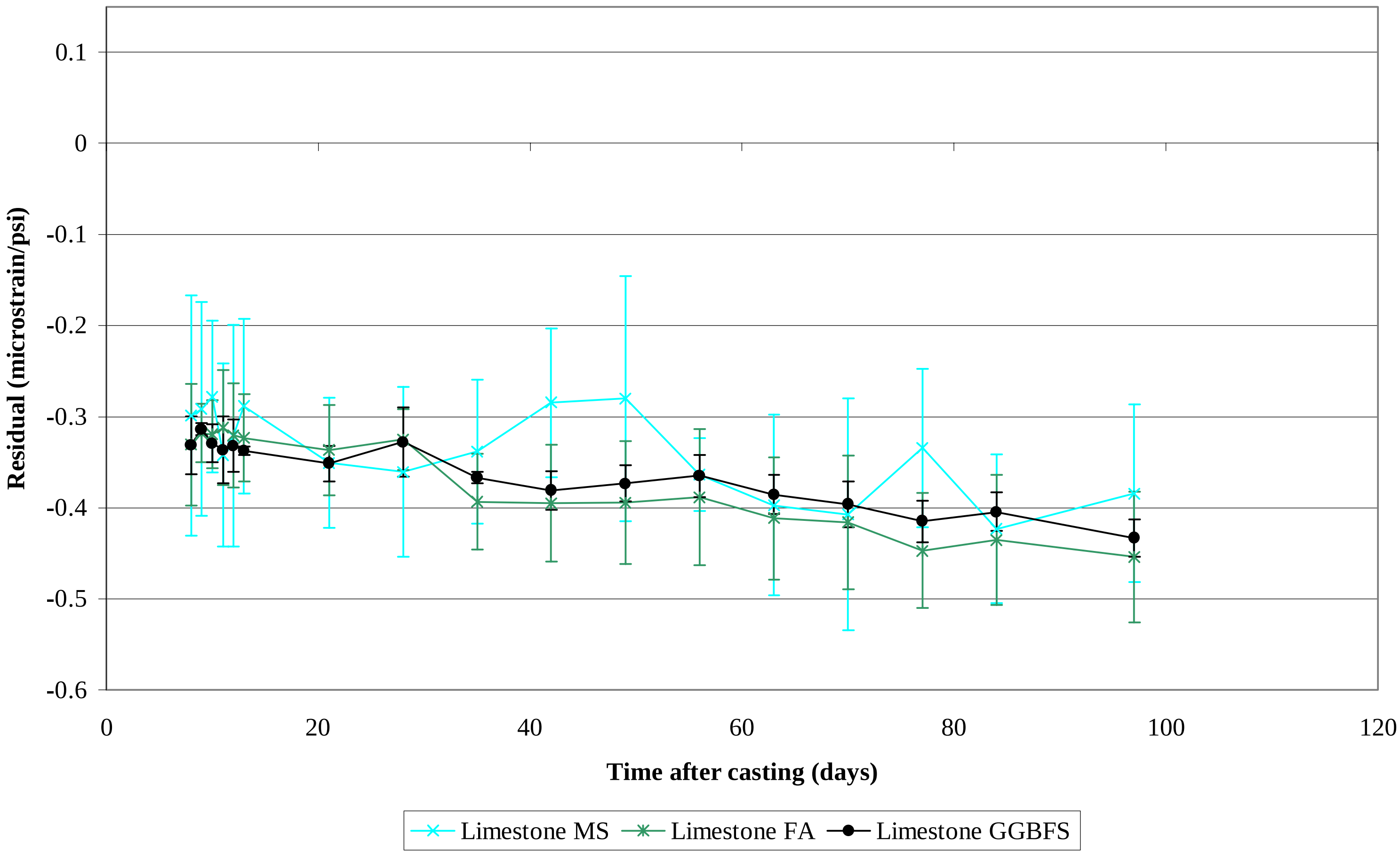

Each data point for a specified time is an average of three measurements. The error bars represent the 95 % confidence interval.

1 psi = 1/145 MPa

FIGURE 33. RESIDUALS OF TOTAL STRAIN OF PORTLAND CEMENT CONCRETE AND SAKATA MODEL

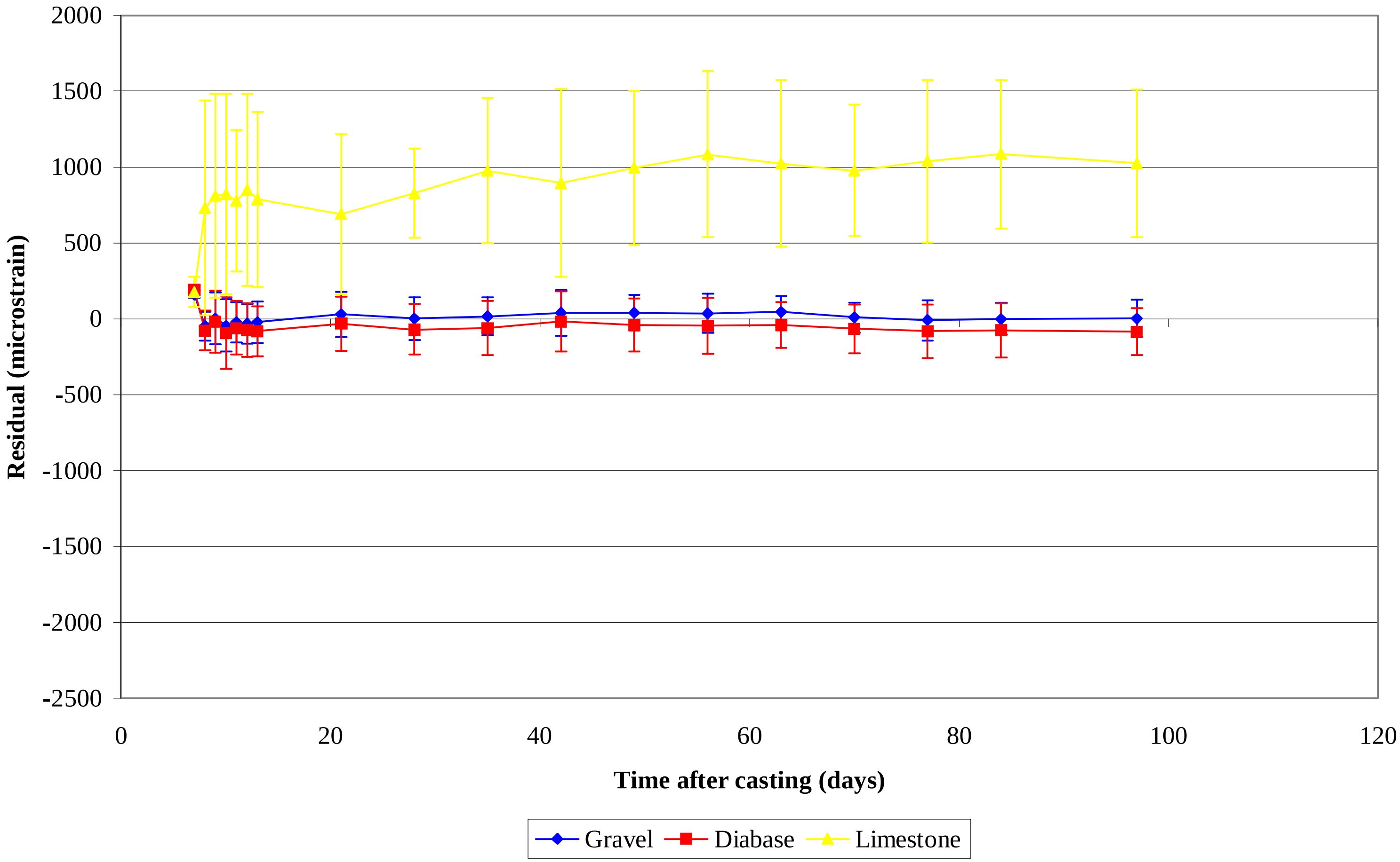

Each data point for a specified time is an average of three measurements. The error bars represent the 95 % confidence interval.

FIGURE 34. RESIDUALS OF DRYING SHRINKAGE OF PORTLAND CEMENT CONCRETE AND SAKATA MODEL

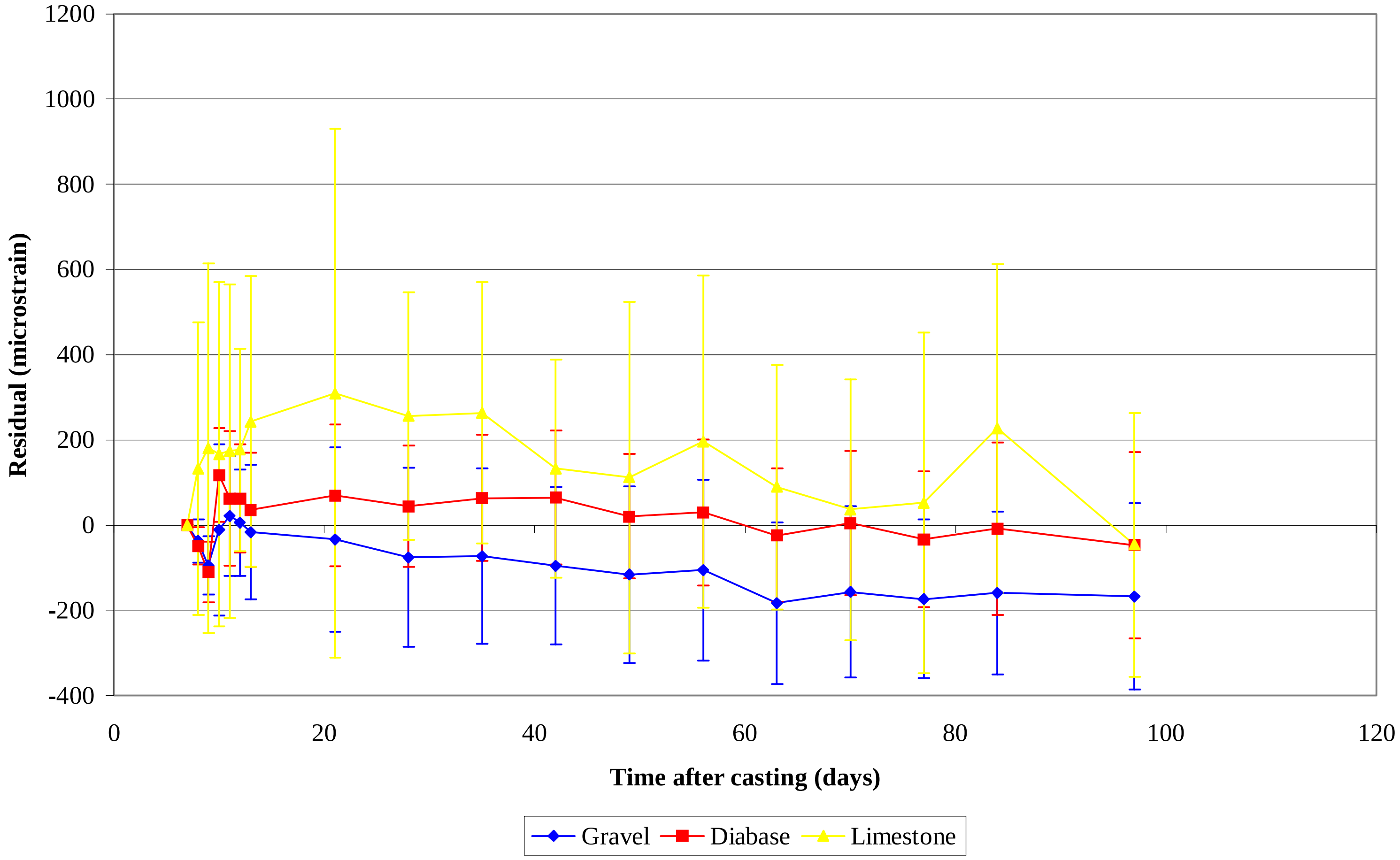

Each data point for a specified time is an average of three measurements. The error bars represent the 95 % confidence interval.

FIGURE 35. RESIDUALS OF BASIC CREEP OF PORTLAND CEMENT CONCRETE AND SAKATA MODEL

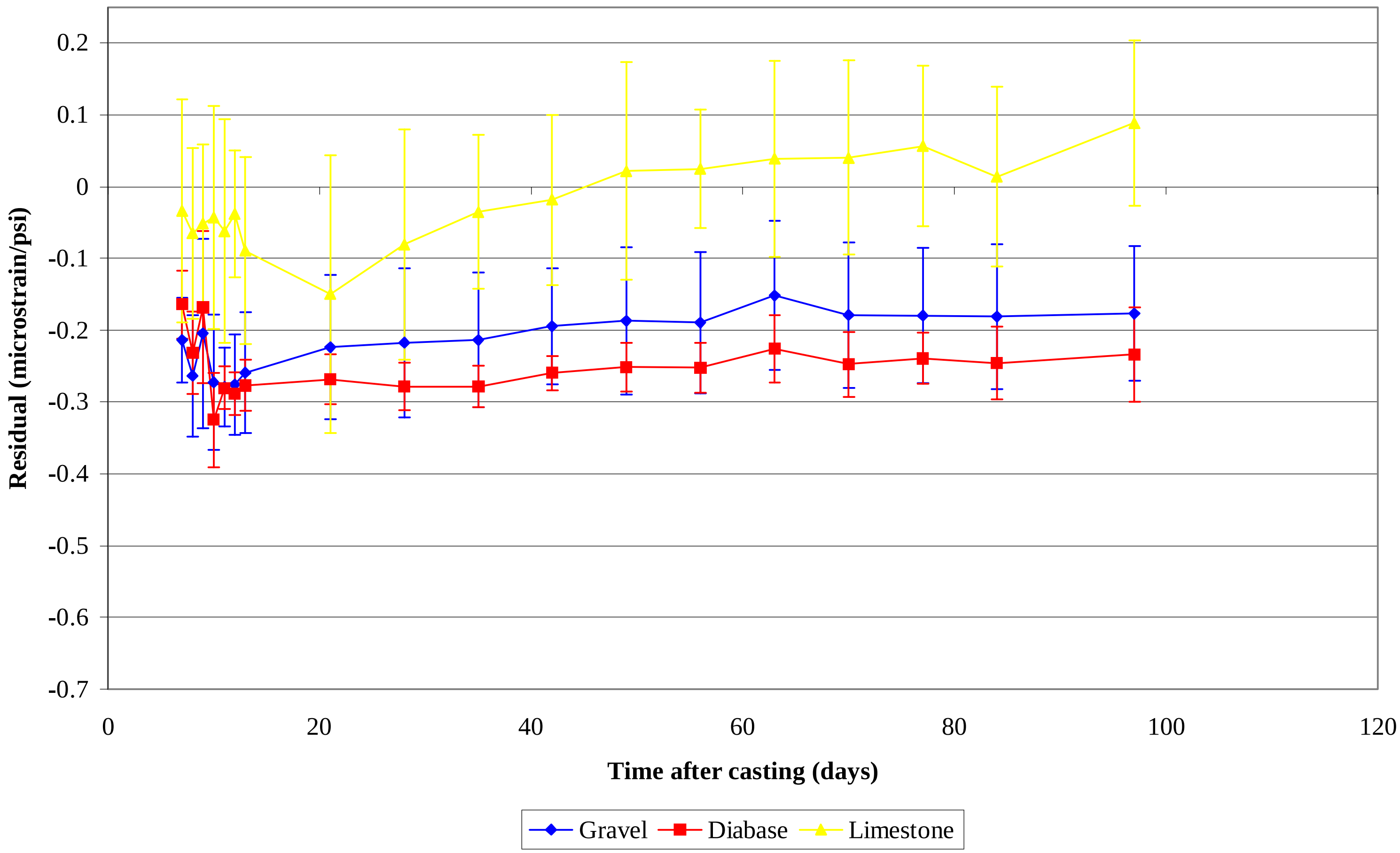

Each data point for a specified time is an average of three measurements. The error bars represent the 95 % confidence interval.

1 psi = 1/145 MPa

FIGURE 36. RESIDUALS OF TOTAL STRAIN OF PORTLAND CEMENT PLUS MINERAL ADMIXTURE CONCRETE AND SAKATA MODEL

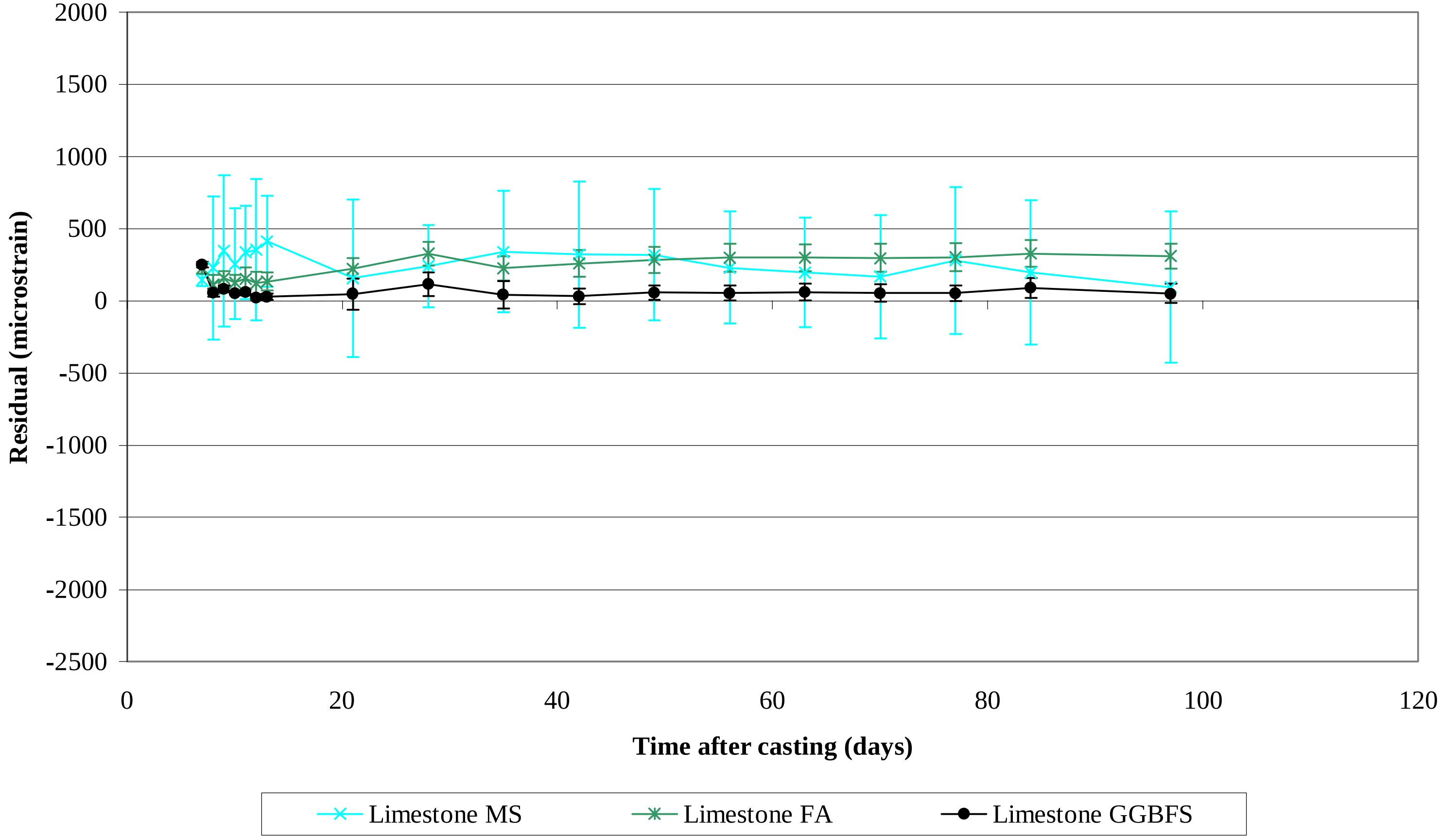

Each data point for a specified time is an average of three measurements. The error bars represent the 95 % confidence interval.

FIGURE 37. RESIDUALS OF DRYING SHRINKAGE OF PORTLAND CEMENT PLUS MINERAL ADMIXTURE CONCRETE AND SAKATA MODEL

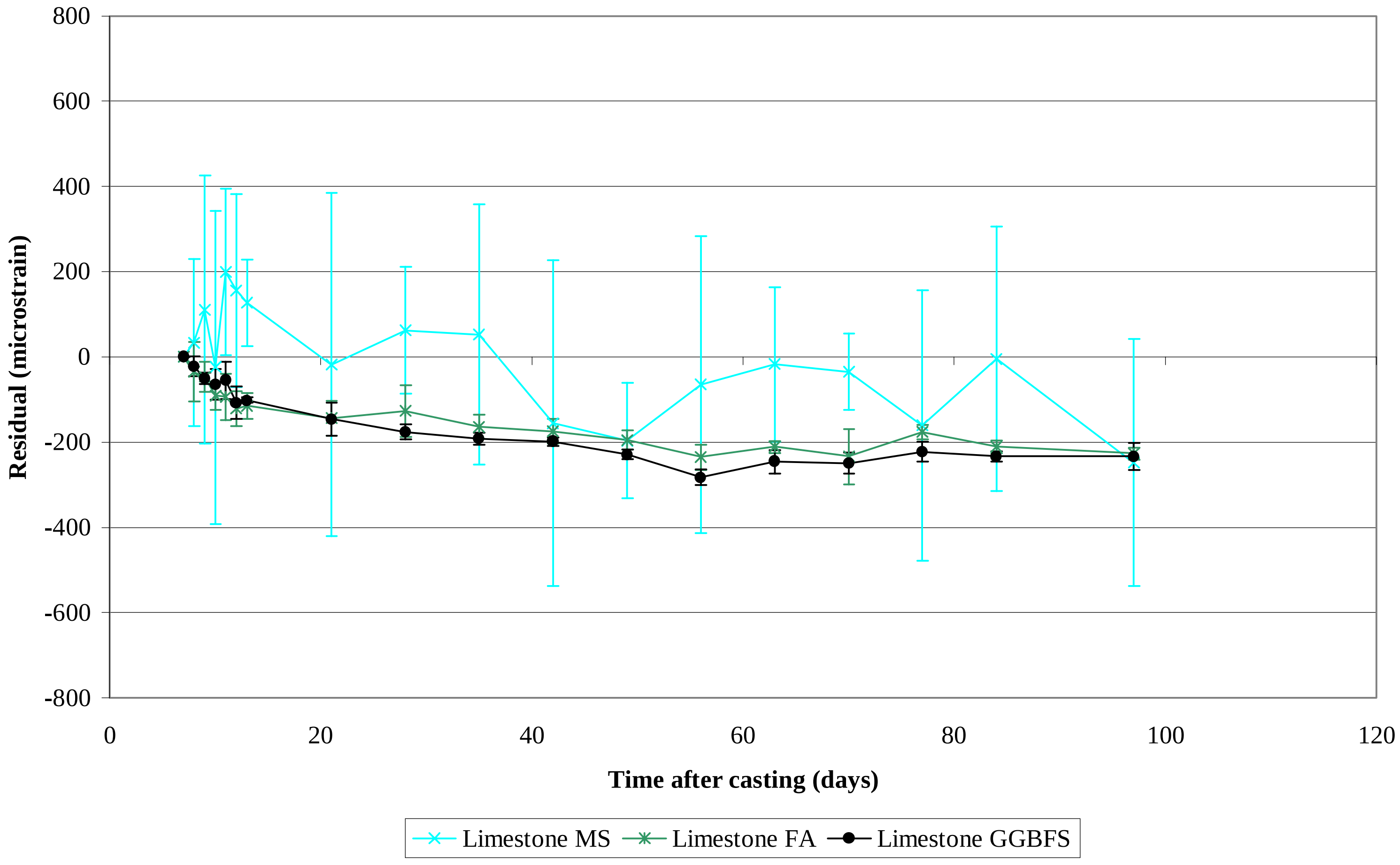

Each data point for a specified time is an average of three measurements. The error bars represent the 95 % confidence interval.

FIGURE 38. RESIDUALS OF BASIC CREEP OF PORTLAND CEMENT PLUS MINERAL ADMIXTURE CONCRETE AND SAKATA MODEL

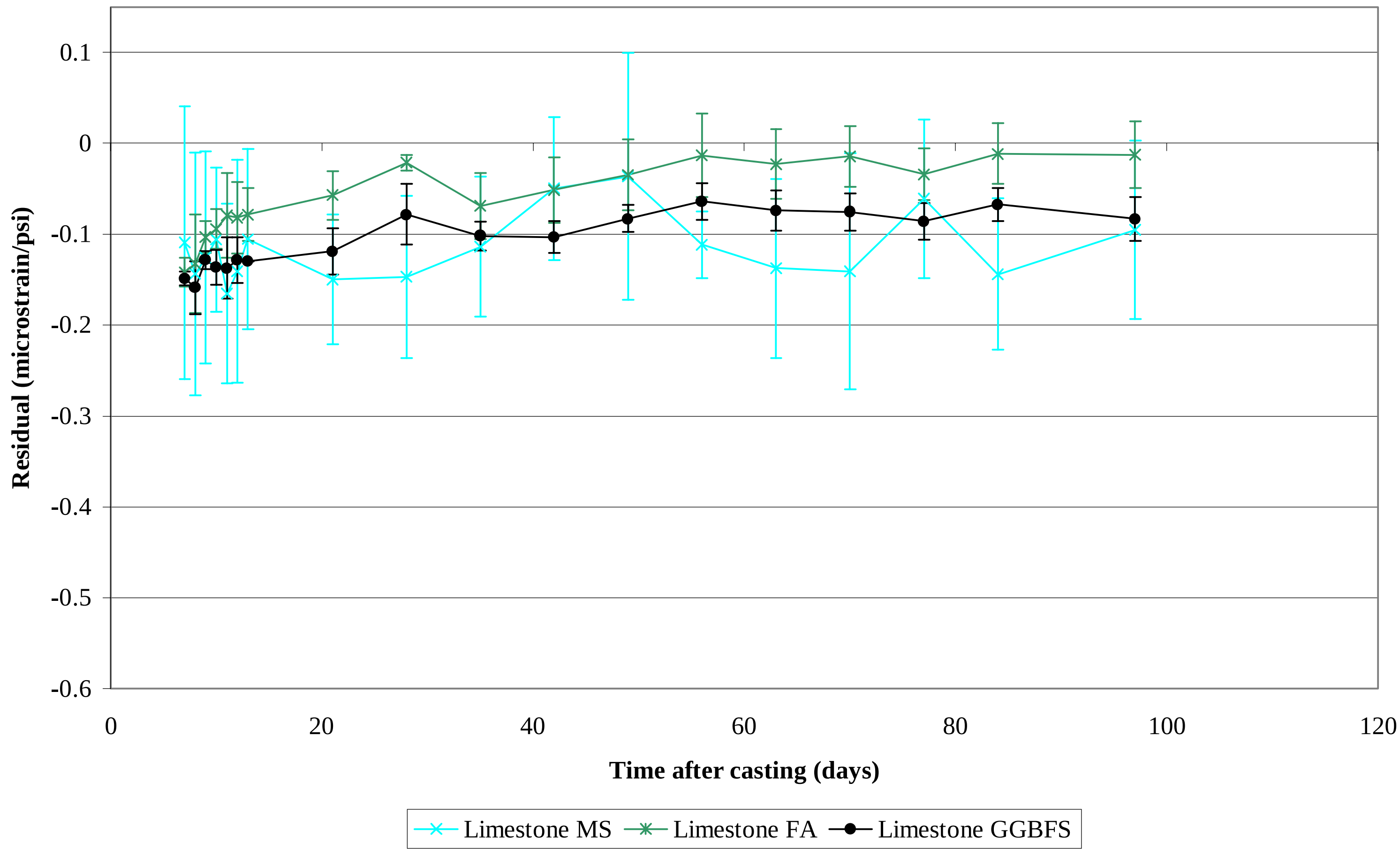

Each data point for a specified time is an average of three measurements. The error bars represent the 95 % confidence interval.

1 psi = 1/145 MPa

FIGURE 39. CHI SQUARED ANALYSIS FOR TOTAL STRAIN OF PORTLAND CEMENT CONCRETE AT 28 DAYS AFTER CASTING

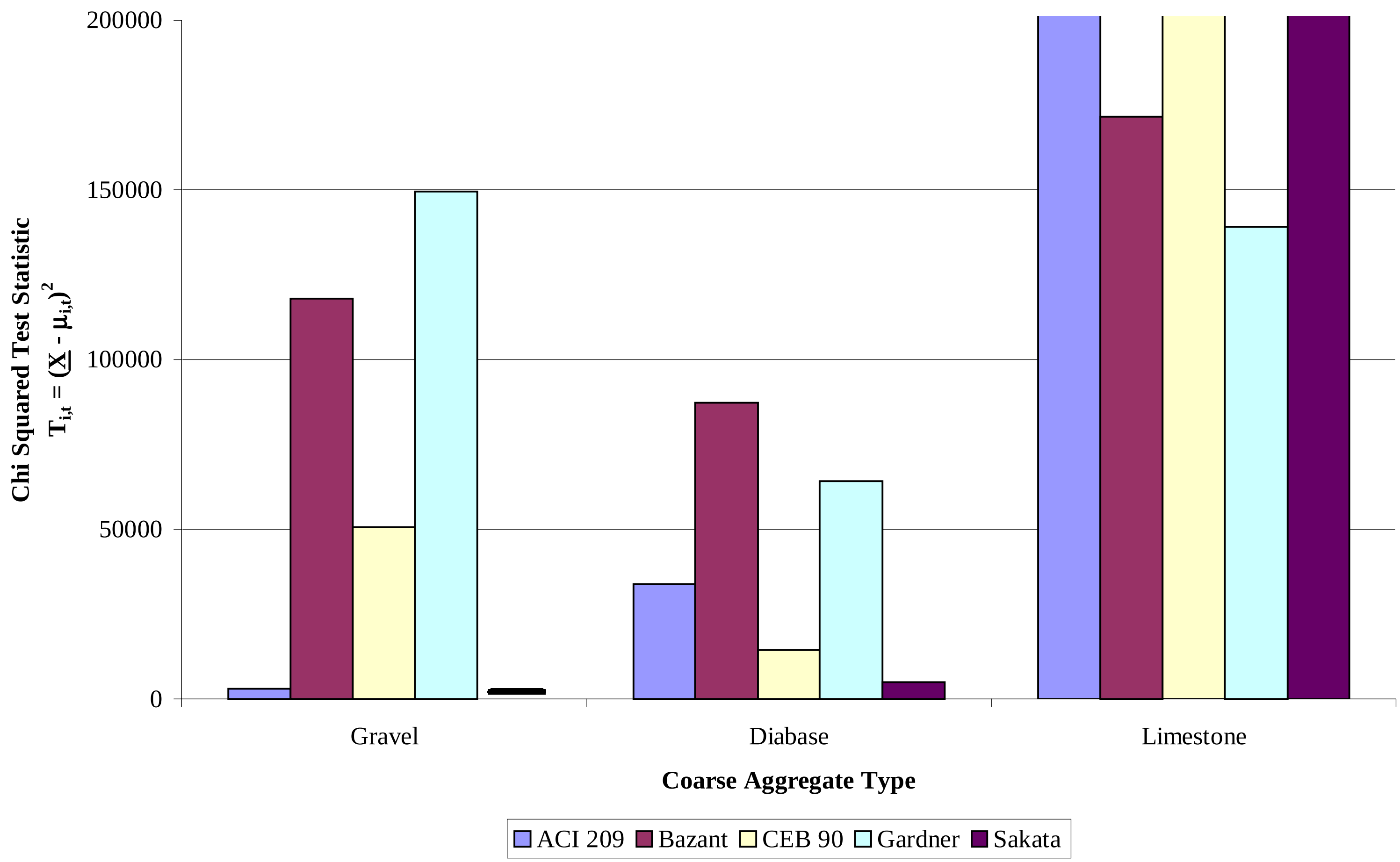

The residual is an average of three values.

FIGURE 40. CHI SQUARED ANALYSIS FOR DRYING SHRINKAGE OF PORTLAND CEMENT CONCRETE AT 28 DAYS AFTER CASTING

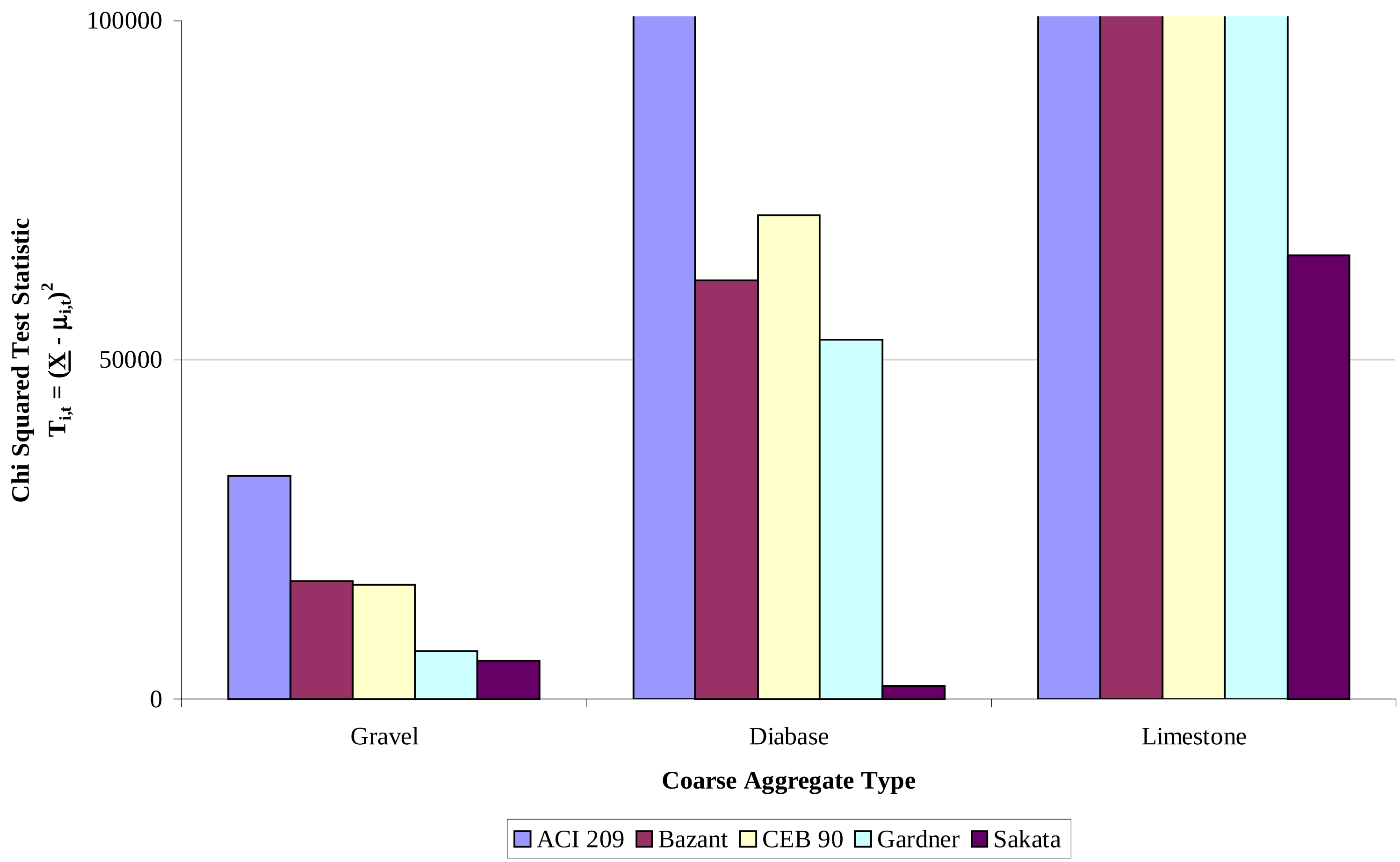

The residual is an average of three values.

FIGURE 41. CHI SQUARED ANALYSIS FOR BASIC CREEP OF PORTLAND CEMENT CONCRETE AT 28 DAYS AFTER CASTING

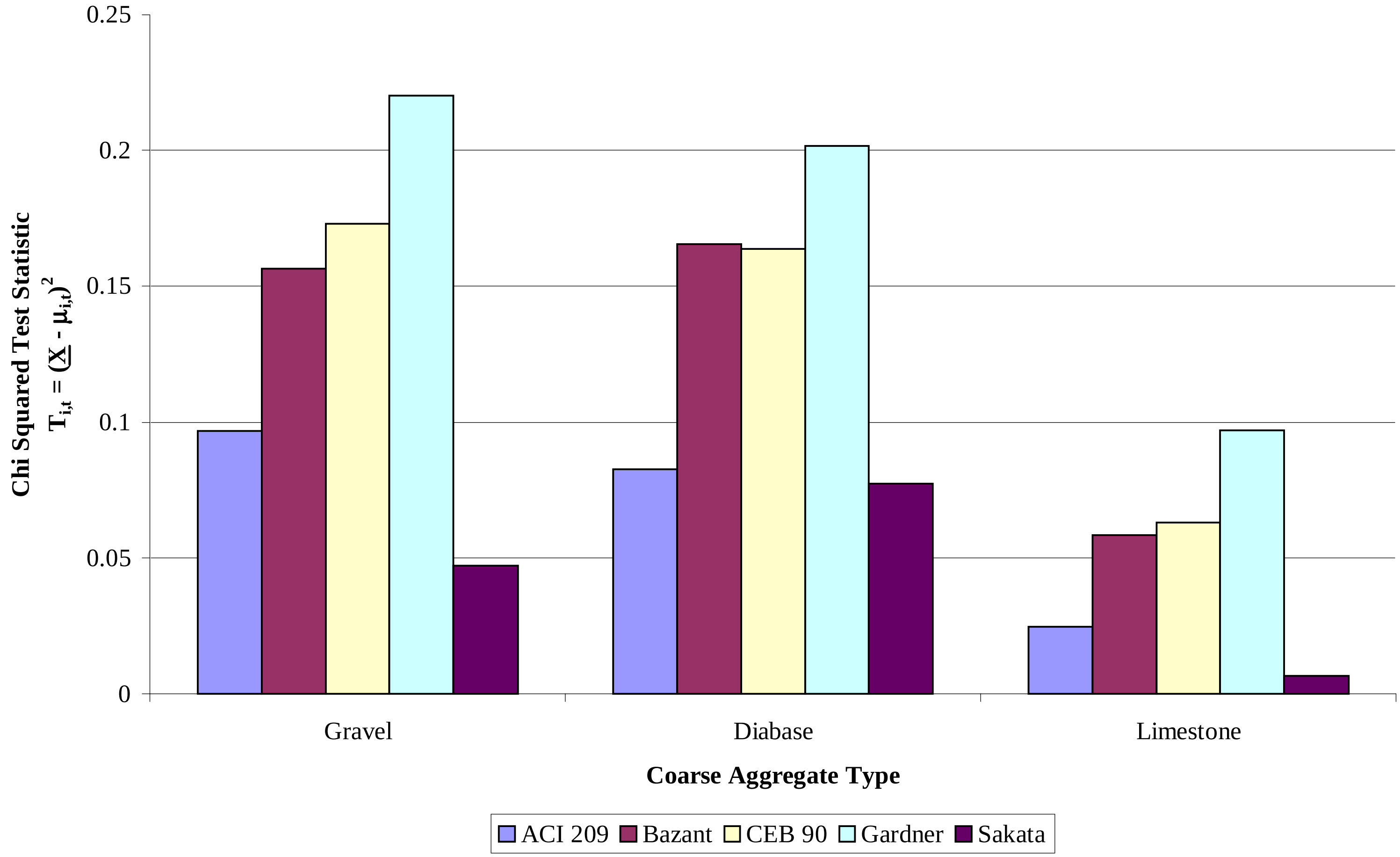

The residual is an average of three values.

FIGURE 42. CHI SQUARED ANALYSIS FOR TOTAL STRAIN OF PORTLAND CEMENT PLUS MINERAL ADMIXTURE CONCRETE AT 28 DAYS AFTER CASTING

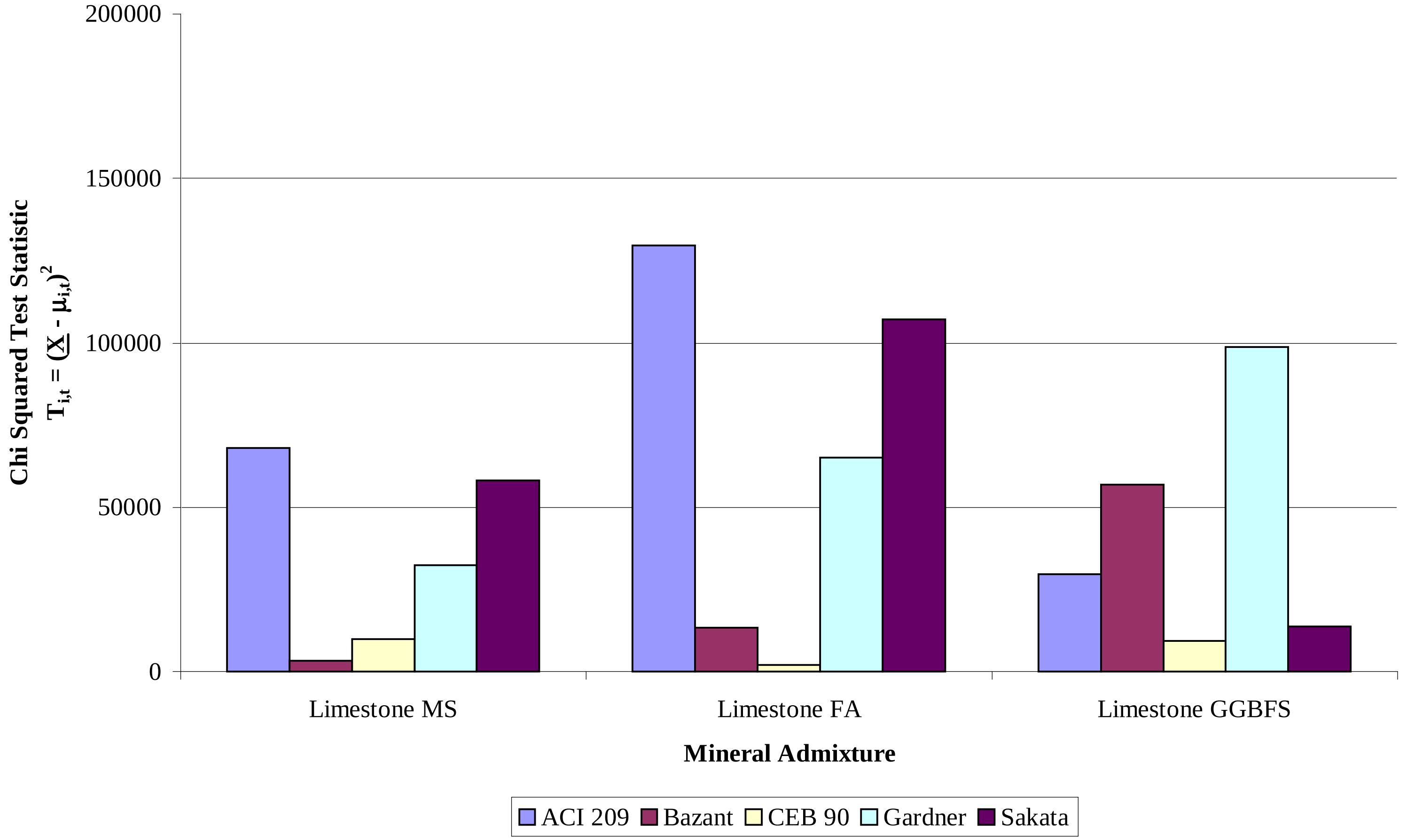

The residual is an average of three values.

FIGURE 43. CHI SQUARED ANALYSIS FOR DRYING SHRINKAGE OF PORTLAND CEMENT PLUS MINERAL ADMIXTURE CONCRETE AT 28 DAYS AFTER CASTING

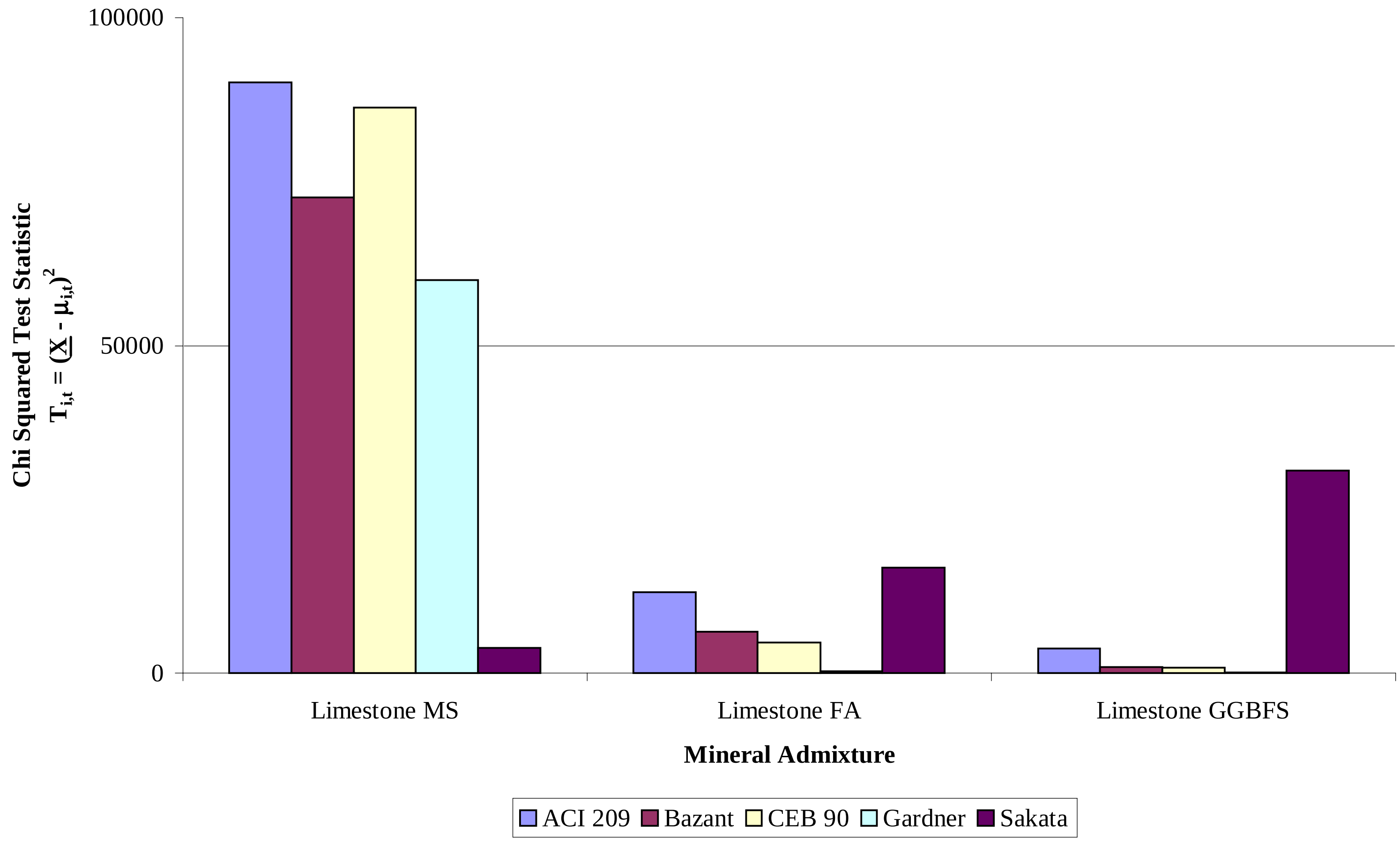

The residual is an average of three values.

FIGURE 44. CHI SQUARED ANALYSIS FOR BASIC CREEP OF PORTLAND CEMENT PLUS MINERAL ADMIXTURE CONCRETE AT 28 DAYS AFTER CASTING

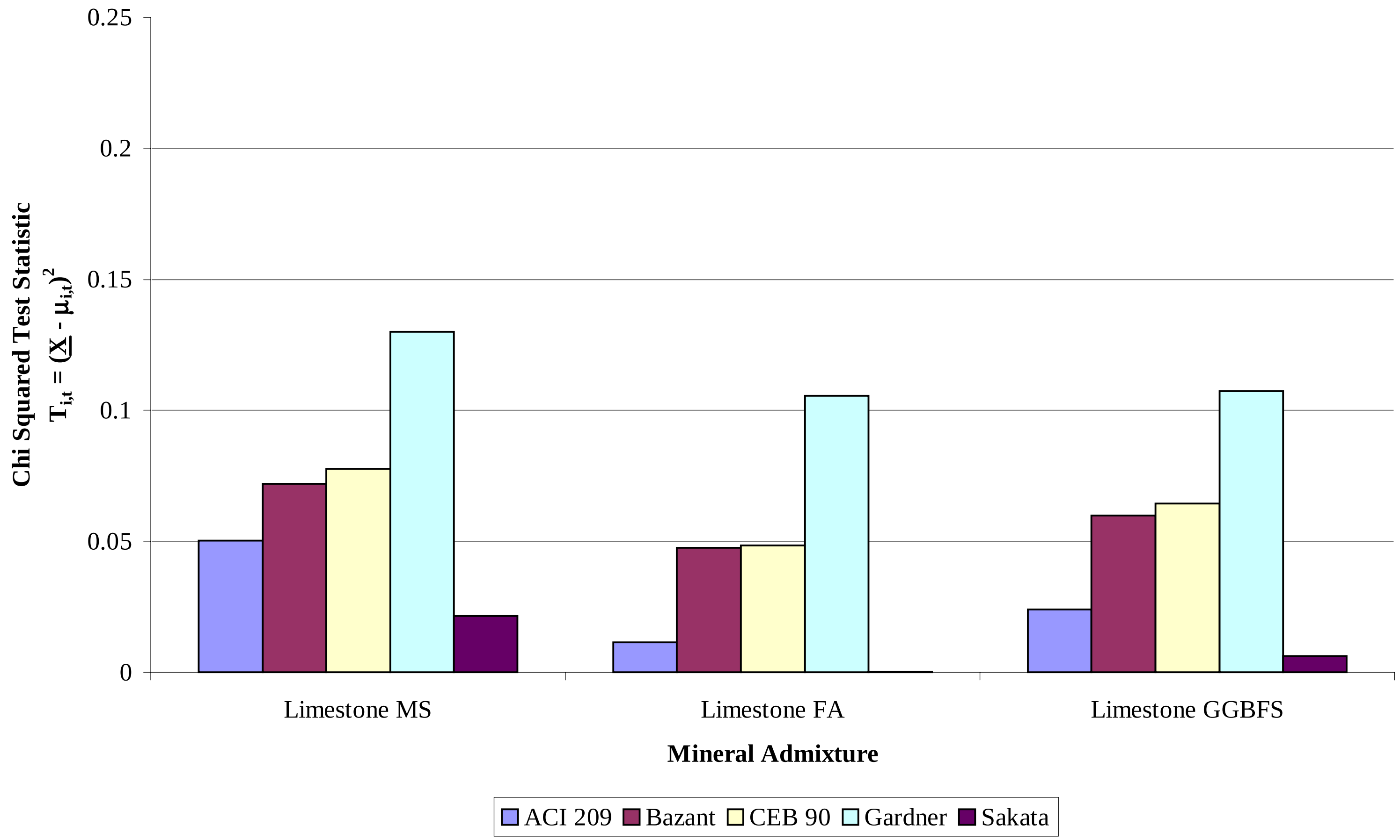

The residual is an average of three values.

FIGURE 45. CHI SQUARED ANALYSIS FOR TOTAL STRAIN OF PORTLAND CEMENT CONCRETE AT 97 DAYS AFTER CASTING

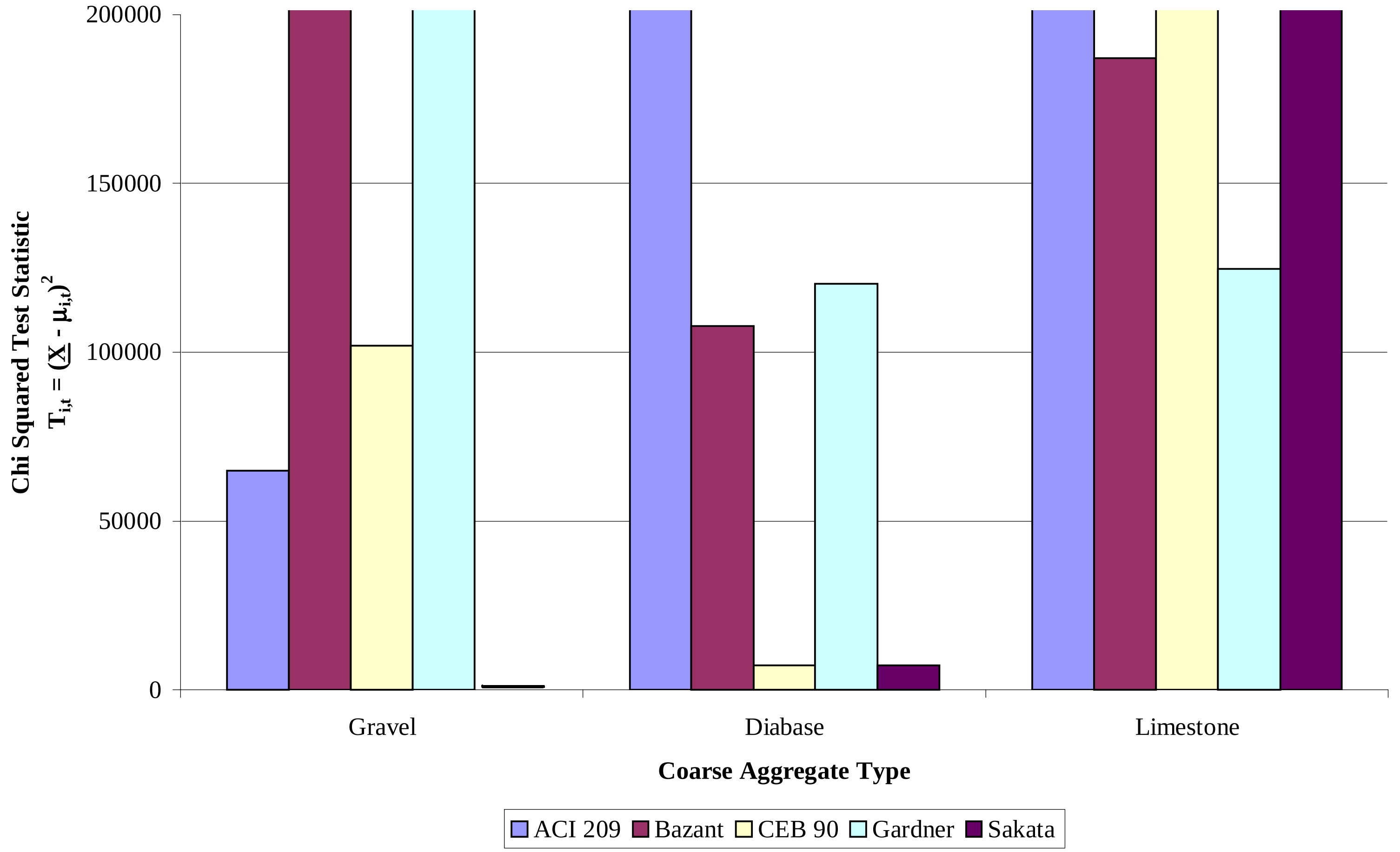

The residual is an average of three values.

FIGURE 46. CHI SQUARED ANALYSIS FOR DRYING SHRINKAGE OF PORTLAND CEMENT CONCRETE AT 97 DAYS AFTER CASTING

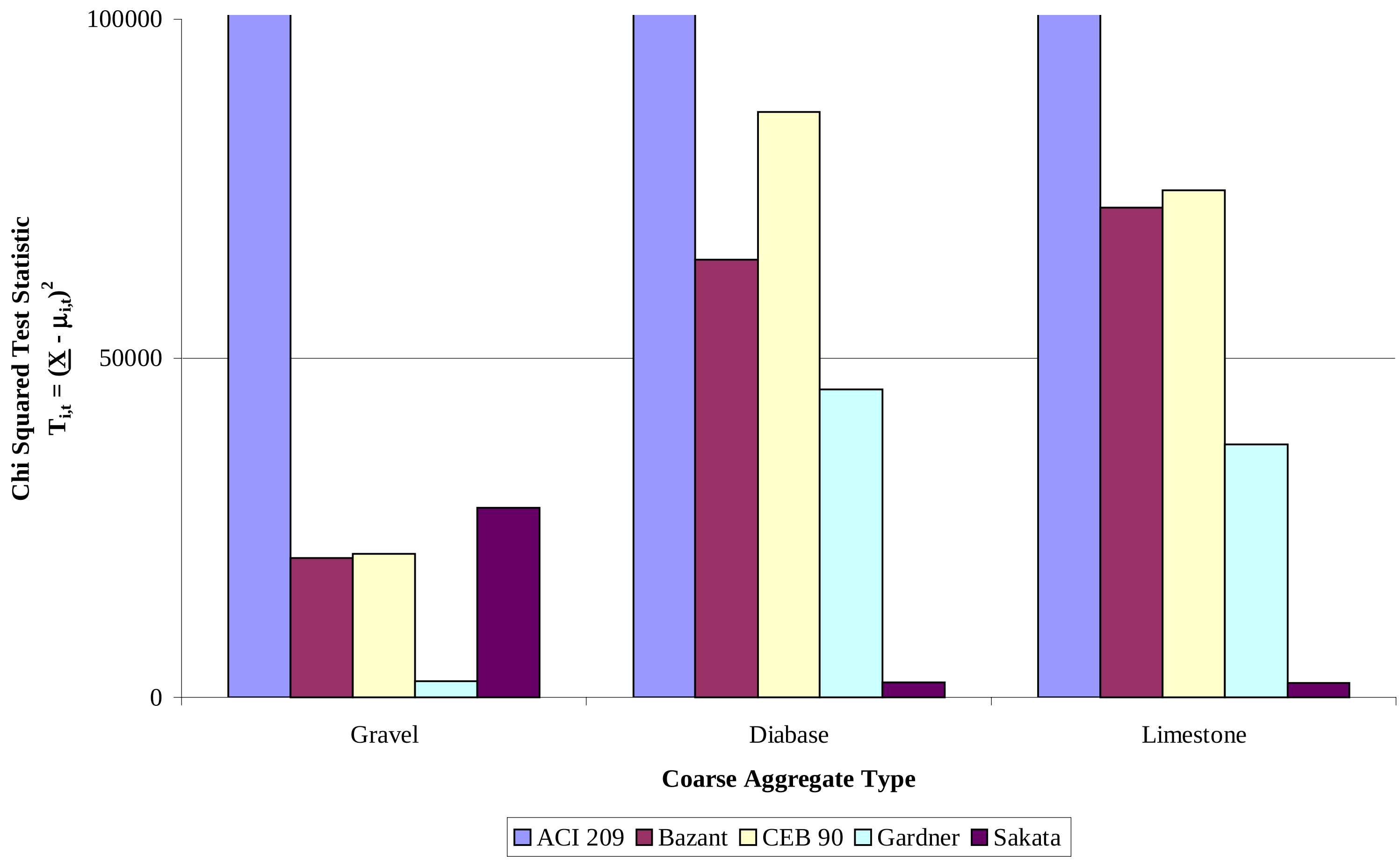

The residual is an average of three values.

FIGURE 47. CHI SQUARED ANALYSIS FOR BASIC CREEP OF PORTLAND CEMENT CONCRETE AT 97 DAYS AFTER CASTING

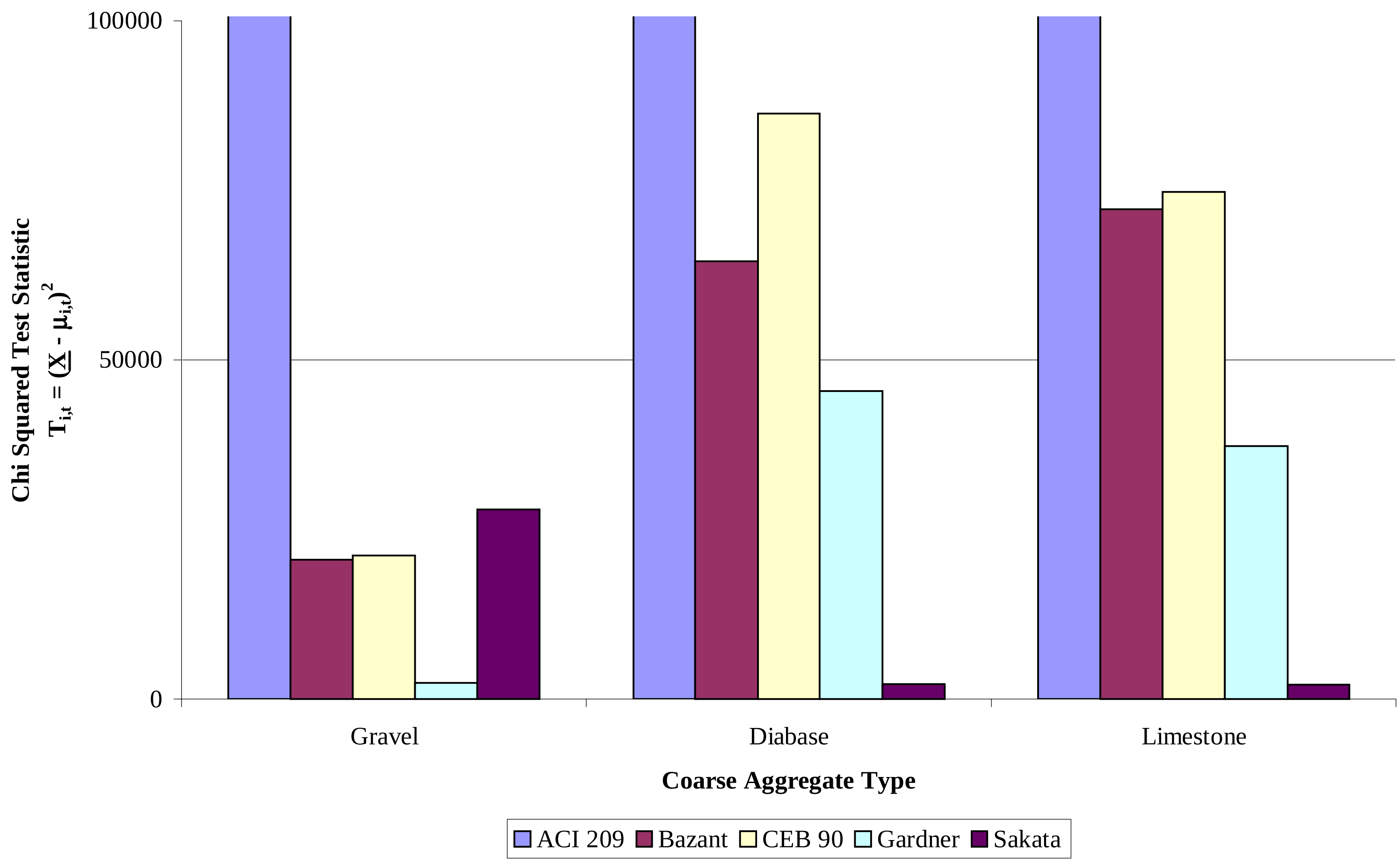

The residual is an average of three values.

FIGURE 48. CHI SQUARED ANALYSIS FOR TOTAL STRAIN OF PORTLAND CEMENT PLUS MINERAL ADMIXTURE CONCRETE AT 97 DAYS AFTER CASTING

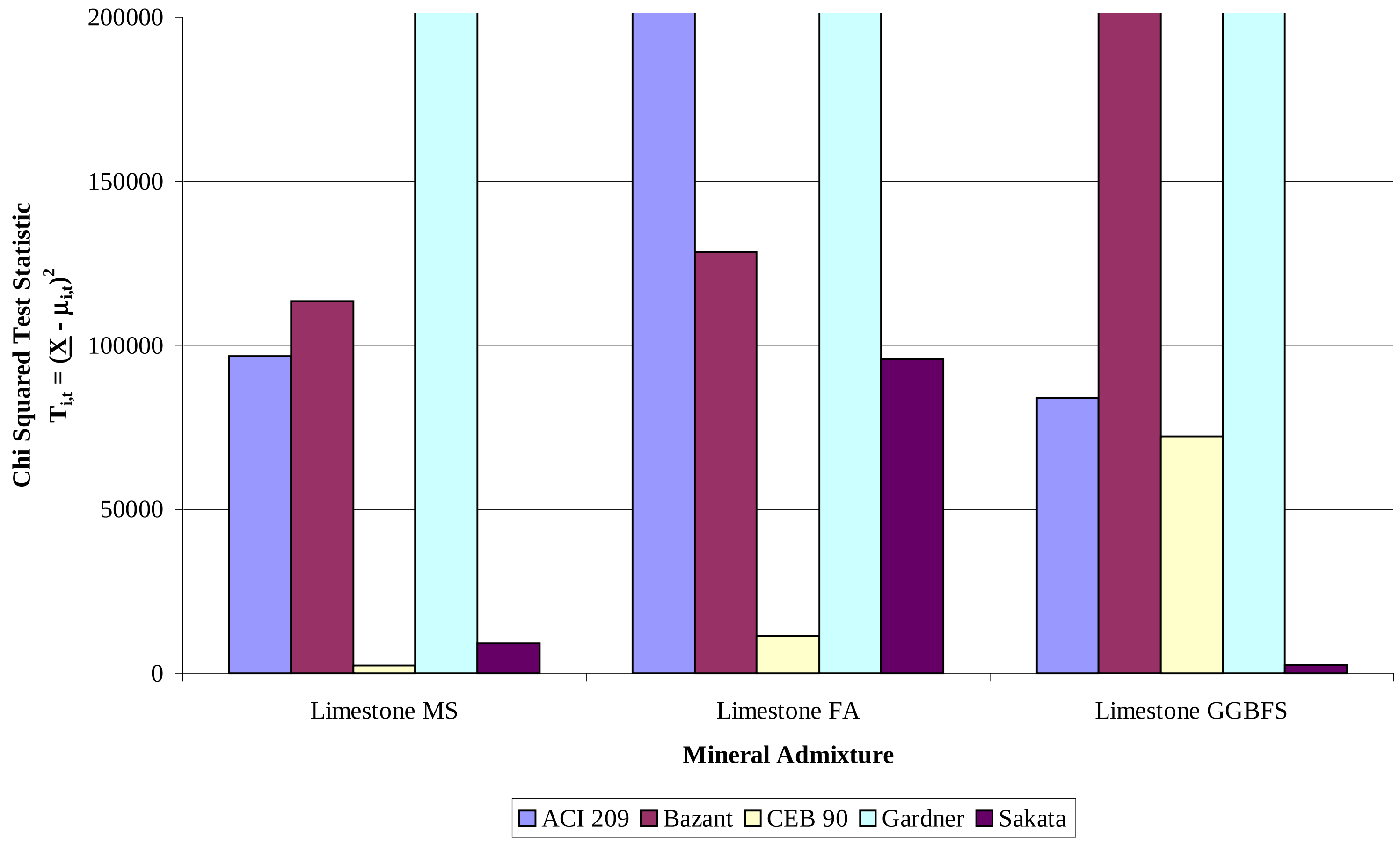

The residual is an average of three values.

FIGURE 49. CHI SQUARED ANALYSIS FOR DRYING SHRINKAGE OF PORTLAND CEMENT PLUS MINERAL ADMIXTURE CONCRETE AT 97 DAYS AFTER CASTING

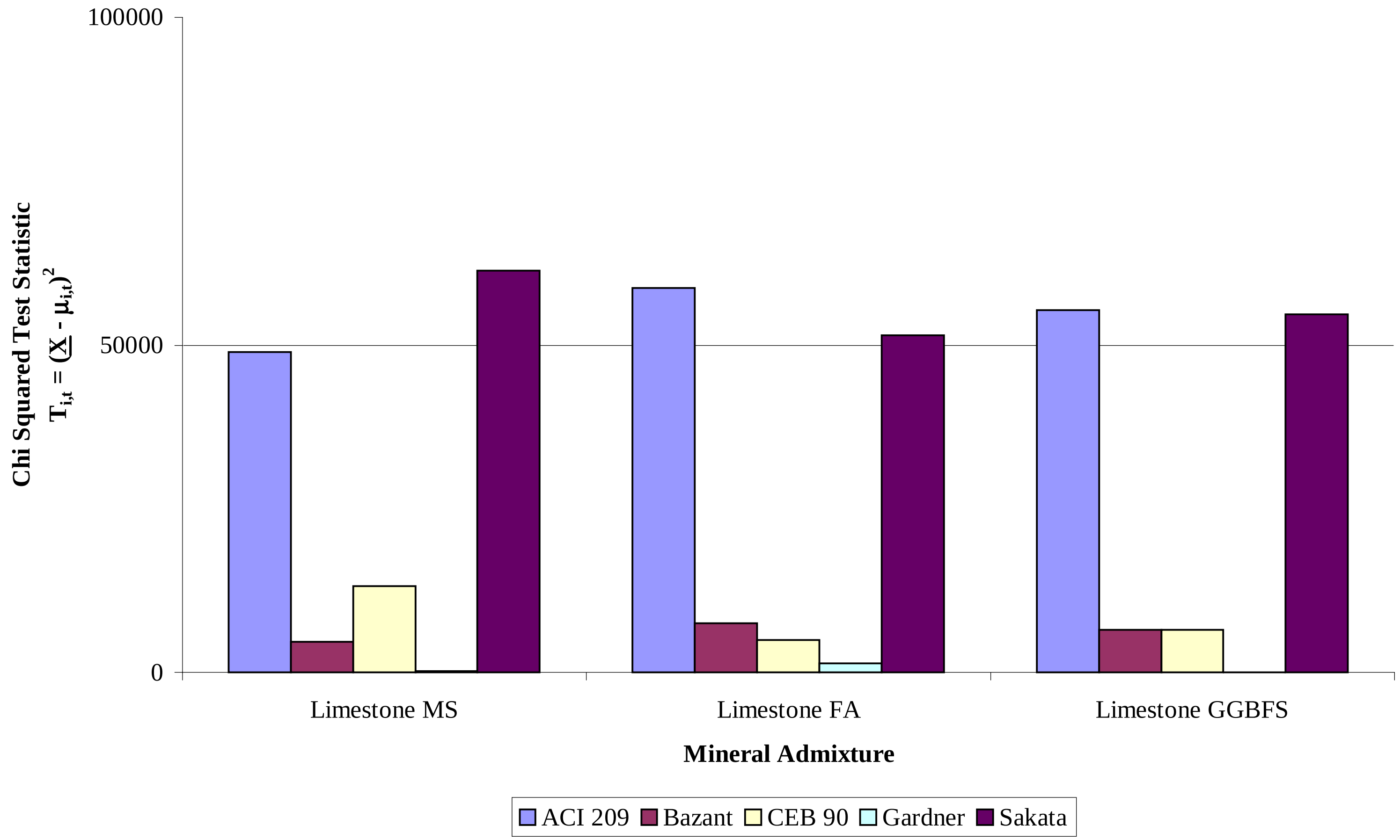

The residual is an average of three values.

FIGURE 50. CHI SQUARED ANALYSIS FOR BASIC CREEP OF PORTLAND CEMENT PLUS MINERAL ADMIXTURE CONCRETE AT 97 DAYS AFTER CASTING

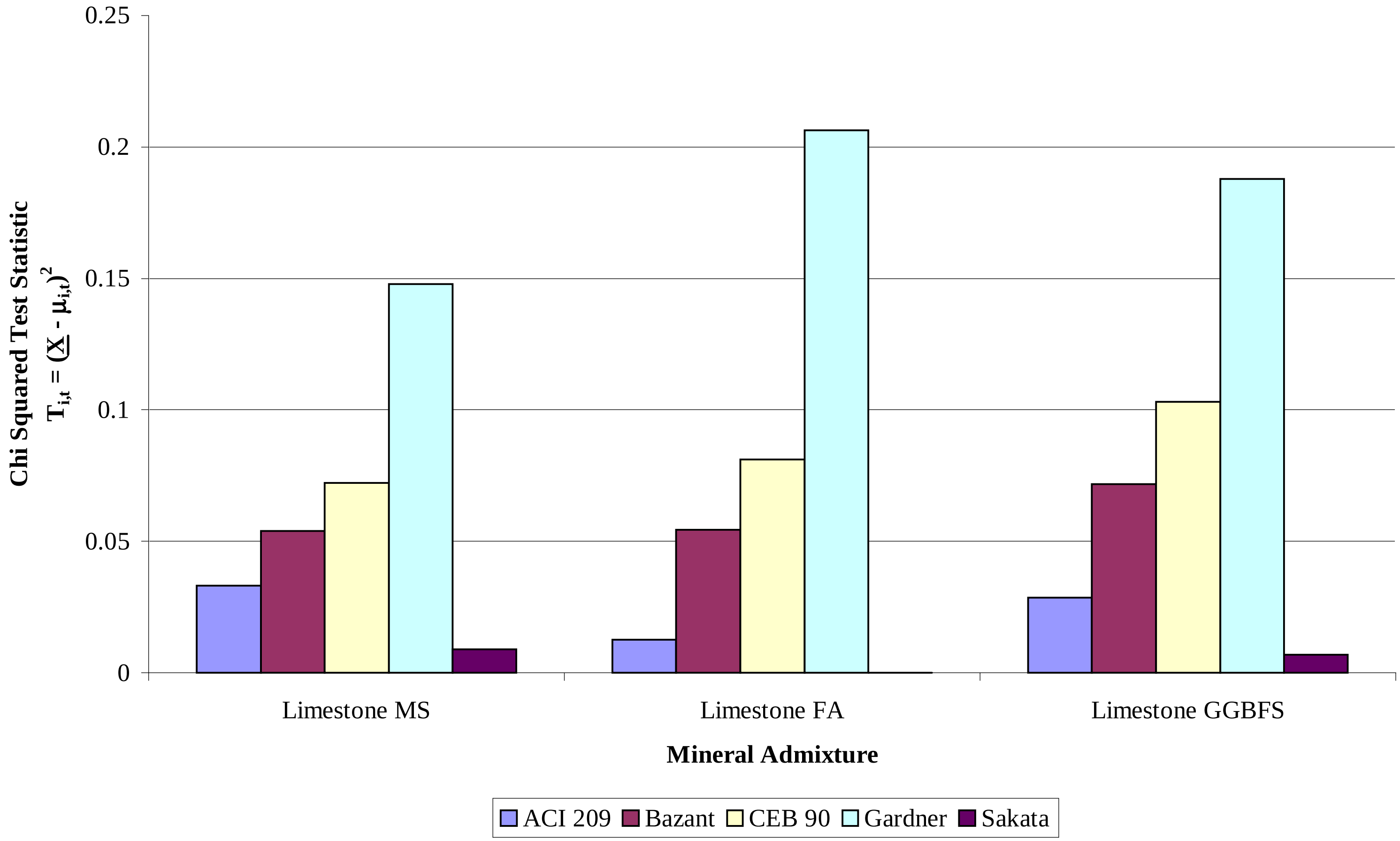

The residual is an average of three values.

FIGURE 51. DIFFERENCE BETWEEN MODELS PREDICTION AND AASHTO LRFD DESIGN VALUES FOR CREEP STRAIN (PERCENT)

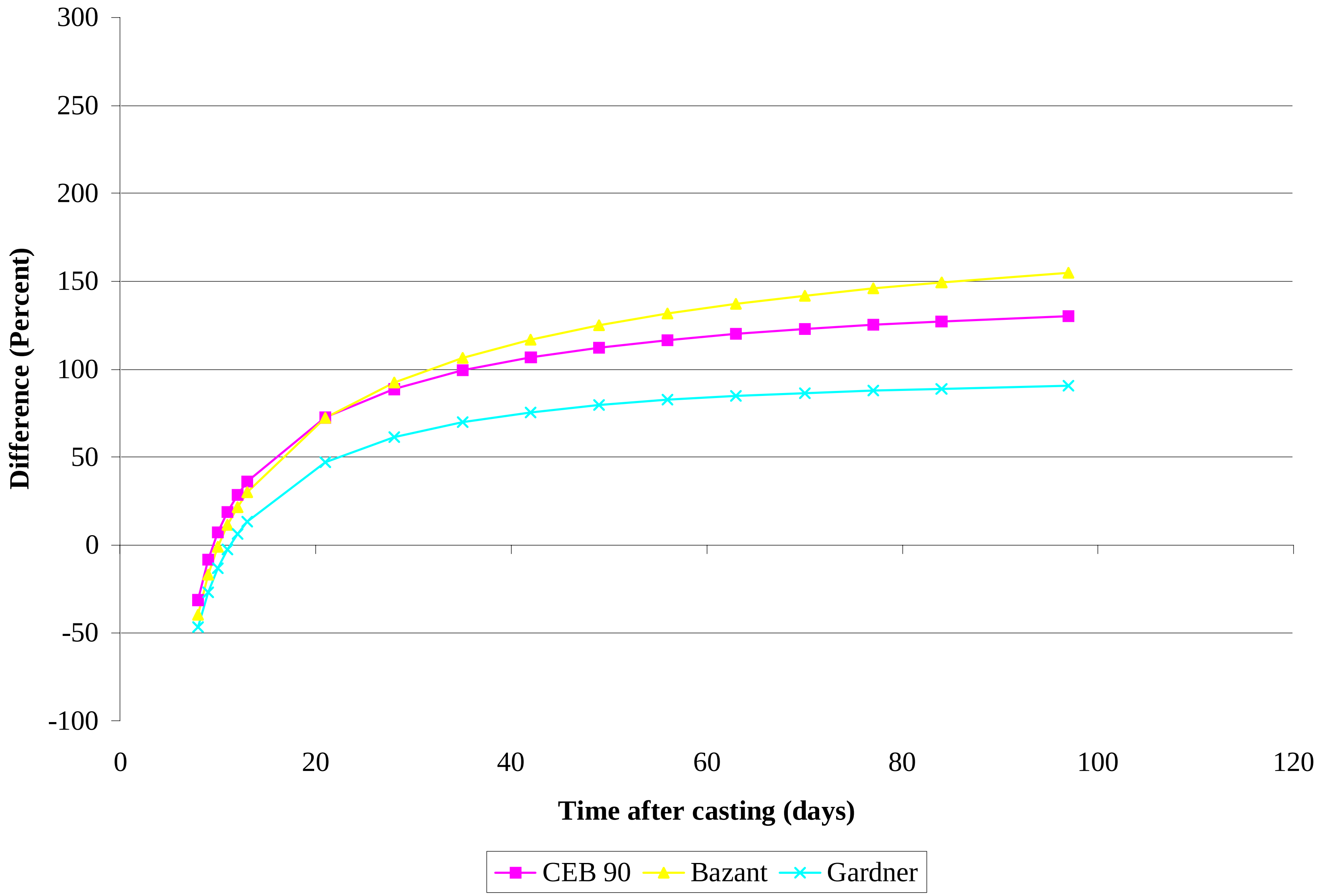

FIGURE 52. DIFFERENCE BETWEEN MODELS PREDICTION AND AASHTO LRFD DESIGN VALUES FOR CREEP STRAIN (PERCENT)

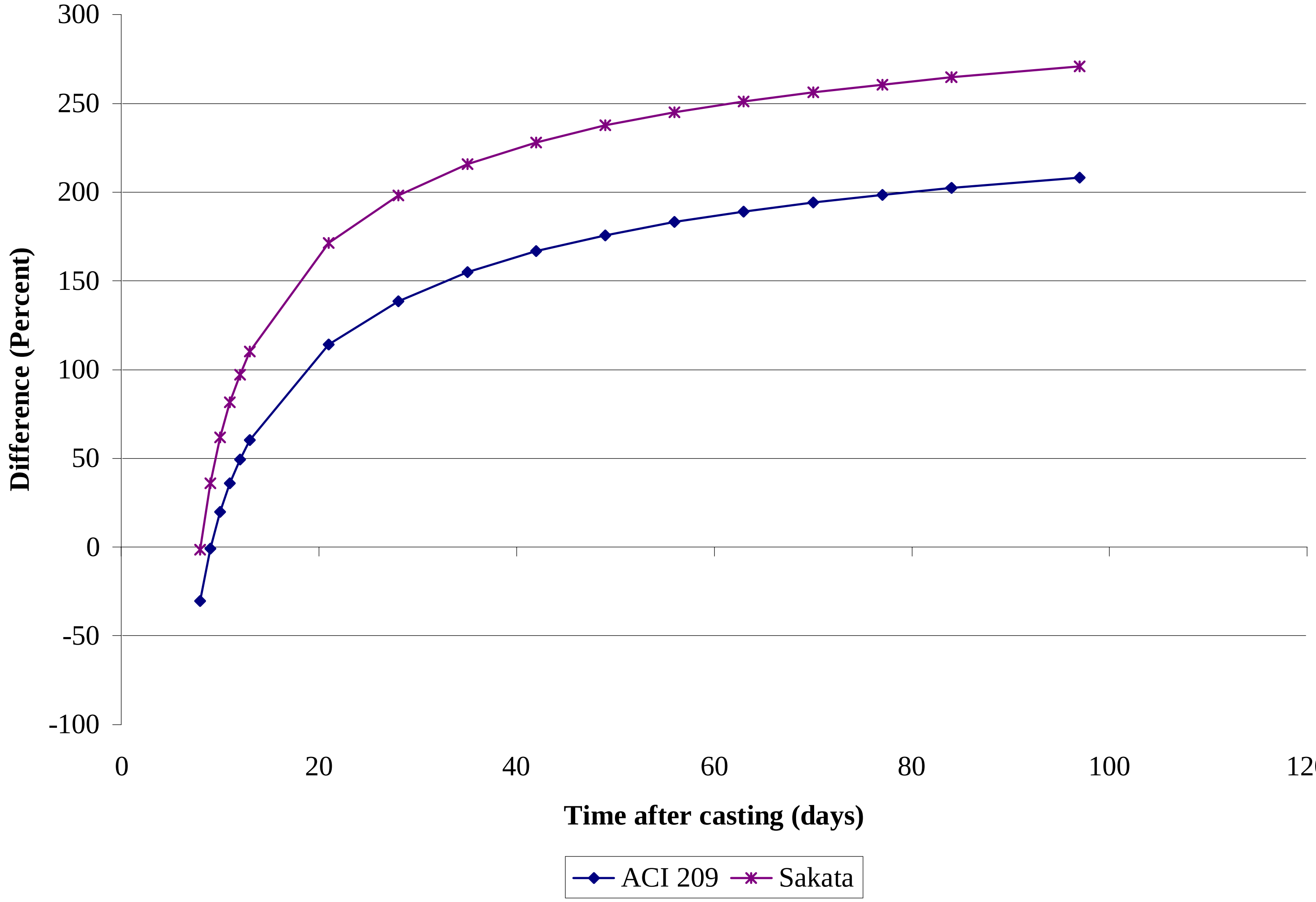

TABLES

TABLE 1. SPECIMENS FOR COMPRESSIVE CREEP TESTING CYCLES

Test Cycle I

Frame 1	Frame 2	Frame 3	Frame 4
Limestone MS B1-S1	Limestone B1-S2	Limestone MS B2-S1	Limestone MS B3-S2
Limestone B2-S1	Limestone B2-S2	Limestone MS B3-S1	Limestone MS B2-S2
Limestone B1-S1	Limestone MS B1-S2	Limestone B3-S1	Limestone B3-S2

Test Cycle II

Frame 1	Frame 2	Frame 3	Frame 4
Diabse B2-S1	Diabase B1-S2	Gravel B2-S1	Gravel B2-S2
Gravel B1-S1	Gravel B1-S2	Gravel B3-S1	Diabase B3-S2
Diabase B1-S1	Diabse B2-S2	Diabase B3-S1	Gravel B3-S2

Test Cycle III

Frame 1	Frame 2	Frame 3	Frame 4
Limestone GGBFS B1-S1	Limestone GGBFS B2-S2	Limestone GGBFS B3-S1	Limestone GGBFS B3-S2
Limestone FA B1-S1	Limestone FA B1-S2	Limestone FA B2-S1	Limestone FA B2-S2
Limestone GGBFS B2-S1	Limestone GGBFS B1-S2	Limestone FA B3-S1	Limestone FA B3-S2

Specimens are labled - (aggregate type - mineral admixture (where applies) - batch number - specimen number)

TABLE 2. A5 GRAVEL BATCH QUANTITIES AND FRESH CONCRETE PROPERTIES

	Dry Batch Mixture Proportions		
Ingredient	**Batch 1**	**Batch 2**	**Batch 3**
Cement Type I/II, kg	18.6	18.6	18.6
Water, kg	7.2	7.2	7.2
Coarse aggregate, kg	48.2	48.2	48.2
Fine aggregate, kg	28.1	28.1	28.1
Total, kg	102	102	102
AEA: Daravair 1000, ml	9	9	9
HRWR: Daracem 19, ml	100	100	100

	Fresh Concrete Properties		
	Batch 1	**Batch 2**	**Batch 3**
w/c	0.35	0.35	0.35
Temperature, C	22	22	22
Slump, mm	65	90	90
Air Content, %	3.5	4.5	5.3
Unit Weight$_{prop}$, kg/m^3	2451	2451	2451
Unit Weight$_{measured}$, kg/m3	2387	2355	2355
Relative Yield, prop/measured	1.03	1.04	1.04

TABLE 3. A5 LIMESTONE BATCH QUANTITIES AND FRESH CONCRETE PROPERTIES

	Dry Batch Mixture Proportions		
Ingredient	**Batch 1**	**Batch 2**	**Batch 3**
Cement Type I/II, kg	17.8	17.8	17.8
Water, kg	6.2	6.2	6.2
Coarse aggregate, kg	44.6	44.6	44.6
Fine aggregate, kg	33.4	33.4	33.4
Total, kg	102	102	102
AEA: Daravair 1000, ml	9	9	9
HRWR: Daracem 19, ml	225	188	174

	Fresh Concrete Properties		
	Batch 1	**Batch 2**	**Batch 3**
w/c	0.33	0.33	0.33
Temperature, C	22	21	22
Slump, mm	100	90	75
Air Content, %	5.0	4.5	5.1
Unit Weight$_{prop}$, kg/m^3	2377	2377	2377
Unit Weight$_{measured}$, kg/m3	2465	2454	2435
Relative Yield, prop/measured	0.963	0.970	0.976

TABLE 4. A5 DIABASE BATCH QUANTITIES AND FRESH CONCRETE PROPERTIES

Dry Batch Mixture Proportions

Ingredient	**Batch 1**	**Batch 2**	**Batch 3**
Cement Type I/II, kg	17.9	17.9	17.9
Water, kg	7.0	7.0	7.0
Coarse aggregate, kg	48.2	48.2	48.2
Fine aggregate, kg	28.3	28.3	28.3
Total, kg	101	101	101
AEA: Daravair 1000, ml	9	9	9
HRWR: Daracem 19, ml	60	60	100

Fresh Concrete Properties

	Batch 1	**Batch 2**	**Batch 3**
w/c	0.39	0.39	0.39
Temperature, C	22	21	22
Slump, mm	75	90	75
Air Content, %	3.1	3.1	3.7
Unit $Weight_{prop}$, kg/m^3	2563	2563	2563
Unit $Weight_{measured}$, kg/m3	2515	2499	2483
Relative Yield, prop/measured	1.02	1.03	1.03

TABLE 5. A5 LIMESTONE GGBFS BATCH QUANTITIES AND FRESH CONCRETE PROPERTIES

	Dry Batch Mixture Proportions		
Ingredient	**Batch 1**	**Batch 2**	**Batch 3**
Cement Type I/II, kg	10.8	10.8	10.8
Slag, kg	7.2	7.2	7.2
Water, kg	6.3	6.3	6.3
Coarse aggregate, kg	44.8	44.8	44.8
Fine aggregate, kg	33.1	33.1	33.1
Total, kg	102	102	102
AEA: Daravair 1000, ml	10	9	9
HRWR: Daracem 19, ml	120	140	130

	Fresh Concrete Properties		
	Batch 1	**Batch 2**	**Batch 3**
w/c	0.33	0.33	0.33
Temperature, C	27	27	25
Slump, mm	65	150	50
Air Content, %	4.8	6.8	4.2
Unit Weight$_{prop}$, kg/m^3	2367	2367	2367
Unit Weight$_{measured}$, kg/m3	2410	2379	2444
Relative Yield, prop/measured	0.982	0.995	0.969

TABLE 6. A5 LIMESTONE FLY ASH BATCH QUANTITIES AND FRESH CONCRETE PROPERTIES

	Dry Batch Mixture Proportions		
Ingredient	**Batch 1**	**Batch 2**	**Batch 3**
Cement Type I/II, kg	15.3	15.3	15.3
Fly Ash, kg	3.6	3.6	3.6
Water, kg	6.3	6.3	6.3
Coarse aggregate, kg	45.1	45.1	45.1
Fine aggregate, kg	31.8	31.8	31.8
Total, kg	102	102	102
AEA: Daravair 1000, ml	10	10	10
HRWR: Daracem 19, ml	125	100	110

	Fresh Concrete Properties		
	Batch 1	**Batch 2**	**Batch 3**
w/c	0.32	0.32	0.32
Temperature, C	28	26	25
Slump, mm	150	65	125
Air Content, %	5.8	4.3	5.3
Unit Weight$_{prop}$, kg/m^3	2355	2355	2355
Unit Weight$_{measured}$, kg/m3	2377	2426	2399
Relative Yield, prop/measured	0.991	0.971	0.982

TABLE 7. A5 LIMESTONE MICROSILICA BATCH QUANTITIES AND FRESH CONCRETE PROPERTIES

	Dry Batch Mixture Proportions		
Ingredient	**Batch 1**	**Batch 2**	**Batch 3**
Cement Type I/II, kg	16.6	16.6	16.6
Microsilica, kg	1.3	1.3	1.3
Water, kg	6.3	5.9	5.9
Coarse aggregate, kg	44.8	44.8	44.8
Fine aggregate, kg	33.1	33.1	33.1
Total, kg	102	102	102
AEA: Daravair 1000, ml	9	9	9
HRWR: Daracem 19, ml	236	264	304

	Fresh Concrete Properties		
	Batch 1	**Batch 2**	**Batch 3**
w/c	0.33	0.31	0.31
Temperature, C	22	22	22
Slump, mm	75	100	75
Air Content, %	4.5	4.4	3.8
Unit Weight$_{prop}$, kg/m^3	2368	2368	2368
Unit Weight$_{measured}$, kg/m3	2441	2435	2478
Relative Yield, prop/measured	0.970	0.972	0.955

TABLE 8. COMPRESSION STRENGTH AND ELASTIC MODULUS OF CONCRETE MIXTURES

Compression Strength (MPa)

Time	Gravel	Diabase	Limestone	Limestone MS	Limestone FA	Limestone GGBFS
7	33	36	44	50	34	41
14	37	40	49	56	42	48
28	42	42	51	63	46	50
56	41	43	52	65	46	47

Elastic Modulus (10^3 MPa)

Time	Gravel	Diabase	Limestone	Limestone MS	Limestone FA	Limestone GGBFS
7	32	41	41	40	39	41
28	34	36	41	41	38	38

The compressive strength and elastic modulus were calculated as an average of six measurements.

TABLE 9. CHI SQUARE ANALYSIS FOR TOTAL STRAIN

Average Total Strain Chi Squared Values (microstrain^2)

	28 Day		97 Day
CEB 90	17300	**Sakata**	23000
Sakata	36790	**CEB 90**	39100
ACI 209	52850	**ACI 209**	159500
Bazant	55810	**Bazant**	170760
Gardner	82030	**Gardner**	326620

Average Drying Shrinkage Strain Chi Squared Values (microstrain^2)

	28 Day		97 Day
Sakata	11738	**Gardner**	9894
Gardner	24111	**Bazant**	20748
Bazant	31784	**CEB 90**	26424
CEB 90	35993	**Sakata**	39541
ACI 209	48057	**ACI 209**	100979

Average Basic Creep Strain Chi Squared Values (microstrain^2)

	28 Day		97 Day
Sakata	0.031	**Sakata**	0.020
ACI 209	0.053	**ACI 209**	0.038
Bazant	0.100	**Bazant**	0.082
CEB 90	0.105	**CEB 90**	0.119
Gardner	0.153	**Gardner**	0.207

APPENDIX A

Creep of Concrete Literature Review and Model Equations

TABLE OF CONTENTS

INTRODUCTION **94**

INFLUENCE OF CONCRETE COMPOSITION ON CREEP **95**

EFFECT OF AGGREGATE 95

EFFECT OF CEMENT TYPE AND FINENESS 96

Ground Granulated Blast Furnace Slag *97*

EFFECT OF CEMENT CONTENT AND WATER CONTENT 98

EFFECT OF MINERAL ADMIXTURES 98

Condensed Silica Fume *98*

Fly Ash *100*

EFFECTS OF CHEMICAL ADMIXTURES 101

EFFECTS OF CURING 101

EFFECTS OF AMBIENT CONDITIONS 101

EFFECTS OF SPECIMEN SIZE 102

HIGH STRENGTH CONCRETE 102

SUMMARY 103

PERFORMANCE SPECIFICATIONS **106**

BRIDGE COMPONENTS 106

Prestressed Members *106*

PORTLAND CEMENT CONCRETE STRUCTURES 106

REPAIR MATERIALS 107

CREEP MODELS **108**

MODEL LIMITATIONS **109**

MODELS: PARAMETERS AND FUNCTIONS **111**

ACI 209 CODE MODEL 111

CEB 90 CODE MODEL 115

THE B3 MODEL 120

THE GZ MODEL 125

THE SAK MODEL 130

REFERENCES 132

INTRODUCTION

Concrete experiences volume changes throughout its service life. The total in-service volume change of concrete is the resultant of applied loads and shrinkage. When loaded, concrete experiences an instantaneous recoverable elastic deformation and a slow inelastic deformation called creep. Creep of concrete is composed of two components, basic creep, or deformation under load without moisture loss and drying creep, or deformation under drying conditions only. Deformation of concrete in the absence of applied load is often called shrinkage.

There are three types of shrinkage; autogeneous, drying, and carbonation shrinkage. Autogeneous shrinkage is the resultant of the hydration process. The hydrated cement paste is smaller in volume than the solid volume of the cement paste and water. Drying shrinkage is caused by the loss of evaporable water. Carbonation shrinkage is caused by the carbonation of hydrated cement products and possibly from the movement of water from the gel pores to the capillary pores.

Creep testing of concrete may be performed on sealed specimens or unsealed specimens. The deformation of sealed-loaded specimens is the resultant of elastic deformation, water movement from the gel pores to the capillary pores, and autogeneous shrinkage. Whereas, the deformation of unsealed-loaded specimens is the resultant of internal moisture movement, moisture loss, autogeneous shrinkage, and carbonation shrinkage. The deformation of unsealed-unloaded, or drying shrinkage is the resultant of moisture loss, autogeneous shrinkage, and carbonation shrinkage. Thus, the difference in deformations between loaded specimens, minus the elastic deformation, and unloaded specimens, is basic creep, which is the resultant of internal moisture movement.

Creep of concrete is normally evaluated using unsealed loaded and unloaded companion specimens exposed at a constant drying environment. Thus, the total deformation may be separated into the elastic compression, basic creep, and drying creep (moisture loss, autogeneous and carbonation shrinkage.)

Carlton and Mistry[1A] discussed the seepage theory of creep. In this theory, the deformation due to creep is attributed to the movement of water between the different phases of the concrete.

When an external load is applied, it changes the attraction forces between the cement gel particles. This change in the forces causes an imbalance in the attractive and disjoining forces. However, the imbalance is gradually eliminated by the transfer of moisture into the pores in cases of compression, and away from the pores in cases of tension.[1A]

INFLUENCE OF CONCRETE COMPOSITION ON CREEP

Factors which contribute to the dimensional changes may be categorized as, mixture composition, curing conditions, ambient exposure conditions, and element geometry. In addition to the above factors, this report shall address creep performance specifications for bridge components and other portland cement concrete structures, repair materials, and alternate construction materials. With respect to mixture compositions, the influence of aggregate type, cement type and fineness, cement and water content, and mineral and chemical admixtures will be addressed.

The literature is abundant with the influence of these parameters on the creep of portland cement concrete. As with all research activities, the study of the creep of concrete has active and dormant periods. The discussion presents a review of the more active 15 year period, from 1985 through 1999.

Effect of Aggregate

The aggregate particles reinforce the cement paste against contraction. The ability of aggregates to restrain movement of a cement paste depends upon the extensibility of the paste, the degree of cracking of the paste, compressibility of the aggregate, and changes in the aggregate moisture content.[2A] Generally, concretes that have aggregates that are hard, dense, and have low absorption and high modulus of elasticity are desirable when concrete with low creep is needed.[2A]

Han and Walraven[3A] examined the effect of aggregate in high strength concrete on creep. The different concrete mixtures included three types of aggregate: crushed gravel, granite, and limestone. Two types of creep tests were conducted. Tests for normal age concrete, 28 days cured, with stress/strength ratio: 15, 35, and 50 %, and tests for early age concrete, 16 hours cured, loaded at: 30, 50, and 70 % of the ultimate strength. The normal age creep tests were conducted at 20 °C, 65 % relative humidity. The early age creep tests were conducted at 20 °C, 50 % relative humidity. The influence of the aggregate used on the creep deformation was significantly less than the early elastic modulus of the concrete, and similar to that of the shrinkage characteristics.[3A]

Alexander[4A] studied the influence of 23 aggregate types on concrete deformation. Shrinkage and creep tests were conducted on 100 x 100 x 200 mm (4 x 4 x 8 in) prisms in a controlled environment, 23 °C (73°F), 60 % relative humidity. Creep tests were conducted for six months after a 28 day fully water cured period, in lime saturated water to allow for minimal effects of hydration. Strains were measured using longitudinal gages on two opposite faces of the prism with a gage length of 100 mm (4 in). The influence of aggregates on creep of concrete had two primary effects: the absorption of the aggregates, and the stiffness of the aggregate relative to the cement paste. The cement paste was the primary source of shrinkage and creep. In summary, aggregate with a lower absorption will therefore produce concrete with lower creep and shrinkage characteristics. It was further determined that higher elastic modulus concrete produce lower creep values. Thus, aggregates affect concrete deformation through water demand, aggregate stiffness and volumetric concentration, and a mechanical bond between the paste and aggregate.[4A]

Collins examined the creep and shrinkage of high strength concrete. Creep and shrinkage tests were conducted according to ASTM C 512. The results demonstrated that a concrete with a large maximum aggregate size and lower paste content will provide more desirable, lower, creep and shrinkage characteristics.[5A]

Effect of Cement Type and Fineness

Cement type and fineness affects the behavior of the concrete during hydration. High early strength cement typically shrinks and creeps more than normal cement. Low heat and portland-pozzolan cements produce larger percentages of gel compared to normal portland cement, thus causing an increase in shrinkage and creep.

Generally, finer cement particles exhibit less shrinkage under moist conditions. The lower the fineness of a low-heat cement, the higher the creep in the concrete. Cement fineness has little influence on the amount of creep of concretes containing ordinary cement.[2A]

Ground Granulated Blast Furnace Slag

GGBFS is similar to fly ash. Slag particles of less than 10 μm contribute to early strengths in concrete up to 28 days; particles of 10 to 45 μm contribute to later strengths, but particles coarser than 45 μm are difficult to hydrate.[6A] Most GGBFS is pulverized below 45 μm. GGBFS may cause an increase in autogeneous shrinkage and early creep, but for later ages, GGBFS has little effect or a reducing effect on creep and shrinkage reduction.[6A]

Alexander[7A] examined the properties of blended cement concrete containing blast furnace slag, and condensed silica fume (CSF). Blend ratios of the GGBFS cements were 50:50 OPC:GGBFS. CFS was blended at 5% of the total cementitious materials. Creep and shrinkage were tested on 100 x 100 x 200 mm (4 x 4 x 8 in) prisms. The specimen were stored in a controlled environment of 23 ± 1 °C (73 °F), 60 ± 5 % relative humidity. Half the prisms were sealed, and the others were left exposed.[7A]

For unsealed prisms, addition of slag increases the specific creep by about 10 % in mixes containing blends of ordinary portland cement and GGBFS compared to ordinary portland cement concrete. Specific creep is defined as the creep strain per unit stress.[7A] For sealed prisms, addition of slag generally reduces shrinkage and specific creep by more than 40 %.

In summary, the addition of GGBFS to plain portland cement has the effect of:

1. Causing an increase in early age creep of unsealed specimens, but having reversing effects on later age specimens.
2. Significantly reducing creep and shrinkage strains for sealed specimens.
3. The magnitude of the variation within-source, and between-source of portland cement may be reduced with the addition of GGBFS, thus producing a more consistent product.[7A]

Effect of Cement Content and Water Content

A higher w/c ratio increases the size of the pores in the cement paste. The water has a more continuous path to flow through the cement paste, and then under a sustained load the water of absorption may be expelled more readily to cause a high rate of creep. When a constant w/c ratio is maintained, creep increases as the slump and cement content increases or as the amount of cement paste is increased.[2A]

Wiegrink, Marikunte, and Shah[8A] examined the creep and shrinkage of high strength concrete. Creep specimens of 400 mm (16 in) long and a 100 mm (4 in) cross section, were cured for two days in 20 °C (68 °F) and 50 % relative humidity. They were then loaded to 40 percent of the maximum three days compressive strength in accordance to ASTM C 512. Observations were that the specific creep decreased with decreasing water content for the conditions of a constant aggregate to cement ratio.[8A]

Effect of Mineral Admixtures

Mineral admixtures have become more popular in concrete mixtures especially for high strength concrete. Typical mineral admixtures used are CSF and fly ash (FA). In general, admixtures that increase the water requirement of concrete increase the creep and shrinkage, and those that decrease the water requirement, decrease the creep and shrinkage.[2A]

Condensed Silica Fume

CSF is an industrial by-product with a particle size distribution of 100 times finer than ordinary portland cement.[6A] The material, which is highly pozzolanic, also creates a greater demand for water or a high range water reducer.[6A]

The specific creep decreases with increasing CFS content.[8A] Alexander[7A] found that the addition of CSF had little effect on unsealed specimens, but further reduced the creep in sealed specimens.

Tazawa and Yonekura[9A] examined creep of concrete with CSF. Specimens were 100 x 100 x 400 mm (4 x 4 x 8 in) prestressed prisms water or autoclaved cured for 28 days. Prestress of stress-strength ratio of 0.3 was used. The specimens were then placed in a controlled environment of 20 °C (68 °F) and 50 % relative humidity or in water at 20 °C (68 °F). Length changes were measured using contact gages and dial gages for 800 days. There was an increase in specific creep of the concrete with CSF compared to the concrete with out CSF at the same compressive strength under both curing conditions. Creep under a low stress-strength ratio, such as 0.3 in this case, is closely related to the pore size distribution and pore volume of the cement paste.[9A]

Ghosh and Nasser[10A] evaluated the creep and shrinkage on 75 x 225 mm (3 x 9 in) cylindrical specimens that were moist cured in water for 28 days. Specimens were tested both in sealed and unsealed conditions. Concrete mixtures with 20 % and 60 % FA replacement levels together with 10 % CSF, 100 % ASTM Type I control cement and 90 % cement plus 10 % CFS were subjected to creep tests at room temperature 21 °C (70 °F) and 50 ± 4 percent relative humidity, under three different stresses 5, 10, and 14 MPa (750, 1500, and 2000 psi.) After 90 days of loading, the 90 % cement plus 10 % CSF concrete creep behavior was not significantly different than that of the 100 % cement concrete. The 20 % as well as the 60 % FA plus 10 % CSF concrete exhibited lower creep values compared with the 100 % cement concrete under both sealed and unsealed conditions.[10A]

Creep and drying shrinkage tests were conducted by; Khatri, Sirivivatnanon and Gross,[11A] on seven day moist cured specimens at 23 ± 2 °C (73 °F), 50 ± 5 % relative humidity. Creep tests were conducted on 150 mm x 300 mm (6 x 12 in) cylinders. The cylinders were loaded up to 40 % of the compressive strength of the concrete. The paste content and water to cement plus pozzolan ratio of all the mixes were held constant. Mixture parameters were:

1. General portland cement (ASTM Type I)
2. High slag cement (65 % slag)
3. Slag cement (35 % slag)
4. Class F fly ash (15 % and 25 % FA)
5. Silica fume (10 % CSF)

Addition of CSF considerably reduces the specific creep of concrete prepared from ordinary portland cement. Concrete with 65 % slag and 10 % CSF, and 35 % slag cement and 10 % CSF, have marginally less creep than the 100 % general portland cement. The concrete with lesser slag cement content in its paste resulted in lower specific creep than general portland cement. Concrete with FA (15 % and 25 %) and 10 % CSF showed far greater reduction in specific creep than general portland cement. The amount of FA, either 15 % or 25 %, was found to have a negligible effect on creep characteristics of triple blend concretes.[11A]

Fly Ash

Both Class C and Class F fly ash were included in the literature review. The particle size distribution, morphology, and surface characteristics of fly ash used as a mineral admixture exercise a considerable influence on the water requirement and workability of freshly made concrete, and the rate of strength development in hardened concrete.[6A]

Particle sizes range from less then 1 μm to 100 μm in diameter, with more than 50 percent under 20 μm.[6A] The Class C high calcium fly ash is more chemically active than the low calcium Class F fly ash.

Tikalsky, Carrasquillo, and Carrasquillo[12A] conducted creep tests according to ASTM C 512. It was found that the addition of fly ash reduced the creep deformation compared to concrete without fly ash. Fly ash replacements ranged from 0 to 35 %. Class F fly ash showed a greater reduction than the Class C fly ash due to a greater pozzolanic nature, which allows the concrete to continue to gain strength over time.[12A]

Sivasundaram, Carette and Malhotra[13A] performed creep tests on 150 x 300 mm (6 x 12 in) cylinders. Seven different Class F fly ashes were examined in the study. Fly ash consisted of 58% of the total cementitious material for Class F fly ash concrete. The concrete containing fly ash had lower overall creep strains compared to those of normal concrete.[13A]

Swamy[14A] determined that fly ash concrete moist cured for 21 days, and loaded at 28 days, with a 50 % replacement, continues to develop strength over time, while the creep and shrinkage values of fly ash concrete were similar to the creep and shrinkage values of ordinary portland cement concrete.[14A]

Carette and Malhotra[15A] conducted creep tests in accordance with ASTM C 512 Test Method. The specimens were loaded at 30 % of their compressive strength. The tests were conducted in a controlled environment of 23 °C ± 1.7 °C (73 °F), 50 % ± 4 % relative humidity. Eleven different fly ashes were tested at a replacement of 20 % by mass. All fly ash concretes were shown to produce considerably lower creep strains, 20 to 45% difference, than the control concrete.[15A]

Effects of Chemical Admixtures

Chemical admixtures such as high range water reducers are in common use. High range water reducers realign the polarity of the water molecules creating a well-dispersed system and greatly enhance the fluidity of the concrete mixture.[6A] Concrete with a low w/c and a high range water reducer produce a concrete with high workability. In general, high range water reducers do not significantly affect the creep of concrete.[15A]

Effects of Curing

In general, the longer the concrete is cured prior to loading, the less creep will occur.[15A,16A] Chern, Wu and Chang[17A] studied the influence of loading age on long term creep of concrete. Creep tests were conducted on 150 x 300 mm (6 x 12 in) unsealed cylinders. Basic creep tests were performed in a controlled environment of 23 °C (73 °F) and 100 % relative humidity. Drying creep tests were conducted in a dry room of 23 °C (73 °F) and 50 % relative humidity. Specimens were immediately loaded after being moist cured for 7, 29, or 94 days. Specimens loaded at younger ages exhibited a greater amount of creep for both the moist specimens and the specimens in the 50 % relative humidity. The age of the concrete when loaded significantly affects the magnitude of both the drying creep and basic creep of concrete. The older the specimen at the time of loading, the less basic creep and drying creep takes place.[17A]

Effects of Ambient Conditions

Temperature and relative humidity affect the shrinkage and creep behavior of concrete. High temperatures increase the creep deformation of concrete, and are more apparent in concrete that has high slag cement content.[16A] At lower relative humidity more creep and shrinkage occur.[16A]

Schwesinger, Ehlert and Wolfel[18A] tested 150 mm diameter 600 mm long (6 x 24 in) concrete cylinders. The specimens were sealed and heated at 20, 60, 100, and 130 ºC (68, 140, 212, and 266 °F). Temperature greater than 60 °C (140 °F) will result in higher creep strains for sealed specimens, loaded before being heated in a 100% relative humidity condition, than for unsealed specimens after being loaded for over 100 hours.[18A]

Effects of Specimen Size

The size and shape of a concrete specimen significantly influence the rate of loss or gain of moisture under given storage conditions, and this affects the rate of volume changes as well as the total expansion or contraction.[2A] The larger the mass subjected to a sustained loading, the less the creep. A larger concrete specimen will have less moisture movement because it is more difficult for the water to travel to the surface.

A non-uniform volume change will occur more commonly in larger masses of concrete due to larger variations of moisture content. Under drying conditions, near surface shrinkage of concrete will develop tensile stresses in the shrinkage zone, which are in equilibrium with residual compressive stresses developed near the center.[2A]

High Strength Concrete

High strength concrete is defined as concrete that has a compressive strength in excess of 40 MPa (6000 psi).[6A] A combination of chemical and mineral admixtures such as: high range water reducers, or pozzolans are added to the concrete mixture to increase its strength.

Smadi, Slate, and Nilson[19A] compared high, medium and low strength concrete. The 28 day compressive strength ranges are 60 to 70 MPa (8,500 to 10,000 psi), 35 to 40 MPa (5,000 to 6,000 psi), and 20 to 25 MPa (3,000 to 3,500 psi) respectively. Tests were conducted on 100 x 200 mm (4 x 8 in) cylinders in either a normal vertical creep frame or a lever arm creep frame depending on the strength of the concrete. The concrete specimens were moist cured until the beginning of the testing period. Testing conditions were 23 °C (72°F) and 50 % relative humidity.[19A]

Smaller magnitudes of creep strain, creep coefficient, and specific creep (the basic creep per unit stress) for high strength concretes was observed as compared to low and medium strength concretes at all stress levels. Final creep of the cement paste increases as the w/c ratio increases. Creep recovery, defined as the instantaneous recoverable deformation the concrete experiences once the load is removed, was also examined. High strength concrete was found to have the greatest creep recovery. The creep recovery was found to be proportional to the applied stress.[19A]

Khan, Cook and Mitchell[20A] conducted creep tests on both sealed and unsealed 100 x 200 mm (4 x 8 in) cylinders loaded between 5 and 22 % of the concrete compressive strength. Test conditions were 20°C ± 1°C (68 °F) and 50 % ± 10% relative humidity. High, medium and normal strength concretes were observed, 30 MPa (4,350 psi), 70 MPa (10,000 psi), and 100 MPa (14,500 psi) respectively. Two curing methods used were, sealed curing and air-dried curing. The CEB-FIP code was used to predict the measured strains.[20A]

Creep strains were found to decrease with increasing concrete compressive strength. High strength concrete was found to be more sensitive to the age of loading than the medium and normal strength concretes. In the case of the sealed curing specimens, the strain development for the normal strength concretes stabilized quicker than the medium or high strength concretes. The air cured concrete exhibited higher creep strains than the sealed specimens, especially when the specimens were loaded at an early age.[20A]

Summary

In summary, concrete experiences volume changes throughout its service life. The total in-service volume change of concrete is the resultant of applied loads and shrinkage. When loaded, concrete experiences an instantaneous recoverable elastic deformation and a slow inelastic deformation called creep. Creep of concrete is composed of two components, basic creep, or deformation under load without moisture loss and drying creep, or deformation under drying conditions only. Deformation of concrete in the absence of applied load is referred to as shrinkage.

Creep of concrete is normally evaluated using unsealed loaded and unloaded companion specimens exposed at a constant drying environment. Thus, the total deformation may be separated into the elastic compression, basic creep, and drying creep.

Factors which contribute to the dimensional changes may be categorized as, mixture composition, curing conditions, ambient exposure conditions, and element geometry.

Generally, concretes that have aggregates that are hard, dense, and have low absorption and high modulus of elasticity are desirable when concrete with low creep is needed. Aggregate with lower absorption will therefore produce concrete with lower creep and shrinkage characteristics. Concrete with higher elastic modulus will produce lower creep values. Thus, aggregates affect concrete deformation through water demand, aggregate stiffness and volumetric concentration, and paste/aggregate interaction. Concrete with a large maximum aggregate size and lower paste content will have lower creep and shrinkage characteristics.

High early strength cement typically shrinks and creeps more than normal cement. Low heat and portland-pozzolan cements produce larger percentages of gel compared to normal portland cement, thus causing an increase in shrinkage and creep. Generally, finer cement particles exhibit less shrinkage under moist conditions. The lower the fineness of a low-heat cement, the higher the creep in the concrete. Cement fineness has little influence on the amount of creep of concretes containing ordinary cement.

The addition of GGBFS to plain portland cement has the effect of causing an increase in early age creep of unsealed specimens, but having a deceasing effect on later age specimens; significantly reducing creep and shrinkage strains for sealed specimens; reducing the magnitude of the variation within-source, and between-source of portland cement, thus producing a more consistent product.

When a constant w/c ratio is maintained, creep increases as the slump and cement content increases or as the amount of cement paste is increased. The specific creep, the creep strain per unit of applied stress, decreases with decreasing water content for the conditions of a constant aggregate to cement ratio.

Concretes with 20 % as well as the 60 % FA plus 10 % CSF were shown to exhibit lower creep values compared with the 100 % cement concrete under both sealed and unsealed conditions. Addition of CSF considerably reduces the specific creep of concrete prepared from ordinary portland cement. Concrete with 65 % slag and 10 % CSF, and concrete with 35 % slag cement and 10 % CSF, have marginally lower creep strains than concrete with 100 % general portland cement. Concrete with lesser slag content in its paste will experience lower specific creep than general portland cement. Concrete with FA (15 % and 25 %) and 10 % CSF may show far greater reduction in specific creep than general portland cement. The amount of FA, either 15 % or 25 %, was found to have a negligible effect on creep characteristics of triple blend concretes.

The addition of fly ash reduced the creep deformation compared to concrete without fly ash with replacements ranging from 0 to 35 %. Class F fly ash may show a greater reduction than the Class C fly ash due to a greater pozzolanic nature, which allows the concrete to continue to gain strength over time.

Specimens loaded at younger ages exhibited a greater amount of creep for ambient conditions of either 100 % relative humidity or specimens in the 50 % relative humidity. The age of the concrete when loaded significantly affects the magnitude of both the drying creep and basic creep of concrete. The older the specimen at the time of loading, the less basic creep and drying creep takes place.

PERFORMANCE SPECIFICATIONS

Bridge Components

Prestressed Members

The major sources of time dependent prestress loss are creep and shrinkage of concrete. Among other factors, the losses are influenced by ambient conditions.

Saiidi et al.[21A] investigated the prestress variation in a prestressed concrete box girder bridge, where ambient relative humidity is highly variable. The creep and shrinkage losses were found to be 30 % higher than those calculated using a time step analysis and 60 % higher than those estimated by AASHTO specifications. This is due to prestress forces changing as a result of seasonal variation of temperature and humidity. The monthly relative humidity that exceeded 50 percent relative humidity increased the camber in the bridge concrete box girder, due to absorption of ambient moisture.[21A]

Densford, Hendrick, and Murray[22A] studied the creep and shrinkage of prestressed steel member bridges. Two W21 x 50 steel beams were used in a composite design with a 7 in concrete slab. Under a sustained loading, the effects of creep and shrinkage became negligible after 100 days. After the 100 days, the camber of the unit varied inversely with the temperature change of the environment without a long-term affect due to the absorption of ambient moisture around the bridge.[22A]

Portland Cement Concrete Structures

Structures using reinforced concrete sections, and steel-concrete composite sections are also susceptible to creep and shrinkage dilemmas.

In composite steel-concrete beams, the concrete slab shrinkage is restrained due to shear forces induced between the concrete and steel connection.[23A] The composite beam will deflect as the concrete slab shrinks with time.[23A] Uy and Bradford[24A] found that composite beams with steel and concrete have significantly less time dependent deformations then those of reinforced concrete beams.

Bakoss et al.[25A] compared long-term deflections of reinforced concrete beams to prediction models. The creep coefficients predicted by ACI 209 model was found to be lower then the measured values. The CEB-FIP model was found to be somewhat higher. The increased shrinkage strain agreed with values of the ACI 209 model and was much higher than the CEB-FIP model prediction.[25A]

High strength concrete beams were tested for long-term deflections and compared to the ACI Building Code predictions, by Paulson, Nilson, and Hover.[26A] The ACI Building Code greatly over estimated the deflections for high strength concrete beams in the range of about 90 MPa (13,000 psi).[26A]

Repair Materials

The repair of concrete will be an issue as long as there are concrete structures. Problems in the past, with durability of repair work, have been excessive.

The magnitude of the shrinkage strain governs formation of cracks, while the magnitude of creep allows for stress relaxation. In order to have a high resistance to cracking, the repair material should have a low elastic modulus, low shrinkage, high tensile strength, and high creep.[27A]

Emberson and Mays[28A] tested repair materials on reinforced concrete members in flexure. Materials with a low modulus value may generate higher stresses in the existing concrete compared to those in the repair material leading to a potential bond failure. In zones of flexural compression, higher deflections and early yielding of the tensile reinforcing steel may occur.[28A]

In the tensile zone, low-modulus materials may generate stress in the existing concrete adjacent to the transverse repair-substrate interface. Conversely, materials with high modulus values place higher demands on interfacial adhesion. Tensile strength of the repair material should always be greater than that of the existing concrete.[28A]

Under sustained loads, the creep deflections of beams may be directly related to the creep characteristics of the repair materials themselves.[28A]

Cleland, Yeoh, and Long[29A] found that epoxy repair materials exhibited less shrinkage than cementitous materials.

CREEP MODELS

Creep coefficient, specific creep, or creep compliance are generally used to describe creep strain by different models. The creep coefficient is defined as the ratio of creep strain (basic plus drying creep) at a given time to the initial elastic strain. The specific creep is defined at the creep strain per unit stress. The creep compliance is defined as the creep strain plus elastic strain per unit stress, whereas the elastic strain is defined as the instantaneous recoverable deformation of a concrete specimen during the initial stage of loading.

Designs typically use one of the two code models to estimate creep and shrinkage strain in concrete, ACI 209 model recommended by the American Concrete Institute or the Eurocode 2 model recommended by the Euro-International Committee. The ASSHTO LRFD is based on the ACI 209 model. Three other models are the B3 model, developed by Bazant, the GZ model, developed by Gardner, and the SAK model developed by Sakata.[30A] A recent comparison of four of these models using the distribution of residuals of the creep compliance showed that the ACI 209, B3, Eurocode, and the GZ models over estimated the creep compliance by 23%, 42%, 39%, and 58%, of the total number of data points and underestimated the creep compliance by 77%, 58%, 61%, and 42% respectively.[31A] The mean coefficient of variation for the residuals for the ACI 209, B3, Eurocode, and GZ models were 38.6%, 32%, 31%, and 31% respectively. Model parameters and functions are presented in the following section.

MODEL LIMITATIONS

Each model has various complexity and limitations. The table below presents each model variable and the corresponding limitations.

Variable	ACI 209	CEB 90	Bazant	Gardner	Sakata
f_{cm} (psi)	-	2,900-13,000	2,500–10,000	2,900-10,000	-
a/c	-	-	2.5-13.5	-	-
c (lbs/ft^3)	-	-	10-45	-	16-31
w/c	-	-	0.35-0.85	0-0.6	0.4-0.6
H (%)	40-100	40-100	40-100	40-100	40-80
Cement Type	I or III	R, SL or RS	I, II or III	I, II or III	I or III
t_o or t_s (moist cured)	≥ 7 days	-	$t_s \leq t_o$	≥ 2 days	≥ 7 days
t_o or t_s (steam cured)	≥ 1-3 days	-	$t_s \leq t_o$	≥ 2 days	≥ 7 days

Where;

f_{cm} = 28 day mean compressive strength

a/c = Aggregate to cement ratio (by weight)

c = Cement content

w/c = water to cement ratio (by weight)

H = Relative humidity

Cement Type

ASTM Type I = Normal portland cement

ASTM Type II = Moderate sulfate resistance cement

ASTM Type III = High early strength cement

R = Equivalent to ASTM Type I

SL = Equivalent to ASTM Type II

RS = Equivalent to ASTM Type III

t_o = Age of concrete at loading

t_s = Age of concrete at the beginning of shrinkage

MODELS: PARAMETERS AND FUNCTIONS

ACI 209 Code Model

Nomenclature

$C_c(t)$	= Creep coefficient at time t
t	= Time after loading (days)
E_{cmto}	= Modulus of Elasticity at age of loading
$\varepsilon(t)$	= Total Strain; instantaneous plus creep and shrinkage
$\varepsilon_s(t)$	= Shrinkage Strain (in/in)
$f_c'(t_o)$	= Mean concrete compressive strength at age of loading (psi)
$f_c'_{28}$	= Mean 28 day compressive strength (psi)
t_o	= Age of concrete loading (days)
γ	= Unit weight of concrete (lbs/yd^3)
t_s	= Time after the beginning of shrinkage (days)
K_{SS}	= Shape and size correction factor for shrinkage
K_{SH}	= Relative humidity correction factor for shrinkage
ε_{shu}	= Ultimate shrinkage strain (in/in)
C_{cu}	= Ultimate creep coefficient
K_{CH}	= Relative humidity correction factor for creep
K_{CA}	= Age at loading correction factor
K_{CS}	= Shape and size correction factor for creep
H	= Relative humidity (%)
V/S	= Volume to surface area ratio (in)

Model

Creep Compliance Function[30A]

$$\text{Compliance function } [\mu\varepsilon / \text{psi}] = \frac{(1 + C_c(t))}{E_{cmto}}$$

Total Strain

$$\varepsilon(t) = \varepsilon_s(t) + \frac{\sigma}{E_{cmto}}(1 + C_c(t))$$

Calculate Compressive Strength:

$$f_c'(t_o) = f_c'{}_{(28)}(t_o / (b+c\, t_o))$$

where;

$f_c'(t_o)$ = compressive strength of concrete at age of concrete loading, t_o

Type of Cement	**Moist Cured Concrete**		**Steam Cured Concrete**	
I	b = 4.0	c = 0.85	b = 1.0	c = 0.95
III	b = 2.3	c =0.92	b = 0.7	c = 0.98

Note: The experimental $f_c'(t_o)$ was used for the calculations to obtain a more accurate value.

Calculate Modulus of Elasticity:

$$E_{cmto} = 33(\gamma)^{3/2}\,(f_c'(t_o))^{1/2}$$

Note: The experimental E_{cmto} was used when calculating the compliance function to obtain a more accurate value.

Calculate Shrinkage Strain:

$$\varepsilon_s(t) = \frac{t_s}{b + t_s} K_{SS}\, K_{SH}\, \varepsilon_{shu}$$

$K_{SS} = 1.14 - 0.09(V/S)$

$\varepsilon_{shu} = 780 \times 10^{-6}$ in/in

Humidity	**Moist Cured Concrete**	**Steam Cured Concrete**
$40\ \% \leq H \leq 80\ \%$	$b = 35$ $t \geq 7$ days $K_{SH} = 1.4 - 0.01H$	$b = 55$ $t \geq 1$ to 3 days $K_{SH} = 1.4 - 0.01H$
$80\ \% \leq H \leq 100\ \%$	$b = 35$ $t \geq 7$ days $K_{SH} = 3 - 0.03H$	$b = 55$ $t \geq 1$ to 3 days $K_{SH} = 3 - 0.03H$

Calculate Creep Strain:

$$\text{Creep Strain} = \frac{\sigma}{E_{cmto}} C_c(t)$$

Where; $$C_c(t) = \frac{t^{0.6}}{10 + t^{0.6}} C_{cu}\, K_{CH}\, K_{CA}\, K_{CS}$$

and

$C_{cu} = 2.35$

$K_{CH} = 1.27 - 0.0067H$

$K_{CS} = 1.14 - 0.09(V/S)$

Moist Cured Concrete	**Steam Cured Concrete**
$t, t_o \geq 7$ days, $H \geq 40\ \%$	$t, t_o \geq 1$ to 3 days, $H \geq 40\ \%$
$K_{CA} = 1.25\,(t_o)^{-0.118}$	$K_{CA} = 1.13\,(t_o)^{-0.095}$

Calculate Creep Compliance Function:

$$\text{Compliance function } [\mu\varepsilon / \text{psi}] = (1 + C_c(t)) / E_{cmto}$$

Calculate Total Strain:

$$\varepsilon(t) = \varepsilon_s(t) + \frac{\sigma}{E_{cmto}}(1 + C_c(t))$$

CEB 90 Code Model

Nomenclature

$\phi(t,t_o)$	= Creep coefficient defining creep between time t and t_o
E_c	= Modulus of elasticity at 28 days (psi)
$E_c(t_o)$	= Modulus of elasticity at age of loading (psi)
$\varepsilon(t)$	= Total strain; instantaneous plus creep and shrinkage (in/in)
$\varepsilon_{cs}(t-t_s)$	= Shrinkage strain between time t and t_s (in/in)
t	= Age of concrete after casting (days)
t_s	= Age of concrete at the beginning of shrinkage (days)
f_{cm}	= Mean 28 day concrete compressive strength (psi)
$f_c'_{28}$	= Specified 28 day concrete compressive strength (psi)
t_o	= Age of concrete at loading (days)
ϕ_o	= Notional creep coefficient
$\beta_c(t-t_o)$	= Coefficient describing creep development with time after loading
ϕ_{RH}	= Factor to allow for relative humidity on the notional creep coefficient (ϕ_o)
$\beta(f_{cm})$	= Factor to allow for effect of concrete strength on the notional creep coefficient (ϕ_o)
$\beta(t_o)$	= Factor to allow for the effect of age of concrete at loading on the notional creep coefficient (ϕ_o)
RH	= Relative humidity (%)
A_c	= Cross-section area of member (in^2)
u	= Perimeter of member in contact with the atmosphere (in)
h_o	= $2A_c/u$ = Notional size of member (in)
β_H	= Coefficient to allow for the effect of relative humidity and the notional member size (h_o) on creep
ε_{cso}	= Notional shrinkage coefficient
$\beta_s(t-t_s)$	= Equation describing development of shrinkage with time
$\varepsilon_s(f_{cm})$	= Factor to allow for the effect of concrete strength on shrinkage

β_{RH} = Coefficient to allow for the effect of relative humidity on the notional shrinkage coeffienct (ε_{cso})

β_{sc} = Coefficient depending on type of cement

β_s = Coefficient to describe the development of shrinkage with time

Model

Creep Compliance Function[30A]

Compliance function [$\mu\varepsilon$/ psi] = $\dfrac{\varphi(t, t_o)}{E_c} + \dfrac{1}{E_c(t_o)}$

Total Strain

$$\varepsilon(t) = \varepsilon_{cs}(t - t_s) + \left[\frac{\varphi(t, t_o)}{E_c} + \frac{1}{E_c(t_o)}\right]\sigma$$

Calculate Mean Concrete Strength:

$$f_{cm} = f'_{c28} + 1200$$

Note: The experimental f'_{c28} was used for the calculations to obtain a more accurate value.

Calculate Tangent Modulus of Elasticity:

$$E_c = (E_{co})(f_{cm} / 1450)^{1/3}$$

$$E_{co} = 3{,}117{,}500 \text{ psi}$$

Calculate Modulus of Elasticity at Age t_o

$$E_c(t_o) = (E_c)\{\exp[0.5S\,(1-(28 / t_o)^{0.5})]\}$$

$$S = \begin{cases} 0.38, \text{ slow hardening cement} \\ 0.25, \text{ normal and rapid hardening cement} \\ 0.2, \text{ rapid hardening high strength} \end{cases}$$

Note: The experimental $E_c(t_o)$ was used for the calculations to obtain a more accurate value.

<u>Calculate Creep Compliance Function:</u>

$$\text{Compliance function } [\mu\varepsilon/\text{ psi}] = \frac{\varphi(t, t_o)}{E_c} + \frac{1}{E_c(t_o)}$$

t = age of concrete after casting

t_o = age of concrete at loading

$$\phi\,(t,t_o) = (\phi_o)\,\beta_c(t-t_o)$$

$$\phi_o = \phi_{RH}\,\beta(f_{cm}) \text{ x } \beta(t_o)$$

$$\phi_{RH} = 1 + \frac{(1 - RH/100)}{0.46(h_o/4)^{1/3}}$$

$$\beta(f_{cm}) = 5.3 / (f_{cm} / 1450)^{1/2}$$

$$\beta(t_o) = (0.1 + t_o^{0.20})^{-1}$$

$$\beta_c(t-t_o) = \frac{(t - t_o)^{0.3}}{\{\beta_H + (t - t_o)\}^{0.3}}$$

$$\beta_H = 150\,[1 + (0.012RH)^{18}]\,(h_o / 4) + 250 \le 1500$$

Calculate Shrinkage Strain:

$$\varepsilon_{cs}(t - t_s) = (\varepsilon_{cso})\ \beta_s\ (t - t_s)$$

$$\varepsilon_{cso} = \varepsilon_s\ (f_{cm})\ (\beta_{RH})$$

$$\varepsilon_s\ (f_{cm}) = [160 + 10\ \beta_{sc}\ (9 - f_{cm} / 1450)] \times 10^{-6}$$

Type of Cement	$\boldsymbol{\beta_{sc}}$
Slow hardening (SL)	4
Normal and rapid hardening (R)	5
Rapid hardening high strength (RS)	8

Humidity	$\boldsymbol{\beta_{RH}}$
40 % ≤ RH ≤ 99 %, stored in air	$-1.55 \times \beta_{ARH}$
RH ≥ 99 %, immersed in water	0.25

$$\beta_{RH} = 1 - (RH/100)^3$$

$$\beta_s(t\text{-}t_s) = \sqrt{\frac{(t - t_s)}{\left\{350\left(\frac{h_o}{4}\right)^2 + (t - t_s)\right\}}}$$

Calculate Creep Compliance Function:

$$\text{Compliance function } [\mu\varepsilon/\text{ psi}] = \frac{\varphi(t, t_o)}{E_c} + \frac{1}{E_c(t_o)}$$

Calculate Total Strain:

$$\varepsilon(t) = \varepsilon_{cs}\ (t\text{-}t_s) + \left[\frac{\varphi(t, t_o)}{E_c} + \frac{1}{E_c(t_o)}\right] \sigma$$

The B3 Model

Nomenclature

$j(t,t')$	= Creep compliance function
q1	= Instantaneous strain due to unit stress
$C_o(t,t')$	= Compliance function for basic creep
$C_d(t,t',t_o)$	= Compliance function for additional creep due to drying
$\varepsilon(t)$	= Total Strain; instantaneous plus creep and drying (in/in)
$\varepsilon_{sh}(t)$	= Shrinkage Strain (in/in)
f_c'	= Mean 28 day concrete compressive strength (psi)
f_{ck}	= Specified concrete compressive strength at 28 days (psi)
E_{28}	= Modulus of elasticity at 28 days (psi)
q2	= Aging visco-elastic compliance
q3	= Non-aging visco-elastic complaince
t	= Age of concrete after casting (days)
t'	= Age of concrete at loading (days)
q4	= Flow compliance
c	= Cement content of concrete (lbs/ft^3)
w/c	= water to cement ratio by weight
a/c	= aggregate to cement ratio by weight
H(t)	= Spatial average of pore relative humidity within cross section
S(t)	= Time function for shrinkage
$\varepsilon_{sh\infty}$	= Ultimate shrinkage strain (in/in)
w	= Water content of concrete (lbs/ft^3)
t_o	= Age of concrete at the beginning of shrinkage (days)
T_{sh}	= Shrinkage half-time (days)
K_s	= Cross section shape factor
V/S	= Volume to surface are ratio (in)
D	= 2(V/S) = Effective cross-section thickness (in)
K_h	= Humidity function for shrinkage

Model

Creep Compliance Function[30A]

$$j(t,t') \; [\mu\varepsilon/ \text{psi}] = q_1 + C_o(t,t') + C_d(t,t',t_o)$$

Total Strain

$$\varepsilon(t) = j(t,t')\sigma + \varepsilon_{sh}(t)$$

Calculate Mean Compressive Strength:

$$f'_c = f_{ck} + 1200$$

Note: Use the experimental mean concrete strength if available.

$$q_1 = \frac{0.6 * 10^6}{E_{28}}$$

$$E_{28} = 57000 \, (f_c')^{1/2}$$

Note: The experimental E_{28} was used when calculating the compliance function to obtain a more accurate value.

$$C_o(t,t') = q_2 \, Q(t,t') + q_3 \ln(1 + (t - t')^n) + q_4 \ln (t / t')$$

t = age of concrete after casting

t' = age of concrete at loading

t_o = age of concrete at the beginning of shrinkage

$$Q(t,t') = Q_f(t') \left[1 + \frac{(Q_f(t'))^{r(t')}}{Z(t,t')^{r(t')}}\right]^{-1/r(t')}$$

$$Q_f(t') = [\ 0.086\ (t')^{2/9} + 1.21\ (t')^{4/9}\ ]^{-1}$$

$$Z(t,t') = (t')^{-m} \ln(1 + (t - t')^n)$$

$$m = 0.5,\ n = 0.1$$

$$r(t') = 1.7\ (t')^{0.12} + 8$$

$$q_2 = 451.1\ (c)^{0.5}\ (f_c')^{-0.9}$$

$$q_3 = 0.29\ (w/c)^4\ q_2$$

$$q_4 = 0.14\ (a/c)^{-0.7}$$

$$C_d(t,t',t_o) = q_5\ [\exp\{-8H(t)\} - \exp\{-8H(t')\}]^{1/2}$$

$$H(t) = 1 - (1-h)\ S(t)$$

$$H(t') = 1 - (1-h)\ S(t')$$

$$q_5 = 7.57 \times 10^5\ (f_c')^{-1}\ \mathrm{ABS}(\varepsilon_{sh\infty})^{-0.6}$$

$$\varepsilon_{sh\infty} = -\alpha_1\ \alpha_2\ (26\ (w)^{2.1}\ (f_c')^{-0.28} + 270) \times 10^{-6}$$

Type of Cement	$\boldsymbol{\alpha_1}$
I	1.0
II	0.85
III	1.1

Type of Curing	α_2
Steamed cured	0.75
Water cured or h = 100 %	1.0
Sealed during curing	1.2

$$S(t) = \tanh \sqrt{\frac{t - t_o}{T_{sh}}}$$

$$S(t') = \tanh \sqrt{\frac{t' - t_o}{T_{sh}}}$$

$$T_{sh} = K_t \, (K_s \, D)^2$$

$$K_t = 190.8 \, (t_o)^{-0.08} \, (f_c')^{-0.25}$$

Type of Member or Structure	K_s
Infinite slab	1.00
Infinite cylinder	1.15
Infinite square prism	1.25
Sphere	1.30
Cube	1.55
Undefined member	1.00

Relative Humidity	K_h
for $h \leq 0.98$	$1 - h^3$
for $h = 1$	-0.2
for $0.98 \leq h \leq 1$	Use linear interpolation

Calculate Shrinkage Strain:

$\varepsilon_{sh}\,(t,t_o) = \varepsilon_{sh\infty}\,K_h\,S(t)$

Calculate Creep Compliance Function:

$j(t,t') \,[\mu\varepsilon/\,psi] = q_1 + C_o(t,t') + C_d(t,t',t_o)$

Calculate Total Strain:

$\varepsilon(t) = j(t,t')\sigma + \varepsilon_{sh}(t)$

The GZ Model

Nomenclature

f_{cm28}	= Mean 28 day concrete compressive strength (psi)
f_{ck28}	= Specified 28 day concrete compressive strength (psi)
t_o	= Age of concrete at loading (days)
K	= Correction term for effect of cement type on shrinkage
E_{cmto}	= Mean modulus of elasticity at age of loading (psi)
f_{cmto}	= Mean concrete compressive strength at age of loading (psi)
E_{cm28}	= Mean modulus of elasticity at 28 days (psi)
$\phi(t_c)$	= Correction term for effect of drying before loading
h	= Relative humidity (decimal)
t	= Age of concrete after casting (days)
V/S	= Volume to surface area ratio
ε_{sh}	= Shrinkage strain (in/in)
ε_{shu}	= Ultimate shrinkage strain (in/in)
$\beta(h)$	= Correction term for the effect of humidity on shrinkage
$\beta(t)$	= Correction term for the effect of time on shrinkage
t_c	= Age of concrete at the beginning of shrinkage (days)
f_{cmtc}	= Mean concrete compressive strength at the beginning of shrinkage
$\varepsilon(t)$	= Total strain; instantaneous plus creep and shrinkage (in/in)

Model

Calculate Mean Compressive Strength:[30A]

Use the experimental mean concrete compressive strength, otherwise:

$$f_{cm28} = f_{ck28} + 1200$$

Calculate Mean Compressive Strength Based on Time:

Use the experimental concrete compressive strength at loading, otherwise:

$$f_{cmto} = f_{cm28} \frac{t_o^{3/4}}{(a + b(t_o)^{3/4})}$$

Cement Type	a	b	K
I	2.8	0.77	1.0
II	3.4	0.72	0.7
III	1.0	0.92	1.33

Calculate Mean Modulus of Elasticity:

Use the experimental Modulus, otherwise:

$$E_{cmto} = 500{,}000 + 52{,}000\,(f_{cmto})^{1/2}$$

Mean Strength and Modulus of Elasticity Based on Time for Experimental Data

Use the experimental E_{c28}, back calculate for f_{cm28} and average it with the experimental f_{cm28} and get the $f_{cm28(average)}$.

$$E_{c28} = 500{,}000 + 52{,}000\,(f_{cm28})^{1/2}$$

From the $f_{cm28(average)}$ calculate the $f_{cmto,}$ and $E_{cmto(average)}$ from the following equations:

$$f_{cmto(average)} = f_{cm28(average)}\ \frac{t_o^{\ 3/4}}{(a + b(t_o)^{3/4})}$$

$$E_{cmto(average)} = 500{,}000 + 52{,}000\,(f_{cmto(average)})^{1/2}$$

Creep Strain

$$\text{Creep Strain} = (\sigma / E_{cmto})\,(1 + \text{Creep Coefficient})$$

If Experimental E_{c28} and E_{cmto} is available then:

$$\text{Creep Strain} = \sigma\,[(1 / E_{cmto(experimental)}) + (\text{creep coefficient} / E_{cmto(average)})]$$

$$\text{Creep coefficient} = [\varphi(t)]\,[\varphi(t_c)]\ \sqrt{\frac{f_{cm28}}{f_{cmto}}}\left[1.5 + (2.86)\sqrt{\frac{4000}{f_{cmto}}}\ \frac{(1 - 1.086h^2)(t - t_o)}{t - t_o + 32(V/S)^2}\right]$$

t_c = age of concrete at beginning of shrinkage

t = Age of concrete after casting

$$\varphi(t) = \frac{7.27 + \ln(t - t_o)}{17.18}$$

$\varphi(t_c) = 1; \qquad \text{If } t_o = t_c$

$$\varphi(t_c) = 1 - \sqrt{\frac{\varepsilon_{sh}(t_o - t_c)}{\varepsilon_{sh}(20000 - t_c)}}\,; \qquad \text{If } t_o > t_c$$

Shrinkage Strain

$$\varepsilon_{sh} = (\varepsilon_{shu})\,\beta(h)\,\beta(t)$$

$$\beta(h) = \begin{cases} 1 - 1.18h^4\,; & \text{for } h < 0.96 \\ 0.0; & \text{for sealed specimens } h = 0.96 \end{cases}$$

$$\beta(t) = \frac{7.27 + \ln(t - t_c)}{17.18} * \frac{t - t_c}{t - t_c + 9.7(V/S)^2}$$

$$\varepsilon_{shu} = 857\ K \left[\frac{f_{cm28}}{f_{cmtc}}\right]^{1/2} \left[\frac{4000}{f_{cm28}}\right]^{1/2} \times 10^{-6}$$

Total Strain

$$\varepsilon(t) = \varepsilon_{sh} + [(\sigma/E_{cmto})(1 + \text{creep coefficient})]$$

If the experimental E_{c28} and E_{cmto} is available then use:

$$\varepsilon(t) = \varepsilon_{sh} + \sigma[(1/E_{cmto(experimental)}) + (\text{creep coefficient}/E_{cmto(average)})]$$

Creep Compliance Function

$$\text{Compliance function} = \frac{(1 + \text{creep coefficient})}{E_{cmto}}$$

If experimental E_{c28} and E_{cmto} is available then:

$$\text{Compliance function} = [(1 / E_{cmto(experimental)}) + (\text{creep coefficient} / E_{cmto(average)})]$$

The SAK Model

Nomenclature

$\varepsilon'_{cs}(t,t_o)$	= Predicted shrinkage strain
ε'_{sh}	= Ultimate shrinkage strain
t	= Age of concrete after casting (days)
t_o	= Age of concrete at the beginning of shrinkage (days)
RH	= Relative humidity (%)
w	= water content of concrete (kg/m^3)
v/s	= volume to surface area ratio
$\varepsilon'_{cc}(t,t',t_o)$	= Predicted specific creep (mm^2/N)
ε'_{bc}	= Basic creep (mm^2/N)
ε'_{dc}	= Drying creep (mm^2/N)
t'	= Age of concrete at loading (days)
c	= cement content of concrete (kg/m^3)
w/c	= water to cement ratio by weight
$E_c(t_o)$	= Modulus of elasticity at age of loading (N/mm^2)
$\varepsilon(t)$	= Total strain; instantaneous plus creep and shrinkage

Model

Calculate Shrinkage Strain:[30A]

$$\varepsilon'_{cs}(t, t_o) = \varepsilon'_{sh}\ [1\text{-}\exp\{-0.108(t\text{-}t_o)^{0.56}\}] \times 10^{-5}$$

$$\varepsilon'_{sh} = -50 + 78\{1\text{-}\exp(RH/100)\} + 38(\ln(w)) - 5[\ln\{(v/s)/10\}]^2 \times 10^{-5}$$

Calculate Creep Strain:

$$\varepsilon'_{cc}(t, t', t_o) = (\varepsilon'_{bc} + \varepsilon'_{dc}) \times [1 - \exp\{-0.09(t - t')^{0.6}\}] \times 10^{-10}$$

$$\varepsilon'_{bc} = 15\ (c + w)^{2.0}(w/c)^{2.4}\ \{\ln(t')\}^{-0.67} \times 10^{-10}$$

$$\varepsilon'_{dc} = 4500\ (w/c)^{4.2}(c + w)^{1.4}\ [\ln\{(v/s)/10\}]^{-2.2}\ \{1 - (RH/100)\}^{0.36}\ (t_o)^{-0.30} \times 10^{-10}$$

Calculate Creep Compliance Function:

$$\text{Compliance function} = \varepsilon'_{cc}(t, t', t_o) + (1 / E_c(t_o))$$

where;

$E_c(t_o)$ is calculated by the CEB 90 method.

Total Strain:

$$\varepsilon(t) = \varepsilon'_{cs}(t, t_o) + \sigma[\varepsilon'_{cc}(t, t', t_o) + (1 / E_c(t_o))]$$

REFERENCES

1A. Carlton, D., and Mistry, N., "Thermo-elastic-creep analysis of maturing concrete". *Computers and Structures*, 1991, v. 40, n. 2, pp. 293-302.

2A. Troxell, George; Davis, Harmer; ad Kelly, Joe. *Composition and Properties of Concrete. Second edition*. New York: McGraw-Hill, pp. 290-320.

3A. Han, N. and Walraven, J. C., "Creep and shrinkage of high strength concrete at early and normal ages".

4A. Alexander, Mark G., "Aggregates and the deformation properties of concrete". *ACI Materials Journal*, November 1996 – December 1996, v. 93, n. 6, pp. 569-577.

5A. Collins, Therese M., "Proportioning high strength concrete to control creep and shrinkage". *ACI Materials Journal,* November 1989 – December 1989, v. 86, n. 6, pp. 567-580.

6A. Mehta, P. K. *Concrete: Structure Properties and Materials*. New Jersey: Prentice Hall 1986, Chapter 6 and Chapter 8.

7A. Alexander, M. G., "Deformation properties of blended cement concretes containing blast furnace slag and condensed silica fume". *Advances in Cement Research,* April 1994, v. 6, n. 22, pp. 73-81.

8A. Wiegrink, Karl; Marikunte, Shashidhara; and Shah, Surendra P., "Shrinkage cracking of high strength concrete". *ACI Materials Journal*, September 1996 – October 1996, v. 93, n. 5, pp. 409-415.

9A. Tazawa, E. and Yonekura, A., "Drying shrinkage and creep of concrete with condensed silica fume". *Special Publication American Concrete Institute* 1991-903, v. 2.

10A. Ghosh, Sujit and Nasser, K. W., "Creep, shrinkage, frost, and sulphate resistance of high strength concrete". *Canadian Journal of Civil Engineering*, June 1995, v. 22, n. 3, pp. 621-636.

11A. Khatri, R. P.; SirivivatnAnon, V.; and Gross, W., "Effect of different supplementary cementitious materials on mechanical properties of high performance concrete". *Cement and Concrete Research,* January 1995, v. 25, n. 1, pp. 209-220.

12A. Tikalsky, P. J.; Carrasquillo, P. M.; and Carrasquillo, R. L., "Strength and durability considerations affecting mix proportioning of concrete containing fly ash". *ACI Materials Journal*, November 1988 – December 1988, v. 85, n. 6, pp. 505-511.

13A. Sivasundaram, V.; Carette, G. G.; and Malhotra, V. M., "Selected properties of high volume fly ash concretes". *Concrete International: Design and Construction*, October 1990, v. 12, n. 10, pp. 47-50.

14A. Swamy, R. N., "Fly ash concrete: potential without misuse". *Materials and Structures Journal*, November 1990, v. 23, n. 138, pp. 397-411.

15A. Carette, G. G., and Mulhotra, V. M., "Characterization of Canadian fly ashes and their relative performance in concrete". *Canadian Journal of Civil Engineering*, October 1997, v. 14, n. 5, pp. 667-682.

16A. Chern, Jenn Chuan and Chan, Yin Wen, "Deformations of concretes made with blast furnace slag cement and ordinary portland cement". *ACI Materials Journal*, July 1989 – August 1989, v. 86, n. 4, pp. 372-382.

17A. Chern, Jenn Chuan; Wu, Yeong Gee; and Chang, Hsing Cheng, "Influence of loading age on long term drying creep of concrete". *Journal of the Chinese Institute of Engineers*, March 1988, v. 11, n. 2, pp. 113-120.

18A. Schwesinger, P.; Ehlert, G.; and Woelfel, R., "Creep of concrete at elevated temperatures and boundary conditions of moisture". *Cement and Concrete Research*, March 1987, v. 17, n. 2, pp. 263-272.

19A. Smadi, Mohammed M.; Slate, Floyd O.; and Nilson, Arthur H., "Shrinkage and creep high, medium, and low strength concretes, including overloads". *ACI Materials* Journal, May 1987 – June 1987, v. 84, n. 3, 224-234.

20A. Khan, Ashrad, A.; Cook, William D.; and Mitchell Denis, "Creep, shrinkage, and thermal strains in normal, medium, and high strength concretes during hydration". *ACI Materials Journal*, March 1997 – April 1997, v. 94, n. 2, pp. 156-163.

21A. Saiidi, M. Saiid; Sheilds, Joseph; O' Connor, Daniel; and Hutchens, Eric, "Variation of prestress force in a prestressed concrete bridge during the first 30 months". *PCI Journal*, September 1996 – October 1996, v. 41, n. 5, pp. 66-72.

22A. Densford, Thomas A.; Hendrick, Thomas L.; and Murray, Thomas M., "Short span prestressed steel bridges". *Engineering Journal of the American Institute of Steel Construction*, March 1990, v. 27, n. 3, pp. 114-120.

23A. Alsamsam, Iyad, "Shrinkage measurements in composite beam slabs". *Procedures of Nondestructive Testing of Concrete Elements and Structures* 215.

24A. Uy, B., and Bradford, M. A., "Service load tests on profiled composite and reinforced concrete beams". *Magazine of Concrete Research*, March 1994, v. 46, n. 166, pp. 29-33.

25A. Bakoss, S. L.; Gilbert, R. I.; Faulkes, K. A.; and Pulamanos, V. A., "Long term deflections of reinforced concrete beams". *Magazine of Concrete Research*, December 1982, v. 34, n. 121, pp. 203-212.

26A. Paulson, Kent A.; Nilson, Arthur H.; and Hover, Kenneth C., "Long term deflection of high strength concrete beams". *ACI Materials Journal*, March 1991 – April 1991, v. 88, n. 2, pp. 197-206.

27A. Emmons, P. H.; Vaysburd, A. M.; Pinelle, D. J.; Poston, R. W.; and McDonald, J. E., "Crack resistant materials – the origin of durability of concrete repair". *Concrete Repair Bulletin*, September 1997 – October 1997, v. 10, n. 5, pp. 20-23.

28A. Emberson, N. K., and Mays, G. C., "Significance and property mismatch in the patch repair of structural concrete – Part 3: reinforced concrete members in flexure". *Magazine of Concrete Research*, March 1996, v. 48, n. 174, pp. 45-57.

29A. Cleland, D. J.; Yeoh, K. M.; and Long, A. E., "Corrosion of reinforcement in concrete repair". *Construction and Building Materials*, June 1997, v. 11, n. 4, pp. 233-238.

30A. Lakshmikantan, S., <u>Evaluation of Concrete Shrinkage and Creep Models</u>. Master of Science Thesis in Civil Engineering, San Jose State University, May 1999.

31A. Al-Manaseer, A., and Lakshmikantan, S., "Comparison between current and future design code models for shrinkage and creep". *Revue francaise degenie civil*, Editors in Chief Culgaro, J. A., and Darue, F., Hermes Science Publications 1999, v. 3, n. 3-4, pp. 39-59.

APPENDIX B

Mix Design

TABLE 1B. CONCRETE AGGREGATE PROPERTIES

Coarse Aggregate Properties

Gradation Particle Size mm	Percent Passing Gravel	Limestone	Diabase	VDOT Spec
25	99	100	99	90-100
19	72	81	79	-
12.7	25	19	34	26-60
9.6	12	3	8	-
4.75	2	0	1	max 7
2.36	0	0	1	max 3
Unit Weight, kg	1673	1577	1752	
Dry Bulk s.g.	2.59	2.81	2.92	
Absorption, %	0.81	0.36	0.73	

Fine Aggregate Properties

Gradation Particle Size mm	Percent Passing FA_{Gravel}	$FA_{Limestone}$	$FA_{Diabase}$	VDOT Spec
9.6	100	100	100	min 100
4.75	99	97	99	94-100
2.36	90	80	83	80-100
1.18	78	70	68	49-85
0.6	46	53	42	25-59
0.3	17	16	12	8-26
0.15	2	2	4	max 10
0.075	0.54	0.40	2.0	-
Fineness Modulus	2.68	2.82	2.92	
Dry Bulk s.g.	2.55	2.59	2.53	
Absorption, %	0.75	0.48	1.04	

Note: Column aggregates are those used in the corresponding concrete mixtures.

TABLE 2B. CEMENT PROPERTIES

Portland Cement Type I/II

Chemical Analysis

Analyte	Percent by Weight DWM-1	DWM-2	ASTM C 150 - 98 Type II
SiO_2	21.25	21.17	20.0 min
Al_2O_3	4.49	4.49	6.0 max
Fe_2O_3	3.04	3.03	6.0 max
CaO	63.51	63.41	-
MgO	2.48	2.5	6.0 max
SO_3	2.47	2.46	3.0 max
Na_2O	0.17	0.17	-
K_2O	0.82	0.81	-
TiO_2	0.21	0.22	-
P_2O_5	0.11	0.11	-
Mn_2O_3	0.06	0.06	-
SrO	0.14	0.14	-
L.O.I. (950 C)	1.06	1.07	3.0 max
Total	99.83	99.65	-
Alkalis as Na_2O	0.72	0.71	*0.6 max

Compounds

Calculated ASTM C 150-97			Mass Estimated by QXRD	
C3S	55	56	65	-
C2S	19	19	16	-
C3A	7	7	4.2	8.0 max
C4AF	9	9	10	-

*Low alkali cement requirement.

TABLE 3B. X RAY ANALYSIS OF MICROSILICA, AND GGBFS

Fly Ash: No information is available.

Microsilica: Predominately amorphous with possibly a trace amount of merwinite ($Ca_3Mg(SiO_4)_2$)

Ground Granulated Blast Furnace Slag: Exhibits a broad mid-angle amorphous material which correlate with the glass chemistry, a few percent of merwinite and less than one percent of both quartz and calcite. Calcite is probably carbonated from lime.

APPENDIX C

Pictures

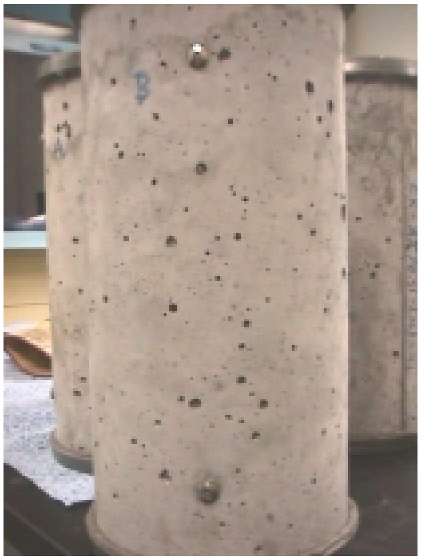

FIGURE 1C. GAGE POINT, SIDE B

FIGURE 2C. CREEP ROOM: FOUR COMPRESSION FRAMES WITH THREE SPECIMENS PER FRAME.

FIGURE 3C. PRESSURE GAGES

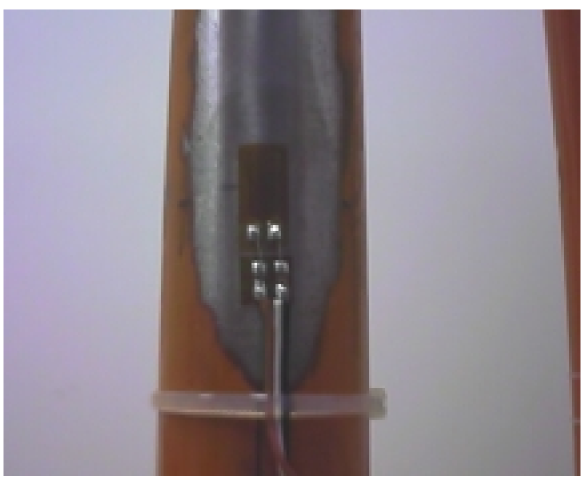

FIGURE 4C. STRAIN GAGE (ONE PER STEEL ROD)

APPENDIX D

Creep Frame Calibration

CREEP FRAME CALIBRATION

The creep frames were calibrated using a load cell, pressure gages, and strain gages. Strain gages A, B, C, and D were placed one on each rod of the frame.

A 220 kip load cell was placed in the frame. Readings were taken from 5 to 40 kips in intervals of 5, and from 40 to 100 kips in intervals of 10. Readings were also taken at 120, 140, and 150 kips.

For each load reading from the load cell, there was a corresponding strain reading (A through D) and gage pressure reading.

This procedure was repeated twice for each frame, four frames total.

To develop a relationship between the load cell measurements, the strain gages, and the gage pressure, four graphs were developed fro each frame:

- Gage pressure readings verses load cell readings
- Strain gage readings verses load cell readings
- Gage pressure readings verses desired concrete pressure
- Gage pressure verses strain gage readings.

Pictures 2C through 4C in Appendix C better illustrate the gages.

FIGURE 1D. FRAME 1 GAGE PRESSURE VS. LOAD

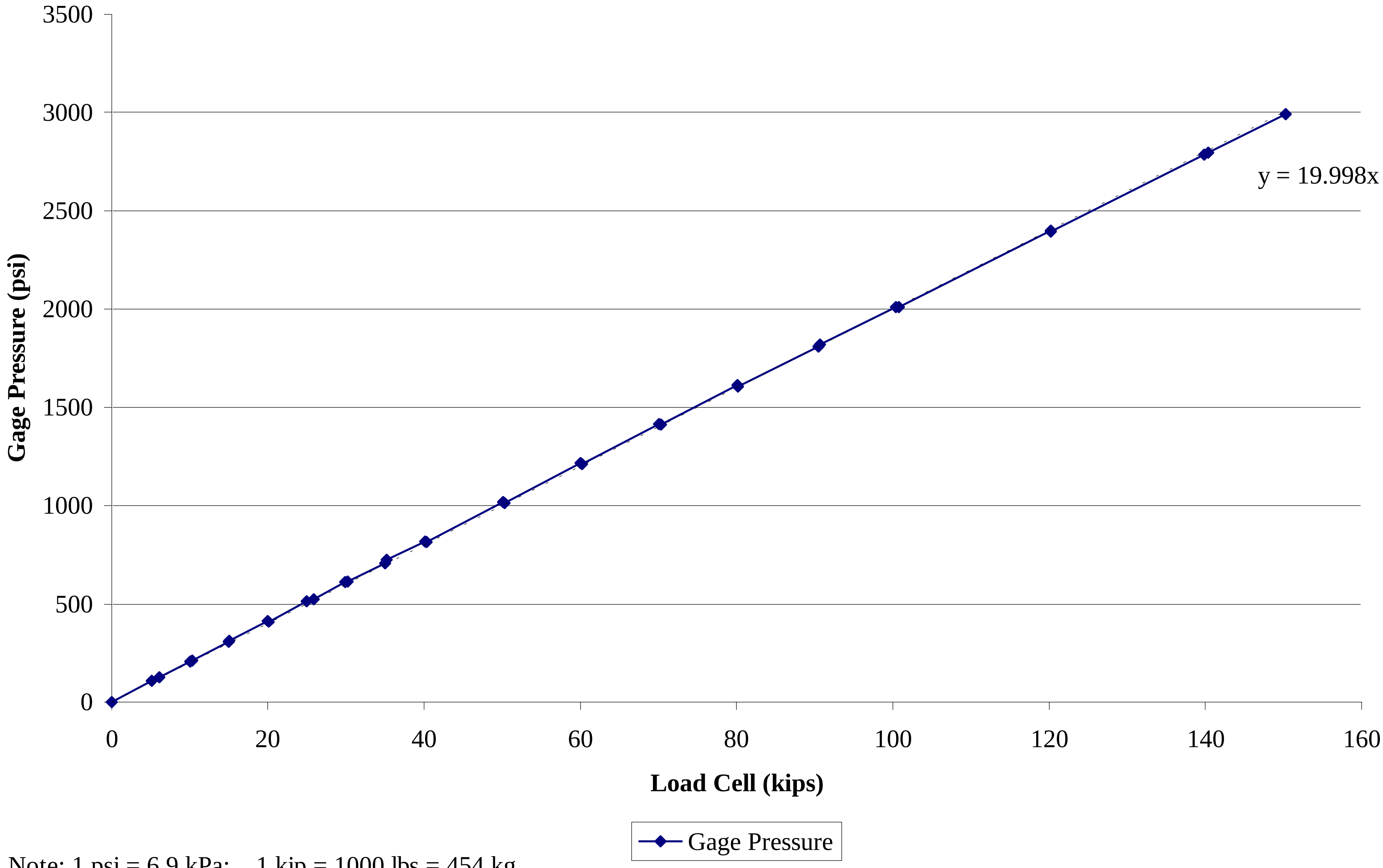

Note: 1 psi = 6.9 kPa; 1 kip = 1000 lbs = 454 kg

FIGURE 2D. FRAME 1 STRAIN VS. LOAD CELL

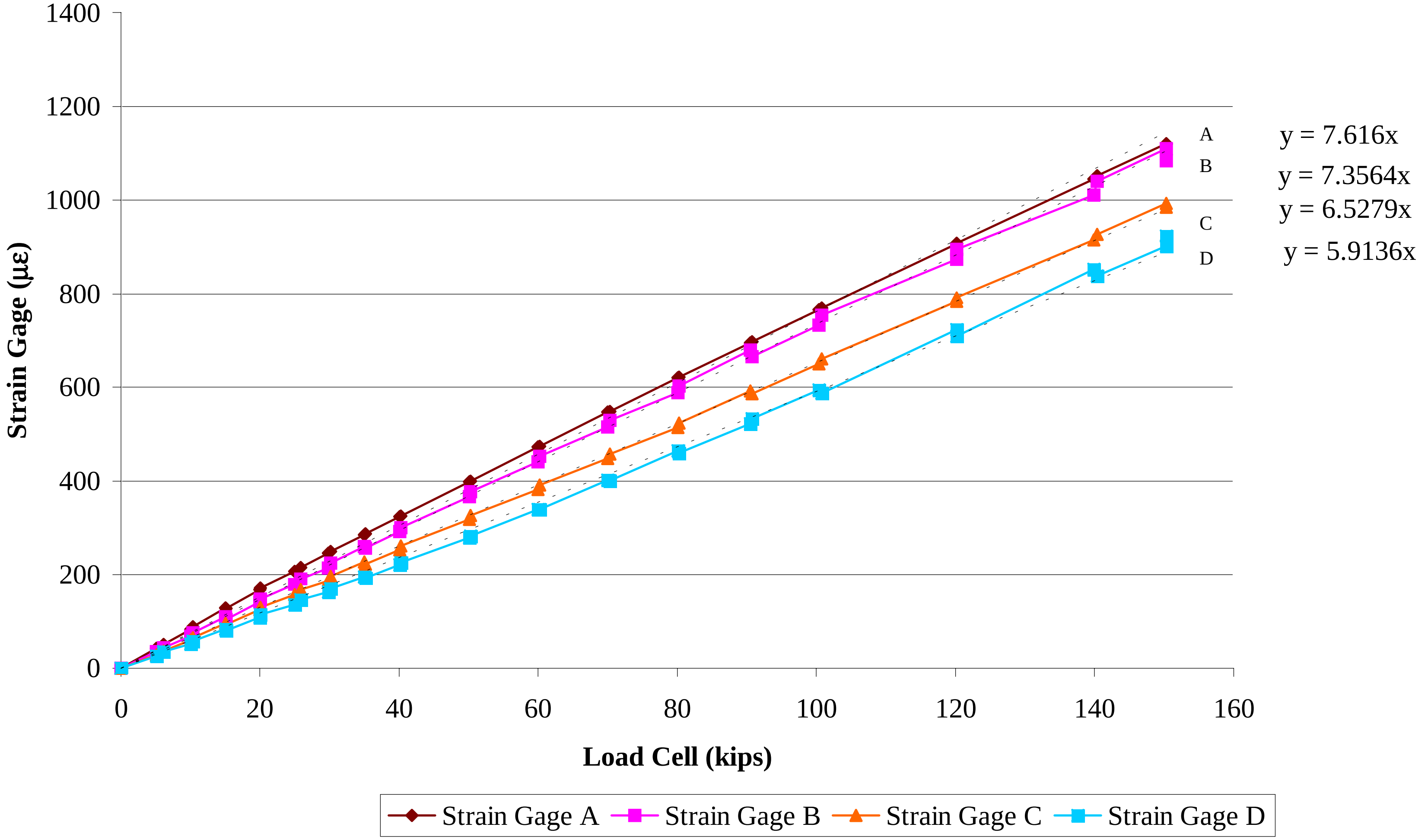

Note: 1 psi = 6.9 kPa; 1 kip = 1000 lbs = 454 kg

FIGURE 3D. FRAME 1 GAGE PRESSURE VS. DESIRED CONCRETE PRESSURE

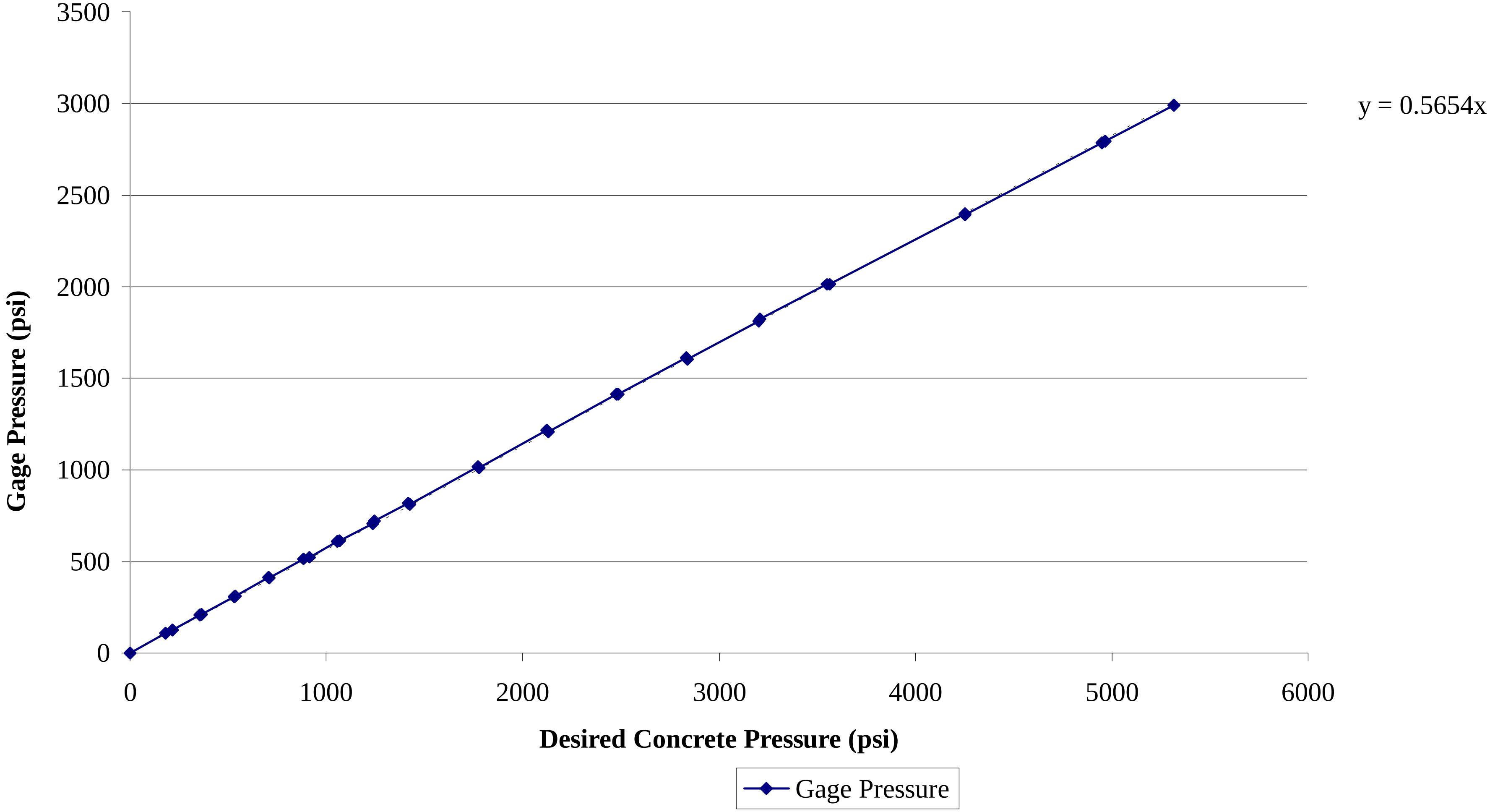

Note: 1 psi = 6.9 kPa;   1 kip = 1000 lbs = 454 kg

FIGURE 4D. FRAME 1 GAGE PRESSURE VS. STRAIN GAGE

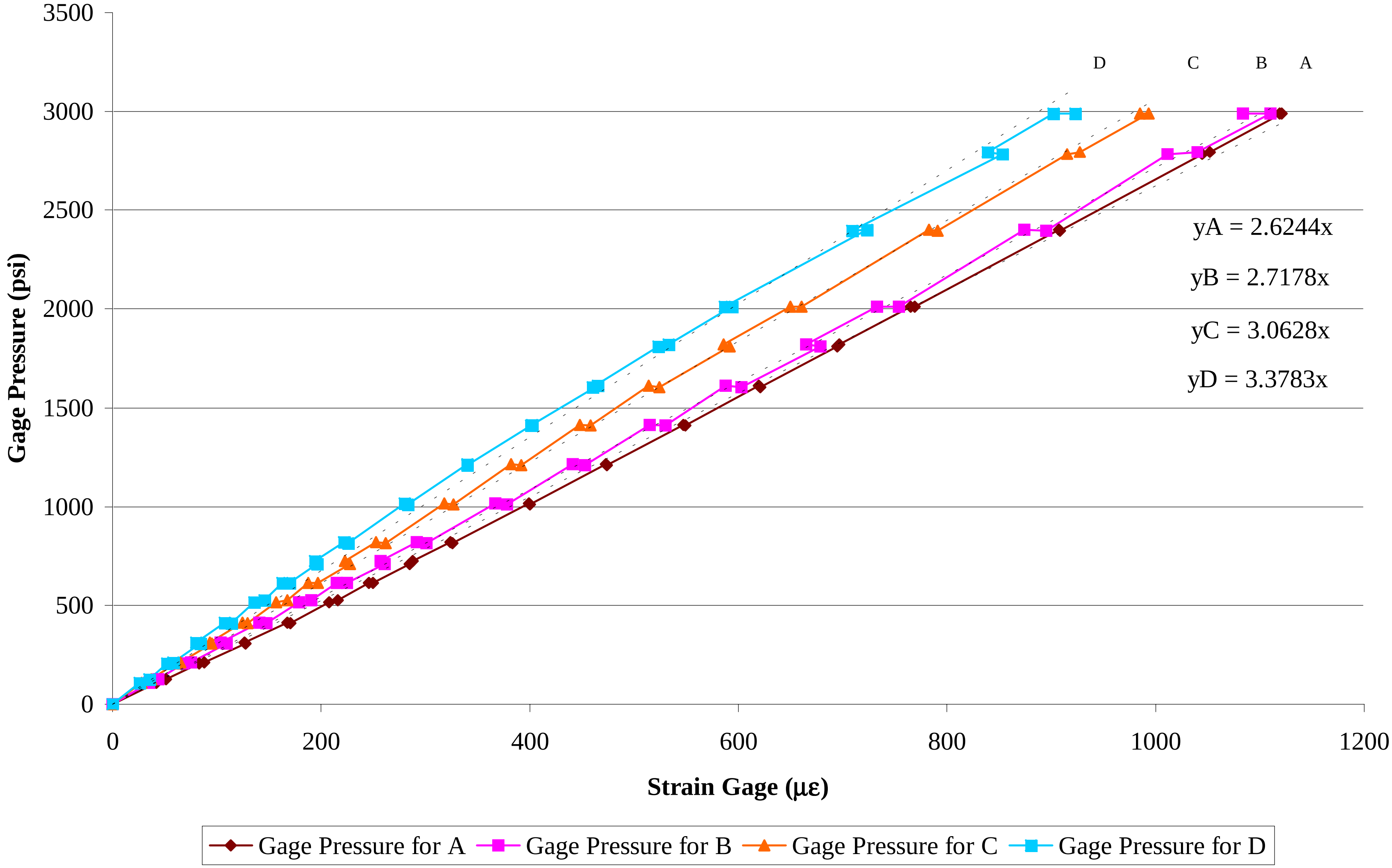

Note: 1 psi = 6.9 kPa; 1 kip = 1000 lbs = 454 kg

FIGURE 5D. FRAME 2 GAGE PRESSURE VS. LOAD CELL

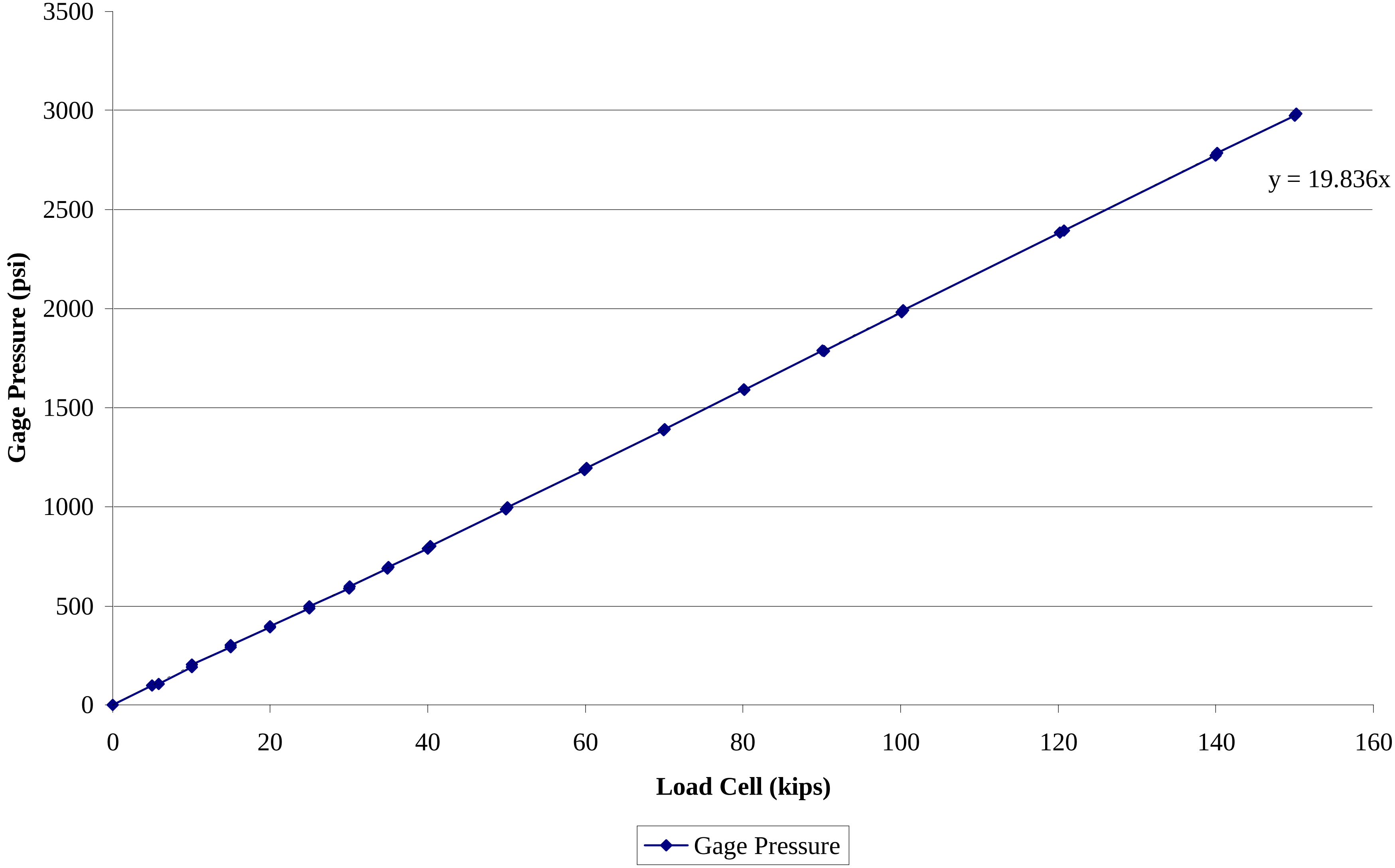

Note: 1 psi = 6.9 kPa; 1 kip = 1000 lbs = 454 kg

FIGURE 6D. FRAME 2 STRAIN VS. LOAD CELL

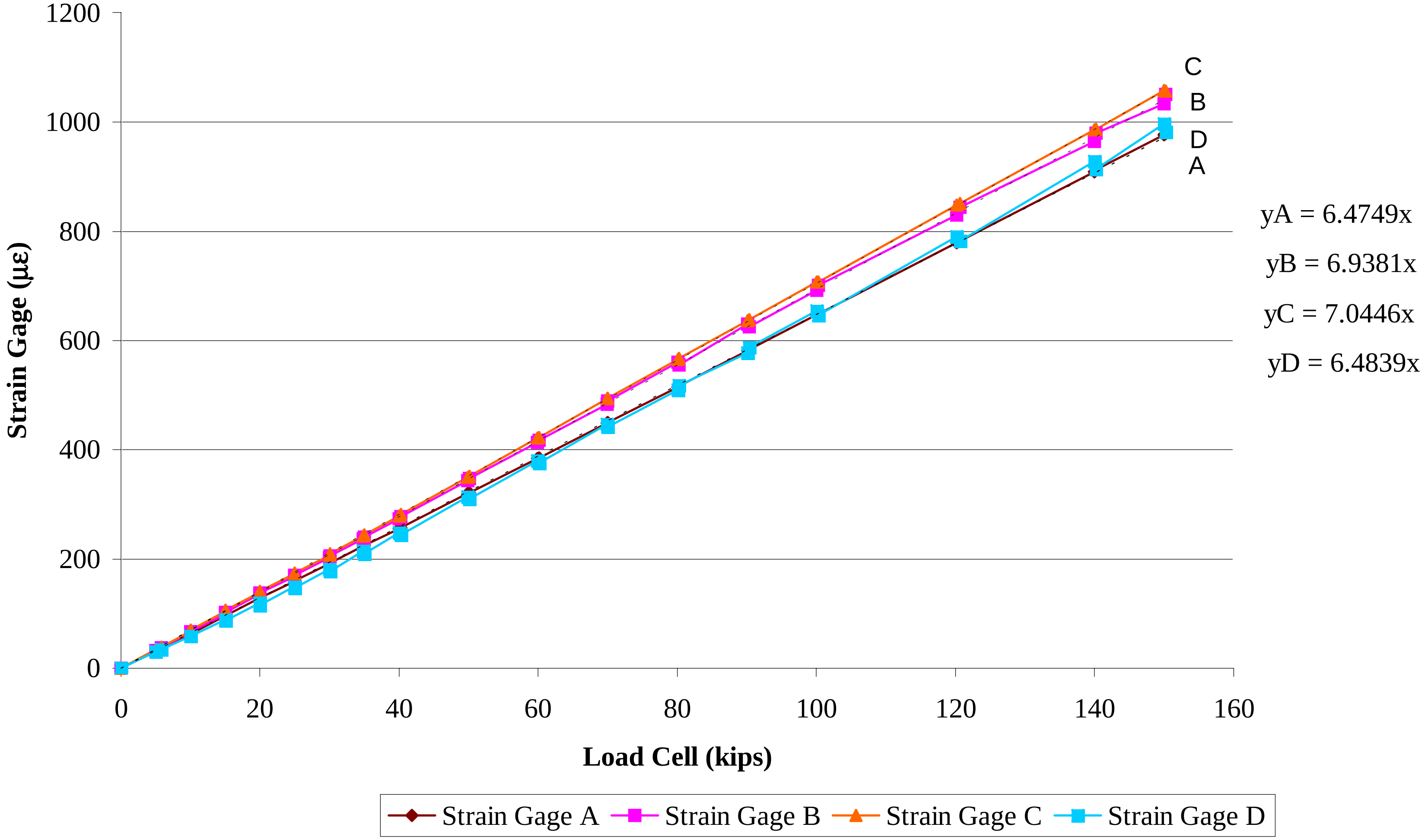

Note: 1 psi = 6.9 kPa; 1 kip = 1000 lbs = 454 kg

FIGURE 7D. FRAME 2 GAGE PRESSURE VS. DESIRED CONCRETE PRESSURE

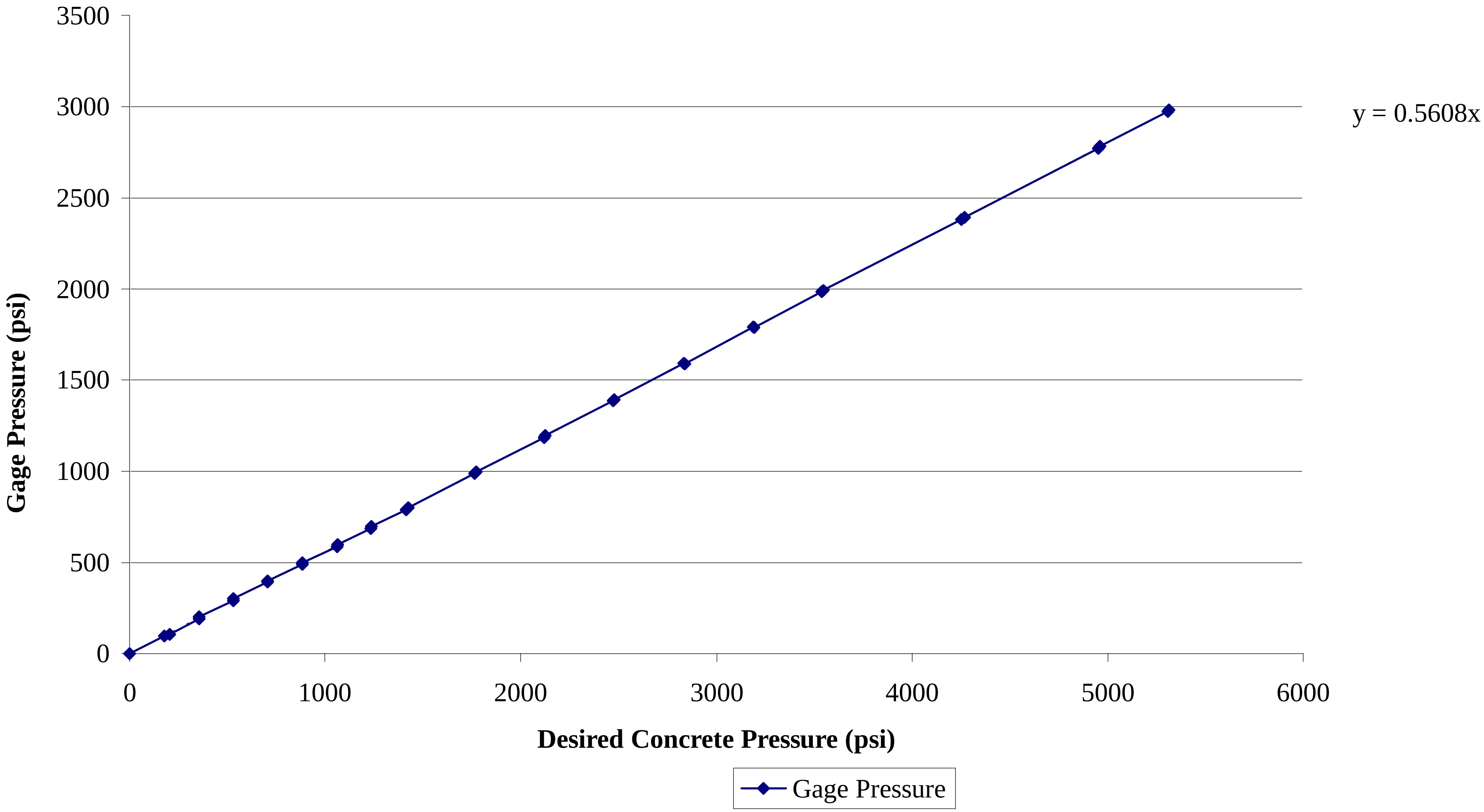

Note: 1 psi = 6.9 kPa; 1 kip = 1000 lbs = 454 kg

FIGURE 8D. FRAME 2 GAGE PRESSURE VS. STRAIN GAGE

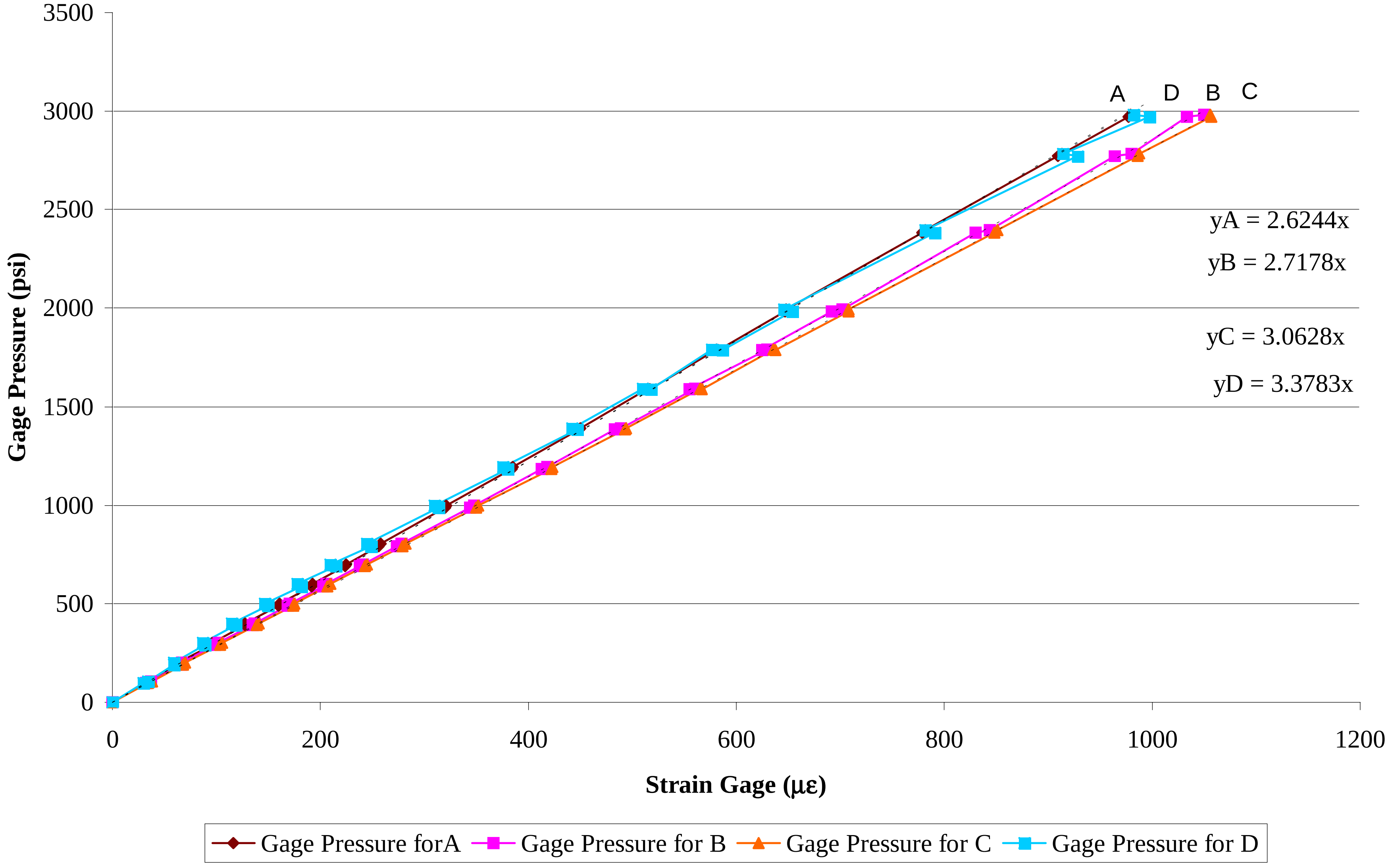

Note: 1 psi = 6.9 kPa; 1 kip = 1000 lbs = 454 kg

FIGURE 9D. FRAME 3 GAGE PRESSURE VS. LOAD CELL

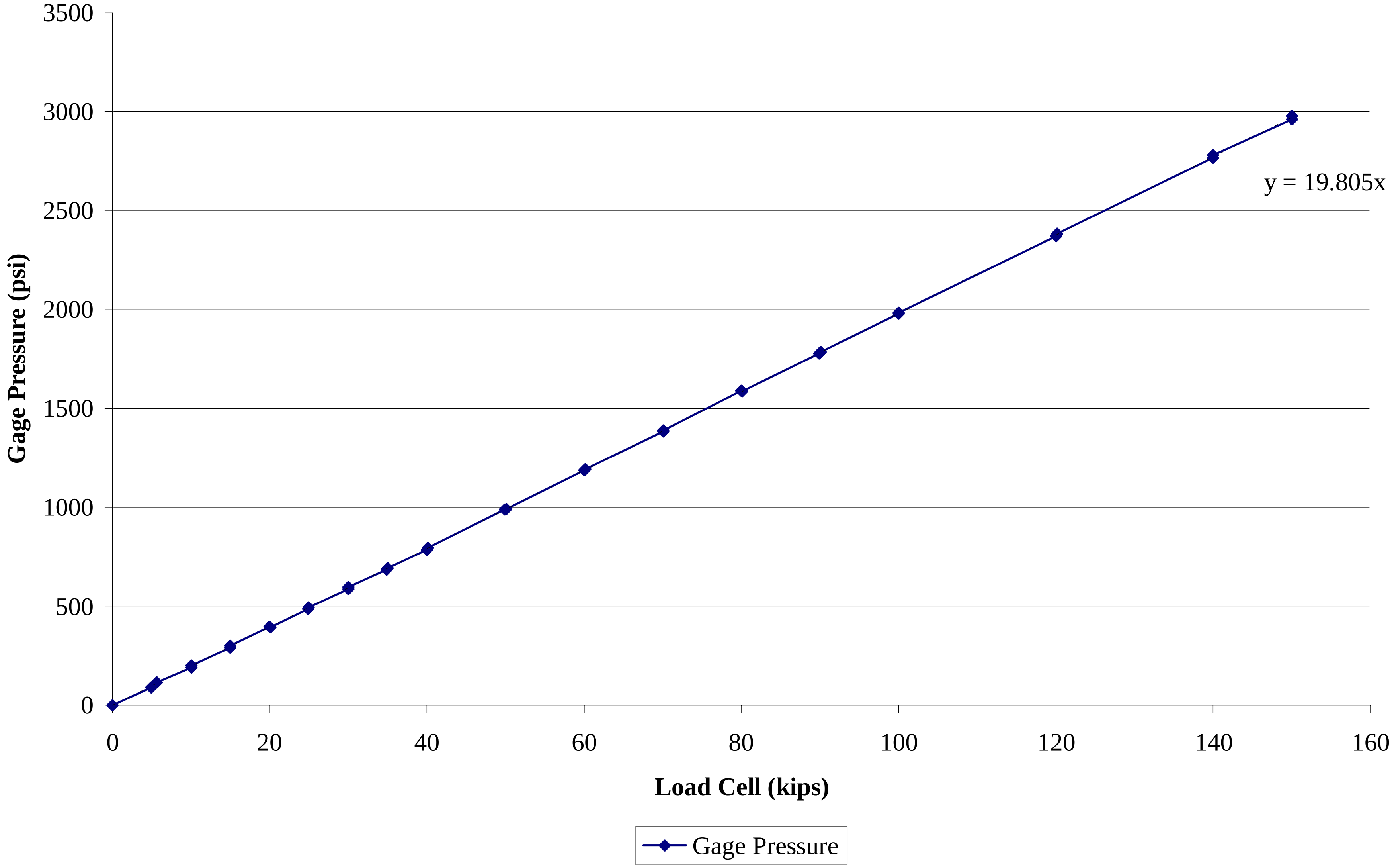

Note: 1 psi = 6.9 kPa; 1 kip = 1000 lbs = 454 kg

FIGURE 10D. FRAME 3 STRAIN VS. LOAD CELL

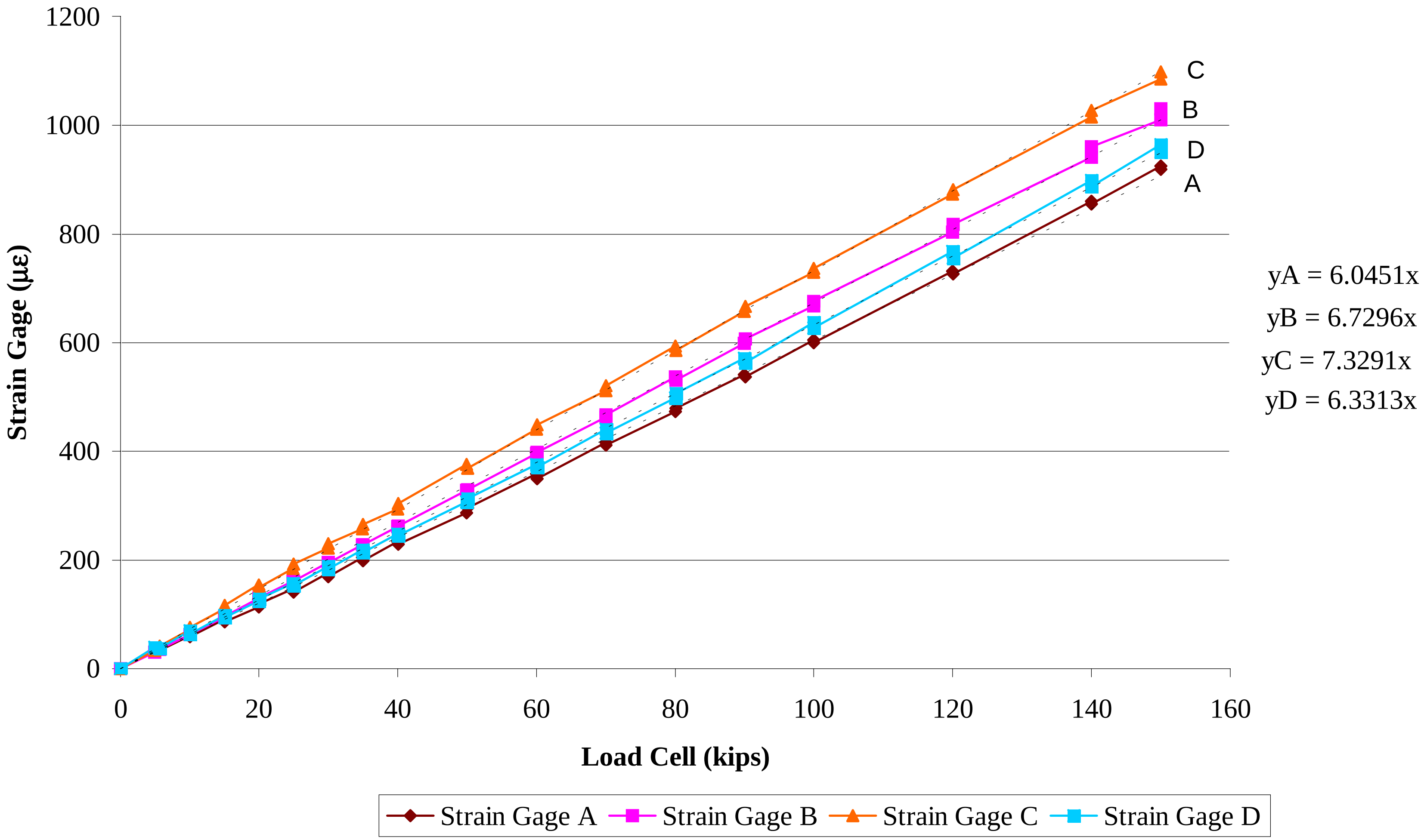

Note: 1 psi = 6.9 kPa; 1 kip = 1000 lbs = 454 kg

FIGURE 11D. FRAME 3 GAGE PRESSURE VS. DESIRED CONCRETE PRESSURE

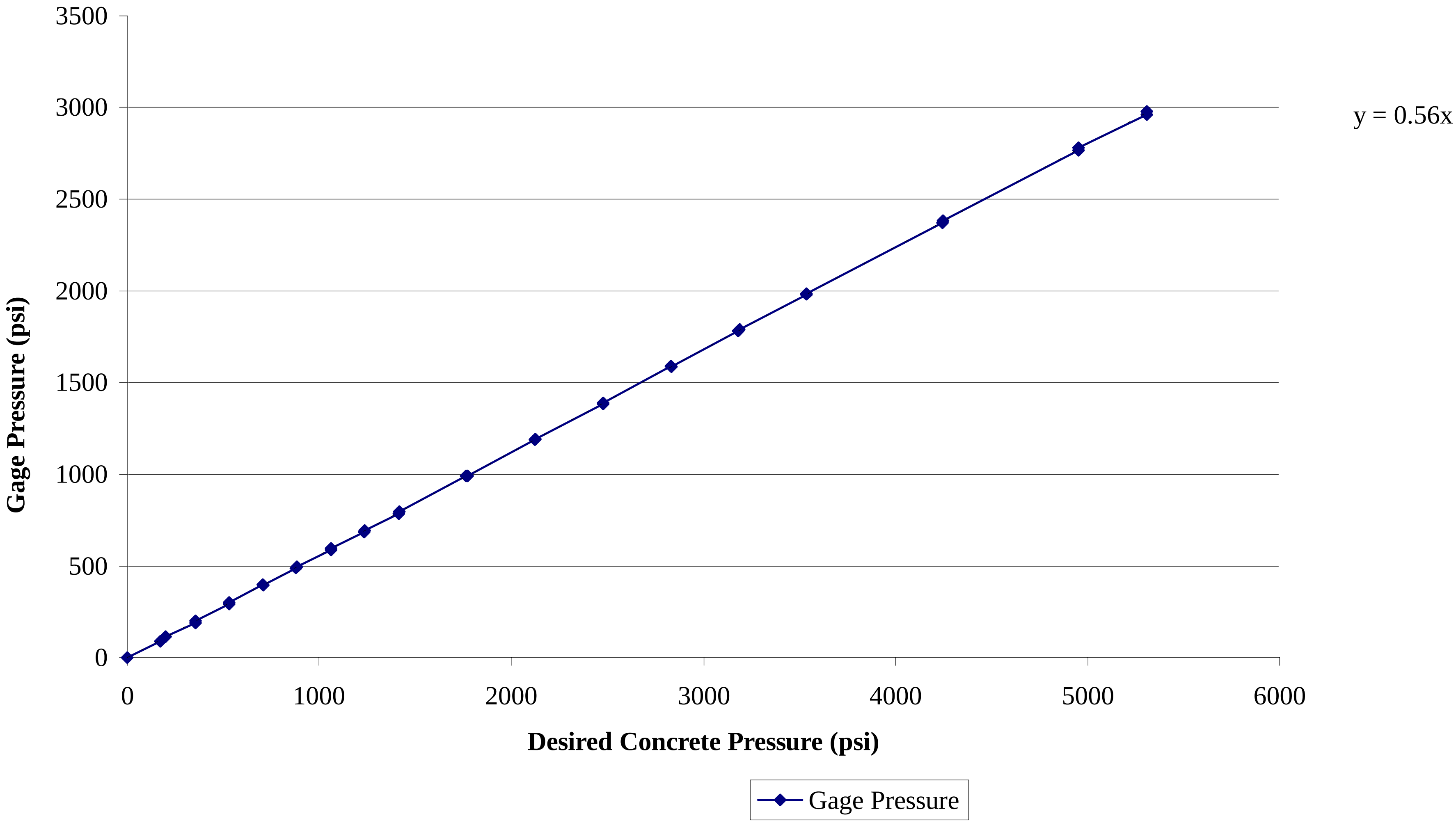

Note: 1 psi = 6.9 kPa; 1 kip = 1000 lbs = 454 kg

FIGURE 12D. FRAME 3 GAGE PRESSURE VS. STRAIN GAGE

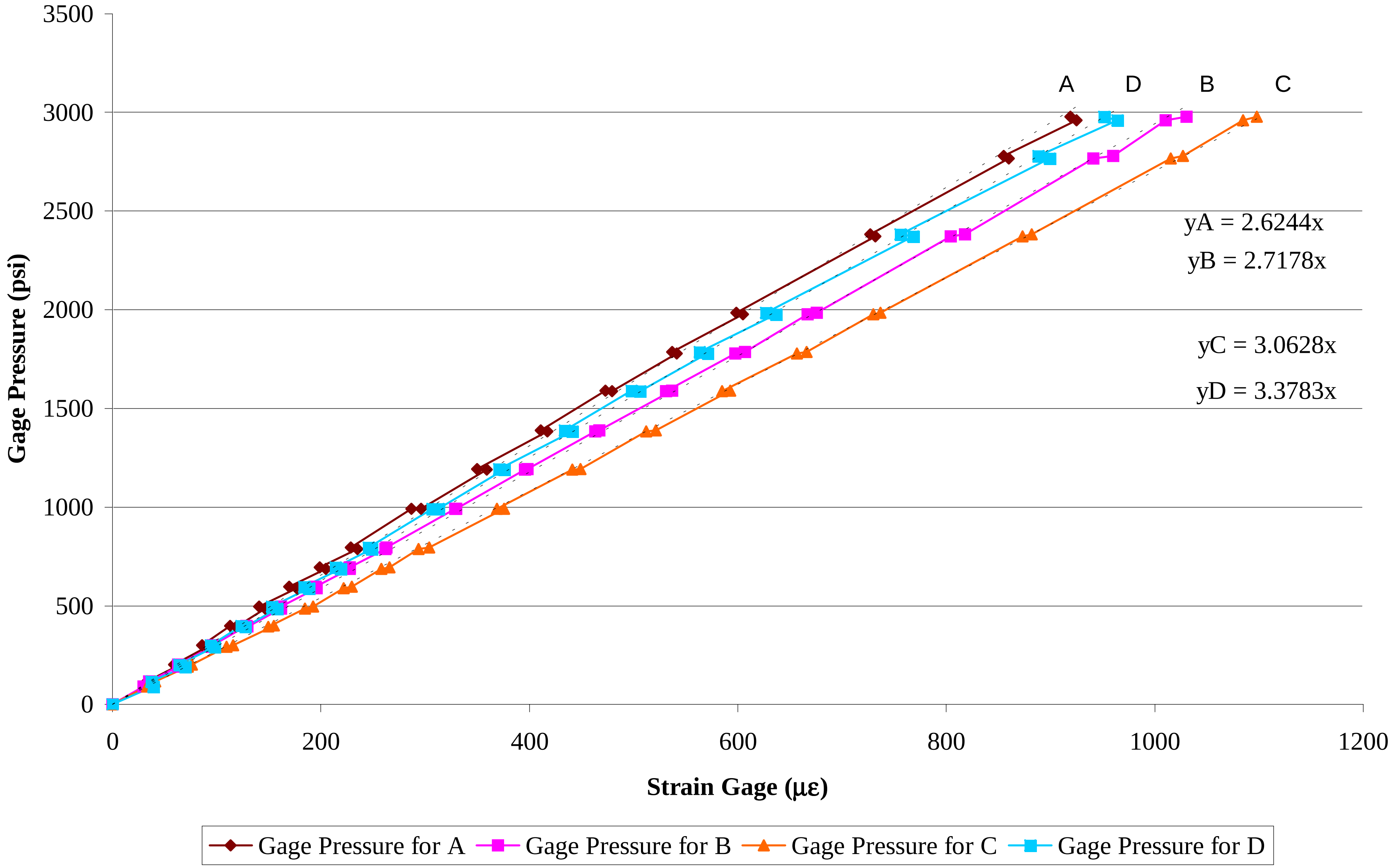

Note: 1 psi = 6.9 kPa; 1 kip = 1000 lbs = 454 kg

FIGURE 13D. FRAME 4 GAGE PRESSURE VS. LOAD CELL

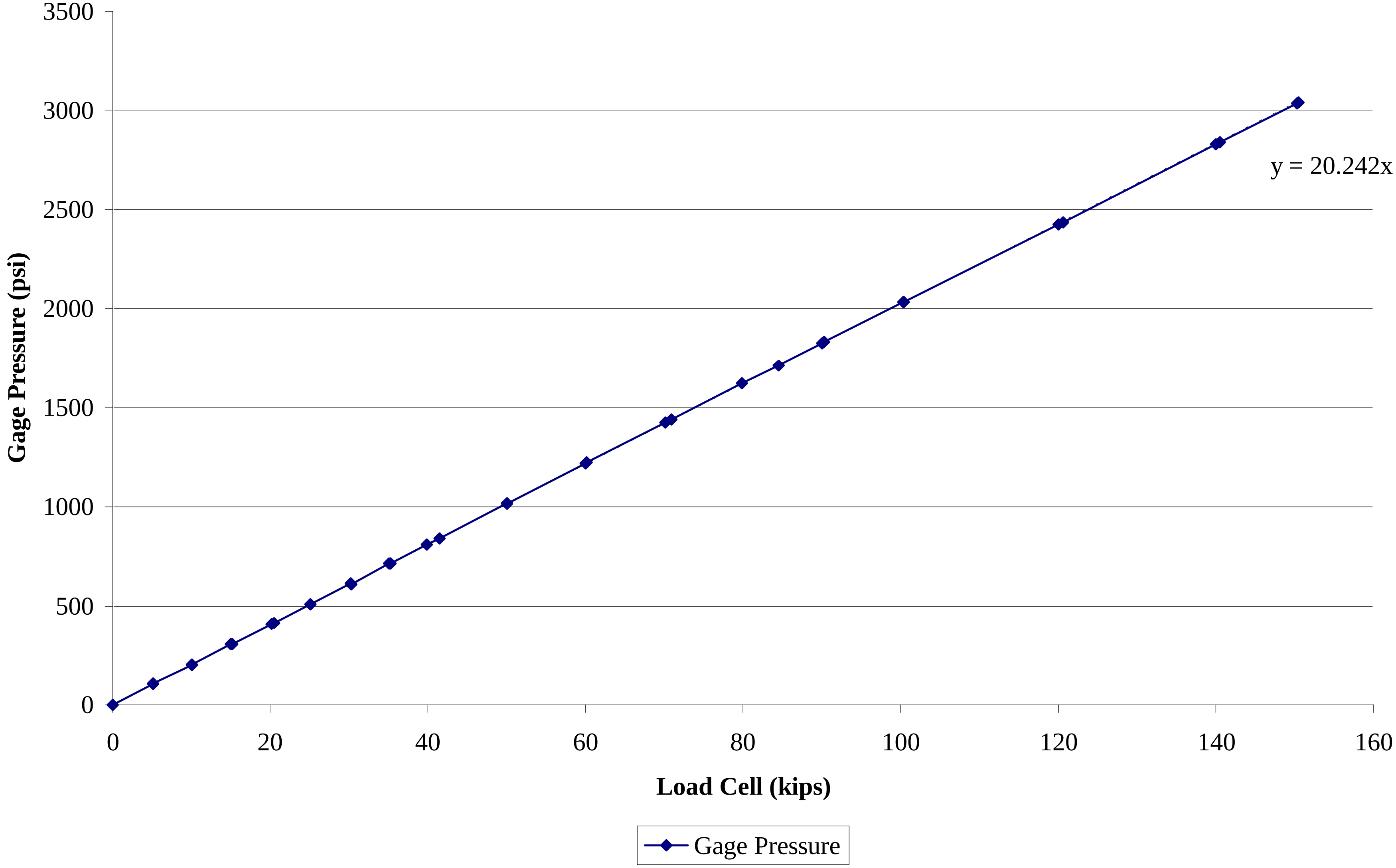

Note: 1 psi = 6.9 kPa;   1 kip = 1000 lbs = 454 kg

FIGURE 14D. FRAME 4 STRAIN VS. LOAD CELL

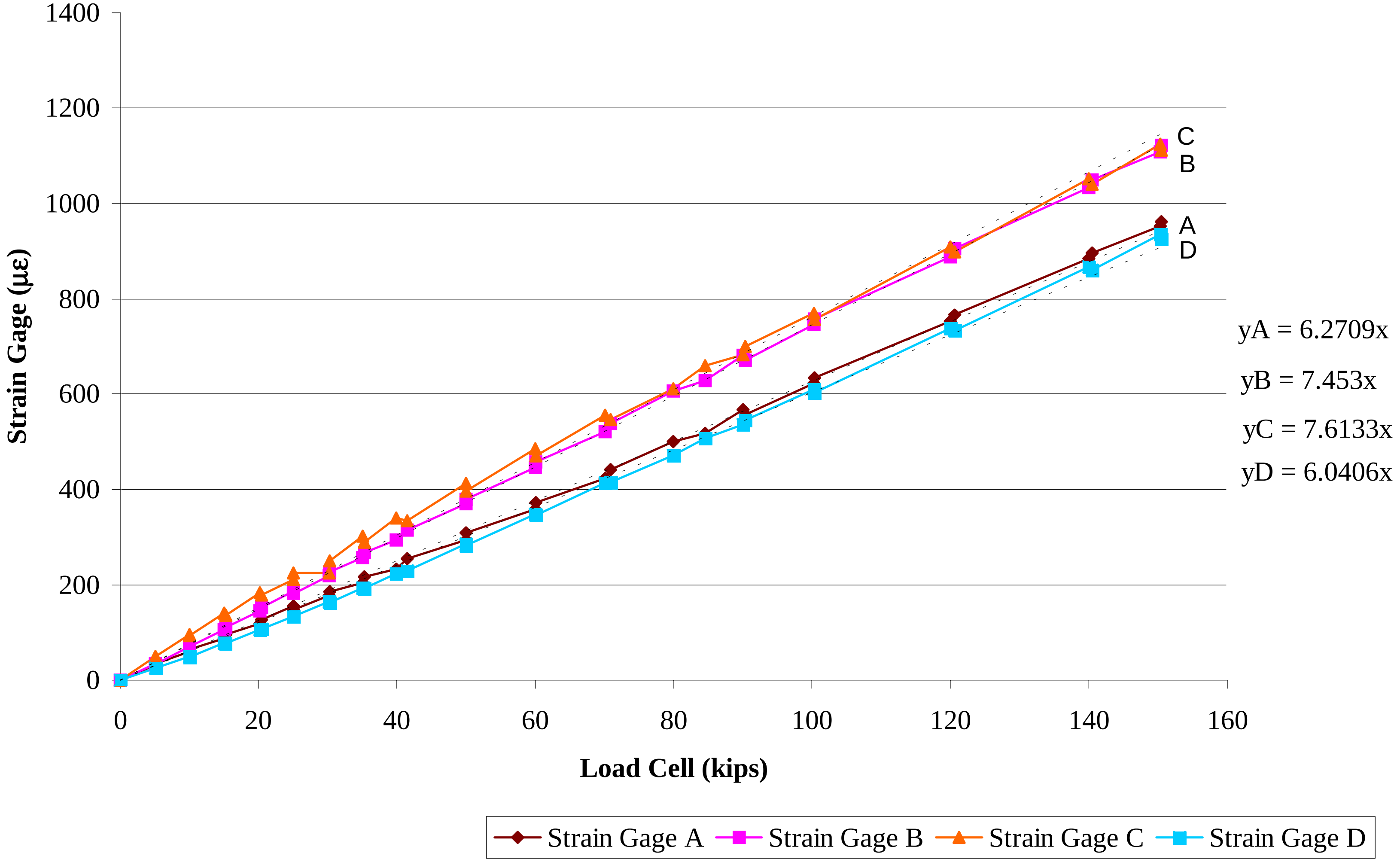

Note: 1 psi = 6.9 kPa; 1 kip = 1000 lbs = 454 kg

FIGURE 15D. FRAME 4 GAGE PRESSURE VS. DESIRED CONCRETE PRESSURE

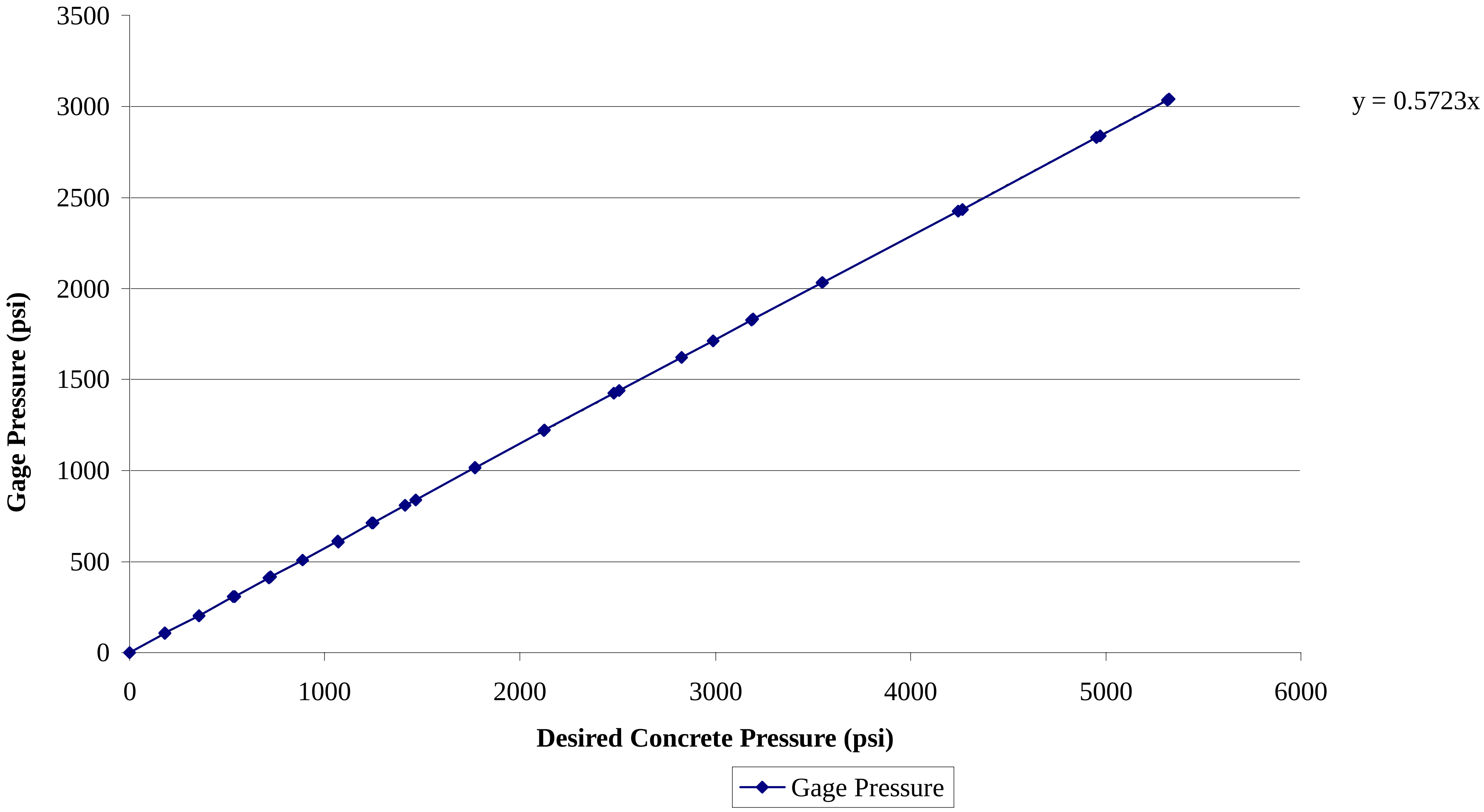

Note: 1 psi = 6.9 kPa; 1 kip = 1000 lbs = 454 kg

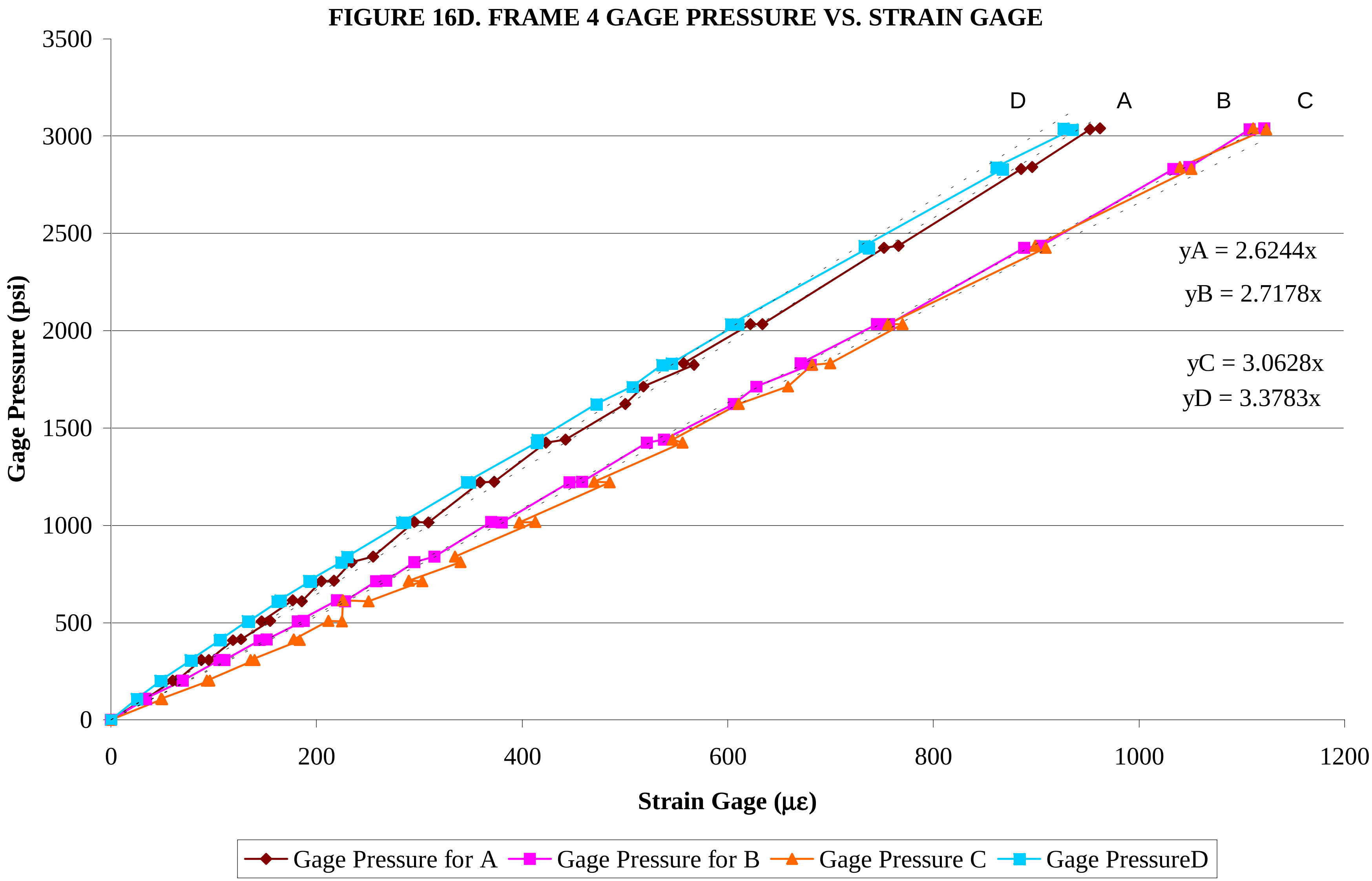

Note: 1 psi = 6.9 kPa; 1 kip = 1000 lbs = 454 k

APPENDIX E

Virginia DOT A-5 Portland Cement Concrete Mixtures

TABLE 1E. VDOT APPROVED A5 PORTLAND CEMENT CONCRETE MIXTURES,

SSD (QUANTITIES/CUBIC METER)

Ingredient	**Gravel**	**Limestone**	**Diabase**
Cement Type I/II, kg	251	386	209
Water, kg	148	138	163
GGBFS, kg	167	-	209
Microsilica, kg	-	30	-
Coarse aggregate, kg	1098	1043	1138
Fine aggregate, kg	627	771	658
Total, kg	2291	2367	2378
w/c or w/(c + p)	0.35	0.33	0.39
Producer	Tarmac America, Inc.	Eastern Vault Co.	Virginia Concrete

TABLE 2E. A5 PORTLAND CEMENT CONCRETE MIXTURES CALCULATED FROM VDOT APPROVED MIXTURES, SSD (QUANTITIES/CUBIC METER)

Ingredient	Gravel	Limestone	Diabase
Cement Type I/II, kg	418	415	419
Water, kg	148	138	164
Coarse aggregate, kg	1098	1043	1138
Fine aggregate, kg	640	781	670
Total, kg	2304	2377	2391
w/c	0.35	0.33	0.39

Ingredient	Limestone	Limestone	Limestone
Cement Type I/II, kg	249	353	386
Water, kg	138	138	138
GGBFS, kg	166	-	-
Fly Ash, kg	-	83	-
Microsilica, kg	-	-	30
Coarse aggregate, kg	1043	1043	1043
Fine aggregate, kg	771	738	771
Total, kg	2367	2355	2367
w/(c + p)	0.33	0.32	0.33

VDOT A5 Specifications	
Minimum Cement Content, kg/m^3	375
Maximum Water, kg water/kg cement	0.4
Consistency, mm of slump	0-100
Air Content, %	4.5 +/- 1.5
Slag Replacement	40 % cement replacement
Fly Ash Replacement	15 % removal of cement, 20% replacement
Microsilica Replacement	7 % cement replacement

APPENDIX F

Measurements of Batch Data

TABLE 1F. DATA FOR A5 GRAVEL PORTLAND CEMENT CONCRETE MIXTURES

	Batch 1			Batch 2			Batch 3		
Time After Casting (days)	**Shrinkage Strain (microstrain)**	**Applied Stress (psi)**	**Total Strain (microstrain)**	**Shrinkage Strain (microstrain)**	**Applied Stress (psi)**	**Total Strain (microstrain)**	**Shrinkage Strain (microstrain)**	**Applied Stress (psi)**	**Total Strain (microstrain)**
7.25	0	1900	566	0	1910	398	0	1910	498
8	37	1900	557	98	1910	391	12	1910	497
9	-22	1910	758	95	1910	447	12	1910	573
10	336	1920	755	96	1920	434	-11	1920	580
11	339	1910	762	117	1920	523	134	1920	655
12	323	1900	787	170	1920	549	111	1920	668
13	348	1910	830	167	1920	580	75	1920	707
14	-	2200	-	-	2160	-	-	2160	-
21	499	2200	1126	212	2160	848	136	2160	1008
28	509	2140	1170	234	2190	937	155	2190	1091
35	552	2320	1310	284	2370	1102	206	2370	1232
42	545	2320	1430	309	2370	1170	232	2370	1302
49	577	2310	1425	314	2360	1245	226	2360	1382
56	618	2370	1511	353	2380	1280	257	2380	1423
63	545	2410	1509	292	2370	1358	228	2370	1505
70	605	2410	1511	320	2370	1358	278	2370	1495
77	588	2400	1572	347	2370	1334	273	2370	1497
84	624	2410	1573	375	2380	1403	301	2380	1546
97	672	2410	1663	370	2370	1432	312	2370	1570

Note: An eight inch gage length was used, the zero was -0.2797 on the digital gage.

TABLE 2F. DATA FOR A5 LIMESTONE PORTLAND CEMENT CONCRETE MIXTURES

Time After Casting (days)	Batch 1 Shrinkage Strain (microstrain)	Batch 1 Applied Stress (psi)	Batch 1 Total Strain (microstrain)	Batch 2 Shrinkage Strain (microstrain)	Batch 2 Applied Stress (psi)	Batch 2 Total Strain (microstrain)	Batch 3 Shrinkage Strain (microstrain)	Batch 3 Applied Stress (psi)	Batch 3 Total Strain (microstrain)
7.25	0	2580	1441	0	2580	1357	0	2400	411
8	480	2550	1617	279	2550	1530	-116	2390	558
9	538	2540	1694	499	2540	1687	-145	2400	723
10	648	2540	1752	345	2540	1716	-62	2410	791
11	619	2530	1680	448	2530	1540	-47	2400	1008
12	547	2580	1886	405	2580	1723	134	2410	938
13	773	2520	1842	388	2520	1597	177	2420	981
14	-	2790	-	-	2790	-	-	2790	-
21	1131	2790	1966	659	2790	1753	38	2790	1157
28	886	2980	2064	572	2980	1862	377	2750	1686
35	890	2970	2394	736	2970	2334	363	2930	1679
42	825	2950	2502	475	2950	2313	401	2920	1524
49	993	2990	2603	416	2990	2395	318	2950	1809
56	903	2960	2734	864	2960	2575	288	2910	1877
63	827	2960	2585	646	2960	2701	327	2950	1844
70	834	2980	2581	573	2980	2562	294	2970	1962
77	945	2980	2822	613	2970	2573	240	2960	1984
84	1129	2950	2845	793	2950	2652	448	2920	2081
97	805	2900	2783	559	2890	2674	259	2930	2050

Note: An eight inch gage length was used, the zero was -0.2797 on the digital gage.

TABLE 3F. DATA FOR A5 DIABASE PORTLAND CEMENT CONCRETE MIXTURES

	Batch 1			Batch 2			Batch 3		
Time After Casting (days)	**Shrinkage Strain (microstrain)**	**Applied Stress (psi)**	**Total Strain (microstrain)**	**Shrinkage Strain (microstrain)**	**Applied Stress (psi)**	**Total Strain (microstrain)**	**Shrinkage Strain (microstrain)**	**Applied Stress (psi)**	**Total Strain (microstrain)**
7.25	0	1900	481	0	1900	613	0	1910	338
8	24	1900	463	13	1900	569	85	1910	340
9	-32	1910	600	0	1910	763	89	1910	404
10	227	1920	605	388	1920	763	212	1920	344
11	228	1910	620	392	1910	813	114	1920	506
12	217	1900	653	396	1900	834	187	1920	528
13	213	1910	693	393	1910	852	170	1920	562
14	-	2200	-	-	2200	-	-	2160	-
21	437	2200	1038	523	2200	1219	237	2160	889
28	463	2140	1116	546	2140	1273	299	2190	996
35	526	2320	1280	621	2320	1463	362	2370	1169
42	572	2320	1425	666	2320	1598	391	2370	1272
49	556	2310	1432	645	2310	1635	391	2360	1356
56	605	2370	1526	697	2370	1722	402	2380	1401
63	576	2410	1569	654	2410	1773	386	2370	1506
70	629	2410	1604	713	2410	1802	422	2370	1513
77	607	2400	1626	685	2400	1839	412	2370	1519
84	645	2410	1675	770	2410	1888	417	2380	1566
97	566	2410	1705	806	2410	1920	423	2370	1649

Note: An eight inch gage length was used, the zero was -0.2797 on the digital gage.

TABLE 4F. DATA FOR A5 LIMESTONE FLY ASH PORTLAND CEMENT CONCRETE MIXTURES

	Batch 1			Batch 2			Batch 3		
Time After Casting (days)	Shrinkage Strain (microstrain)	Applied Stress (psi)	Total Strain (microstrain)	Shrinkage Strain (microstrain)	Applied Stress (psi)	Total Strain (microstrain)	Shrinkage Strain (microstrain)	Applied Stress (psi)	Total Strain (microstrain)
7.25	0	1780	408	0	1970	526	0	1960	472
8	117	1780	486	11	1970	630	12	1960	584
9	103	1780	605	66	1970	713	41	1960	659
10	84	1780	604	45	1970	725	28	1960	681
11	128	1780	644	50	1970	812	40	1960	733
12	105	1790	645	41	1970	804	48	1960	727
13	118	1790	687	66	1970	827	78	1960	771
14	-	2440	-	-	2410	-	-	2390	-
21	198	2440	1098	136	2410	1167	134	2390	1084
28	229	2390	1264	283	2400	1373	175	2390	1277
35	263	2710	1365	216	2580	1373	227	2570	1267
42	288	2710	1399	241	2580	1490	248	2570	1388
49	288	2720	1477	248	2580	1564	271	2570	1459
56	259	2720	1528	225	2580	1627	277	2570	1515
63	300	2720	1574	288	2580	1656	312	2570	1549
70	354	2720	1598	296	2580	1692	238	2570	1578
77	373	2720	1637	384	2580	1728	354	2570	1611
84	366	2720	1680	345	2580	1773	345	2570	1672
97	366	2720	1721	346	2580	1788	368	2570	1685

Note: An eight inch gage length was used, the zero was -0.2797 on the digital gage.

TABLE 5F. DATA FOR A5 LIMESTONE GGBFS PORTLAND CEMENT CONCRETE MIXTURES

	Batch 1			Batch 2			Batch 3		
Time After Casting (days)	**Shrinkage Strain (microstrain)**	**Applied Stress (psi)**	**Total Strain (microstrain)**	**Shrinkage Strain (microstrain)**	**Applied Stress (psi)**	**Total Strain (microstrain)**	**Shrinkage Strain (microstrain)**	**Applied Stress (psi)**	**Total Strain (microstrain)**
7.25	0	1780	413	0	1780	388	0	1960	427
8	70	1780	475	73	1780	447	36	1960	526
9	55	1780	580	68	1780	524	78	1960	573
10	76	1780	582	113	1780	541	50	1960	588
11	121	1780	613	144	1780	568	69	1960	648
12	95	1790	613	100	1780	563	39	1960	629
13	107	1790	648	102	1780	595	95	1960	641
14	-	2400	-	-	2430	-	-	2390	-
21	152	2400	1016	188	2430	944	120	2390	811
28	186	2390	1129	191	2380	988	163	2390	1118
35	198	2710	1248	221	2700	1168	204	2570	1022
42	236	2710	1280	244	2700	1172	227	2570	1129
49	227	2720	1348	245	2700	1255	234	2570	1202
56	189	2720	1391	223	2700	1287	209	2570	1247
63	238	2720	1445	284	2700	1332	272	2570	1283
70	277	2720	1472	305	2700	1365	262	2570	1301
77	305	2720	1495	345	2700	1390	324	2570	1338
84	324	2720	1573	341	2700	1452	321	2570	1388
97	321	2720	1573	371	2700	1448	367	2570	1393

Note: An eight inch gage length was used, the zero was -0.2797 on the digital gage.

TABLE 6F. DATA FOR A5 LIMESTONE MICROSILICA PORTLAND CEMENT CONCRETE MIXTURES

	Batch 1			Batch 2			Batch 3		
Time After Casting (days)	Shrinkage Strain (microstrain)	Applied Stress (psi)	Total Strain (microstrain)	Shrinkage Strain (microstrain)	Applied Stress (psi)	Total Strain (microstrain)	Shrinkage Strain (microstrain)	Applied Stress (psi)	Total Strain (microstrain)
7.25	0	2580	1073	0	2400	420	0	2400	613
8	304	2550	1309	-37	2390	413	77	2390	589
9	545	2540	1505	104	2400	570	33	2400	755
10	495	2540	1297	-67	2410	563	-68	2410	829
11	560	2530	1358	303	2400	730	232	2400	943
12	571	2580	1596	205	2410	692	248	2410	902
13	413	2520	1498	234	2420	920	343	2420	1018
14	-	2790	-	-	2790	-	-	2790	-
21	684	2790	1683	12	2790	703	148	2790	982
28	566	2980	1588	314	2750	986	375	2750	1368
35	760	2970	1968	335	2930	1201	260	2930	1389
42	670	2950	2084	80	2920	1152	87	2920	1438
49	398	2990	2092	242	2950	1248	163	2950	1506
56	780	2960	1985	235	2910	1291	259	2910	1409
63	673	2960	1973	444	2950	1273	364	2950	1484
70	586	2980	2026	442	2970	1231	456	2970	1500
77	709	2970	2249	209	2970	1330	241	2960	1595
84	873	2950	2191	384	2920	1296	416	2920	1488
97	632	2920	2128	155	2930	1178	231	2930	1491

Note: An eight inch gage length was used, the zero was -0.2797 on the digital gage.

VITA

Richard Meyerson was born in Staten Island, New York on October 19, 1976 to Saul and Gail Meyerson. He grew up in Staten Island, attending Staten Island Technical High School. After graduating high school in 1994, Richard attended Rutgers, The State University of New Jersey. Richard graduated Rutgers with a Bachelor's of Science in Civil Engineering in 1998. He then pursued a graduate degree at Virginia Tech. Upon completion of his Master's Degree from Virginia Tech in February 2001, Richard plans on becoming a bridge engineer.